JIMMA UNIVERSITY

SCHOOL OF GRADGUATE STUDIES

JIMMA INSTITUTE OF TECHNOLOGY

DEPARTMNT OF CIVIL ENGINEERING

GEOTECHNICAL ENGINEERING CHAIR

PERFORMANCE PREDICTION OF FLEXIBLE PAVEMENT: CASES STUDY THE ROAD FROM JIMMA TO BONGA TOWN.

A THESIS SUBMITTED TO THE SCHOOL OF GRADUATE STUDIES JIMMA UNIVERSITY, JIMMA INSTITUTE OF TECHNOLOGY, DEPARTMENT OF CIVIL ENGINEERING IN PARTIAL FULFILMENT OF THE REQUIREMENTS FOR THE DEGREE OF MASTERS OF SCIENCE IN CIVIL ENGINEERING (GEOTECHNICAL ENGINEERING).

BY

TEWODROS MEZMUR (B.SC)

MARCH, 2020

JIMMA ETHIOPIA

JIMMA UNIVERSITY

SCHOOL OF GRADGUATE STUDIES

JIMMA INSTITUTE OF TECHNOLOGY

DEPARTMNT OF CIVIL ENGINEERING

GEOTECHNICAL ENGINEERING CHAIR

PERFORMANCE PREDICTION OF FLEXIBLE PAVEMENT: CASES STUDY THE ROAD FROM JIMMA TO BONGA TOWN.

A THESIS SUBMITTED TO THE SCHOOL OF GRADUATE STUDIES JIMMA UNIVERSITY, JIMMA INSTITUTE OF TECHNOLOGY, DEPARTMENT OF CIVIL ENGINEERING IN PARTIAL FULFILMENT OF THE REQUIREMENTS FOR THE DEGREE OF MASTERS OF SCIENCE IN CIVIL ENGINEERING (GEOTECHNICAL ENGINEERING).

BY

TEWODROS MEZMUR (B.SC)

MAIN ADVISOR: Prof. ANAND M.H

CO ADVISOR: DAMTEW TSEGE (PhD)

MARCH, 2020

JIMMA ETHIOPIA

DECLARTION

This paper is my original work and it has not been present for a degree in any other University.

Tewodros Mezmur

Signature_____Date_____

The thesis submitted for examination with my approval as University Supervisor Adviser

Main adviser: Prof. Anand M.H

Signature  Date_____

Co- Adviser. Damitew Tsige (PhD)

Signature_____Date_____

ACKNOWLEDGMENT

First praise and glory be to Almighty God for best owing me strength with health and power to complete this work.

I would like to all my deepest thanks to the Ethiopian Road Authority (ERA), for its kind help, support, and sponsorship of this study program for the M.Sc and to all my lecturers who have taught me in Jimma University and Jimma Institute of Technology, thank you for all the knowledge and guidance.

Also, I would like to say thanks a lot to my adviser Anand M.H (Prof) and co-adviser Damitew Tsige (Dr) for their continuous unlimited help and kind support in preparing my thesis.

Finally, my special thanks go to my parents, brothers and sisters who are always been there in times of difficulties and giving me moral support to complete this research work.

ABSTRACT

Road structure deformation is a critical issue for flexible pavement. Pavement distress such as fatigue cracking and rutting deformation are the most serious for pavement sustainability. Due to repetitive traffic loading during its service life and environmental factors causes pavement distress, which affects the serviceability and durability of pavement structures.

Particularly, In Ethiopia several roads are failed before they gave full service. This study aims to conduct future performance of a pavement structure, evaluate existing pavement structure and mechanistic response. Therefore, to achieve the objective of the study, nonlinear finite element and multi-layer leaner elastic methods are utilized for analyses of flexible pavement structural response mechanism. In Situ Pavement structures and mechanical property of flexible pavement evaluated by Dynamic Cone Penetrometer (DCP), and multi-layer elastic and finite element used for analysis of pavement structural response by utilizing JULEA and ABAQUS software respectively. Finally predicting on service performance of flexible pavement comparatively based on JULEA and ABAQUs critical strain result by using asphalt institute (AI) distress prediction model. From the study, the results of road section number one, two and three are drawn as (a) pavement thickness and strength (CBR) of granular base course (200 mm, 71%), (200 mm, 79%) and (200 mm, 71%) respectively. (b)For sub-base course pavement thickness and CBR values are (200 mm, 31%), (175 mm, 33%) and (275 mm, 21%) respectively. (c)Subgrade soil had infinite thickness with CBR value of 10%, 20% and 6% respectively. (d)Asphalt concrete had similar thickness 50 mm for all section. (e) the Resilient modulus (elastic modulus) of base course 269 Mpa, 288 Mpa and 267Mpa, sub-base course 158 Mpa, 165 Mpa and 123 Mpa, and subgrade soil 77 Mpa, 120 Mpa and 55 Mpa respectively. It was concluded that from JULEA multilayer elastic analysis, vertical compressive strain predicted as 0.075 damage ratio and 13 year of minimum pavement performance. However, from ABAQUS nonlinear finite element analysis of section one, vertical compressive strain value at top of subgrade soil predicted as 0.060 damage ratio and 16 year of minimum pavement performance. Therefore, it is concluded that so that, 13 years are taken as governing predicted performance year for Jimma-Bonga flexible pavement road.

Key Words: Flexible Pavement, performance, prediction, in situ condition, Dynamic cone penetration, PCASE'S DCP, Mechanistic response, ABAQUS and JULEA, Asphalt Institute

TABLE OF CONTENT

DECLARTION ..... **I**
ACKNOWLEDGMENT ..... **II**
ABSTRACT ..... **III**
TABLE OF CONTENT ..... **IV**
LIST OF TABLE ..... **VI**
LIST OF FIGURE ..... **VII**
ACRONYMS ..... **IX**
CHAPER ONE **1**
1.1. BACKGROUND 1
1.2. PROBLEM STATEMENT 3
1.3. RESEARCH QUESTIONS 3
1.4. OBJECTIVES 4
1.4.1 General Objective *4*
1.4.1 Specific Objectives *4*
1.5. SIGNIFICANCE OF THE STUDY 4
1.6. SCOPES AND LIMITATION OF THE STUDIES 5
CHAPTER TWO **6**
LITRATURE REVIEW **6**
2.1 INTRODUCTION 6
2.2 EVALUATION OF IN SITU PAVEMENT LAYERS WITH THE DYNAMIC CONE PENETROMETER (DCP) 9
2.2.1 PRINCIPLE 11
2.2.2 EXISTING CORRELATIONS BETWEEN DCP AND CALIFORNIA BEARING RATIO (CBR) 15
2.2.3 EXISTING CORRELATION BETWEEN DCP AND ELASTIC MODULI 17
2.3. MECHANISTIC MODEL 19
2.3.1 RESILIENT MODULUS 20
2.3.2 HIERARCHAL APPROACH 23
2.3.3 FINITE ELEMENT MODEL 25
2.3.4 LAYER ELASTIC MODEL 27
2.4. CAUSES AND EMPIRICAL PREDICTION OF PAVEMENT DAMAGE 29
2.4.1 Fatigue Cracking Models *31*
2.4.2 Rutting *33*
CHAPTER THREE **36**
MATERIALS AND METHOD **36**
3.1. STUDY AREA 36
3.2. CLIMATE CONDITION OF THE AREA 36
3.3. GEOLOGY OF THE AREA 37

3.4. CONSTRUCTION HISTORY OF PAVEMENT 37
3.5. SAMPLING PROCEDURES 38
3.6. SAMPLING TECHNIQUE 38
3.7. DATA PROCESSING AND ANALYSIS 39
3.8. STRENGTH (CBR) AND THICKNESS OF PAVEMENT LAYERS 39
3.9. ELASTIC MODULUS OF PAVEMENT LAYERS 40
3.10. POISONS RATIO 40
3.11. ASSUMPTIONS OF MECHANISTIC PAVEMENT RESPONSE ANALYSIS 40
3.12. TRAFFIC LOAD 41
3.13. MECHANISTIC PAVEMENT RESPONSE ANALYSIS 41
3.14. PERFORMANCE PREDICTION OF FLEXIBLE PAVEMENT 42
3.14.1. AI Fatigue Distress *42*
3.14.2. AI Rutting Distress *42*

CHAPTR FOUR 44

RESULT AND DISCUSSION 44

4.1. PAVEMENT EVALUATION RESULT 44
4.2. DYNAMIC MODULUS RESULT 52
4.3. MECHANISTIC RESPONSE RESULT 55
4.4. EMPIRICAL PERFORMANCE PREDICTION RESULT 63

CHAPTER FIVE 66

CONCLUTION AND RECOMMENDATION 66

5.1. CONCLUSION 66
5.2. RECOMENDATION 67

REFERENCE 68

APPENDIX 74

LIST OF TABLE

Table 2. 1 Coefficient in rutting and cracking distress models 34
Table 3. 1 Rainfall figures along the route 36
Table 3. 2 Jimma-Bonga flexible pavement road sections 36
Table 4. 1 Section one PCASE DCP analysis result. 44
Table 4. 2 Section two PCASE DCP analysis result 45
Table 4. 3 Section three PCASE DCP analysis result 47
Table 4.4 Average CBR and thickness result of pavement sections 48
Table 4. 5 Climate data of Jimma. 49
Table 4. 6 AASHTO Typical moduli value for common paving materials 51
Table 4. 7 Pavement Material Properties (source: ERA 2013). 52
Table 4. 8 Jimma-Bonga road pavement layers CBR value and elastic modulus 52
Table 4. 9 Average pavement layers Elastic modulus, thickness and poisons ratio of Jimma-Bonga road. 53
Table 4. 10 JULEA Critical strain at the bottom of asphalt and at top of subgrade soil results 61
Table 4. 11 ABAQUS analysis critical strain result at the bottom of asphalt and top of sub-grade soil 62
Table 4. 12 Pavement Performance prediction result base on JULEA result 62
Table 4. 13 Pavement performance prediction based on ABAQUS result 63
Table 4. 14 Comparative pavement performance prediction based on JULEA and ABAQUS 64

LIST OF FIGURE

Figure 2. 1 DCP test equipment……...10
Figure 2. 2 Dynamic Cone Penetrometer Schematic (Source: MnDOT DCP Design)……...12
Figure 2. 3 The Dynamic Cone Penetration (DCP) Test Procedure (Salgado and Yoon, 2003) 13
Figure 2. 4 DCPI Profile of a Flexible Pavement (Gudishala, 2004).....14
Figure 2. 5 Correlation chart between CBR vs DCPI 16
Figure 2. 6 Comparison of Different CBR-Moduli Relationships (Wu and Sargand, 2007).....16
Figure 2. 7 Spread of wheel-load though pavement structure (ERA, 2002). 19
Figure 2.8: Resilient Modulus from Simplified Stress-Strain Diagram……..21
Figure 2.9 Deformation Response of a Pavement under cyclic Loading (Huang, 1993)……22
Figure 2. 10 Critical stress and strain in a flexible pavement (ERA, 2002)……30
Figure 2.11: Illustration of AI Fatigue Damage Model……..….31
Figure 2.12: Illustration of AI Rutting Damage Model……...33
Figure 3. 1 Jimma –Bonga road alignment(Google map, 2012).....35
Figure 3. 2 Sample Collection.....37
Figure 4. 1 Section one average thickness of Asphalt, Base, Sub-base and Sub-grade pavement layers 43
Figure 4. 2 Section two average thickness of Asphalt, Base, Sub-base and Sub-grade pavement layers 45
Figure 4. 3 Section three average thickness of Asphalt, Base, Sub-base and Sub-grade pavement layers.....47
Figure 4.4: PCASE climate analysis result……..49
Figure 4.5 pavement evaluation result of section one……50
Figure 4.6 pavement evaluation result of section two……50
Figure 4.7 pavement evaluation result of section three……...51
Figure 4. 8 ABAQUS Vertical stress of section one, two and three results 55
Figure 4. 9 Vertical stress result of ABAQUS and JULEA 57
Figure 4. 10 Horizontal strain result from ABAQUS 57
Figure 4. 11 Horizontal strain result of ABAQUS and JULEA.....58
Figure 4. 12 Vertical strain result of ABAQUS for section one, two and three 60

Figure 4. 10 Vertical strain result of ABAQUS and JULEA 61

ACRONYMS

AASHTO	American association of state highway transport office
AI	Asphalt institute
ASTM	American Society for Testing and Materials
^0C	Degree Celsius
CBR	California Bearing Ratio
DCP	Dynamic Cone Penetrometer
DCPI	Dynamic Cone Penetration Index
E_{11}/ ε_{xx}	Horizontal strain along x- axis
E_{22}/ ε_{yy}	Vertical strain along y- axis
EIA	Environmental impact analysis
ERA	Ethiopia road authority
ESAL	Equivalent standard axle load
^0F	Degree Fahrenheit
FWD	Falling weight deflectometer
M-E	Mechanistic-empirical
MEPDG	Mechanistic-empirical pavement design Gide
MLET	Multilayer elastic theory
MnDOT	Minnesota department of transportation
NCHRP	National Cooperative Highway Research Program
PMS	Pavement management systems
S_{22}	Vertical stress along y- axis
USACE	U.S. Army Corps of Engineers

CHAPER ONE
INTRODUCTION

1.1. Background

Flexible Pavement road is modern construction way of road infrastructure in the world from different material layers property and thickness in order to distribute traffic load in to each layers without excessive deformation and deterioration during service life. In many countries, flexible pavements deteriorate before design service life or before expecting traffic service life (Huang, 2004). Actually flexible pavement roads are failed under the influence of traffic loads, clime condition and construction problem. However, the major causes of flexible pavement distress are heavy traffic loads induced stress on pavement structure. The stresses caused by heavy loads may result in micro cracking in asphalt materials and may cause permanent deformation in pavement layers. Performance prediction of flexible pavement needed in order to keep pavement health condition before they reach total damage or out of function. Fatigue crack and rutting deformation are the most predicted critical distress of flexible pavement, which are induced by heavy traffic load long wheel path. Ideally, pavement performance predictions are performed for such type of distresses or deteriorations through a comprehensive evaluation of in situ pavement layers with the Dynamic Cone Penetrometer (DCP), mechanistic response analysis of pavement structure and empirical prediction of pavement service life. Unfortunately, the process of all distress or deterioration of pavement material is quite complex and difficult to predict.

Early deformation of pavement before reaching design life is one of main problem of pavement road in Ethiopia (Wayessa, 2017). Jimma-Bonga flexible pavement road branch are found in south west Ethiopia at Jimma district road network. Total length of 107 Km Jimma-Bonga road are divide into three sections depending on construction history in order to evaluate, analysis and predict in situ performance of each pavement section properly. The stud carried out in each section of pavement including evaluation of in situ pavement layers with dynamic cone penetration (DCP) test, mechanistic response analysis of pavement structure in terms of stress, strain and displacement and finally empirical prediction of pavement service life by using fatigue and rutting distress model of asphalt institute (AI). The mechanistic approach was performed based on result of in situ evaluation of elastic modulus and thickness

of pavement layers in each section from DCP data analysis, at ERA standard manual conditions as close as possible to what they are in the designing of road structure. An empirical approach is one, which based on the results of mechanistic response analysis. This means that the relationship between the input values and pavement failure were arrived through in situ DCP test, mechanistic approach and empirical prediction approach.

According to ASTM D 6951 dynamic cone penetrometer (DCP) have been used for evaluation of in situ engineering properties of geo-materials including pavement base courses, sub-bases, and subgrade layers. DCP is one of the primary tools for assessing the in situ strength and thickness of unbound pavement layers. The U.S. Army Corps of Engineers (USACE) has adopted the DCP for use in the evaluation of existing unbound pavements. On this study, consider the USACE's recommended procedures for using the DCP to evaluate in situ pavement materials. The regression models are presents to describe the relationship between the penetration rate or DCP index and the California Bearing Ratio (CBR). However, the Analysis for interpreting DCP results is present in terms of CBR and thickness of pavement layers in each section of road. The results of the analyses express that the correlations provide a simple means of obtaining estimates of key material properties. The techniques and relationships described in this paper provide a relatively reliable means of estimating in situ material properties with the DCP.

The mechanistic analysis performed based on multi-layer elastic method and finite element method for better quantify strain values of pavement structure in order to get realistic value of pavement performance service life for future. The mechanistic – empirical method mixed the elements of mechanistic modeling and performance models in calculating performance prediction of the road on service life. Analysis of flexible pavement is based on elastic multilayer structure and finite element method for computation of stresses and strains at the critical location using a linear layered elastic method (Kim, 2007). Finite element method is a solution tool for analyzing of various types of structures. This technique provides a methodology to solve the complex problems related to the pavement structures. The main benefits of the finite element method are its suitability and flexibility for analysis of the different boundary conditions and different materials properties.

The purpose of this thesis is evaluating in situ flexible pavement layers for use of mechanistic procedure (layered elastic analysis) to predicate (estimate) on service performance of pavement based on mechanical response. The use of layered elastic analysis and finite element method concept is necessary in that it is based on the elastic theory (Yang, 1973) and can be used to investigate excessive horizontal tensile strain at the bottom of the asphalt layer (fatigue cracking) and excessive vertical compressive strain on top of the subgrade (Rutting deformation) in asphalt pavement.

1.2. Problem statement

Road structure deformation is a critical issue for flexible pavement. Mostly fatigue cracking and rutting deformation are considering the most serious mechanism of distress in asphalt pavements (Oscarsson, 2007). Due to repetitive traffic loading that the road experiences during its service life combined with environmental factors causes rutting deformation and fatigue crack, which ultimately degrade and reduces the serviceability and durability of pavement structures. Most of the flexible pavement roads in our country are start to deform before expected period due to fatigue crack and rutting deformation (Wayessa, 2017). Transient strain at the bottom of asphalt are responsible for occurrence of fatigue crack and vertical compressive strain founded at the top of subgrade are responsible for occurrence of rutting deformation.

Mechanistic-empirical based pavement performance prediction procedures are being developed in different countries such as Europe and North America with the main purpose to adequately predict pavement response and performance (AMADEUS, 2000; Cost333, 1999; Bayomy and Abo-Hashema, 2001). The use of multi-layer elastic and finite element model through JULEA and ABAQUS software package allow to model pavement structure, which is accommodating stiffness of the asphalt road layers, granular base, sub-base and subgrade materials. Linear elastic model is most commonly uses for performance prediction and evaluation of flexible pavement section. Linear elastic model are worked based on linear elastic theory of constitutive relationship by assuming the load come from vehicles is distributed over the pavement structure properly in order to enforced deflection of the road.

1.3. Research Questions

The research questions that this study attempts to clarify about performance prediction of flexible pavement under traffic load are as follows**:**

1. How can Dynamic Cone Penetrometer (DCP) evaluate in Situ Pavement Layers?
2. Can multilayer elastic and finite element method analyze mechanistic response of flexible pavement?
3. Can we predict the performance of pavement comparatively based on critical strain?

1.4. Objectives

1.4.1 General Objective

This research is aim Performance prediction of flexible pavement: For the road from Jimma to Bonga town.

1.4.1 Specific Objectives

- To evaluate in Situ Pavement Layers with Dynamic Cone Penetrometer (DCP).
- To analyze mechanistic response of flexible pavement based on multilayer elastic and finite element method.
- To predict the performance of pavement comparatively based on critical strain.

1.5. Significance of the study

Pavement performance prediction allow to forward prediction of future condition based on present condition of pavement under a defined range of future loading, rehabilitation and maintenance scenarios. The successful implementation of pavement management systems (PMS) is strongly dependent upon how will future pavement condition, as predicting by the performance prediction models of the system, observing behavior of pavement and local engineering knowledge of the pavement damage consideration. Therefore, accurate prediction of pavement performance is very important for efficient management, rehabilitation and maintenance of the road infrastructure.

This research significantly studied to accommodate the idealistic pavement formulation and actual condition of pavement through in situ evaluation, numerical (mechanistic) and empirical methods. The research is diagnostic, deterministic, illustrative, predictive and informative for pavement rehabilitation program, for new pavement designers, for pavement

management and maintenance work. Therefore, the output of this research will be user full for designer, government and any researchers for further investigation of the problems and to take remedial measures in our study area, which is Jimma- Bonga road.

1.6. Scopes and limitation of the Studies

The scope of work included the following for performance prediction of section one, two and three:

- Use DCP data to back calculate the pavement layer modules, which are important input to structural analysis. The nonlinear behavior of base and sub-base was modeled by using (Witczak and Uzan, 1988). But, subgrade soil material behavior considered as linear because of nonlinearity effect of subgrade are small (Huang, 2004).
- Use PCASE software package of DCP, CLIMATE and JULEA program.
- Use finite element (ABAQUS) and multilayer elastic (JULEA) program to calculate critical strains. The horizontal tensile strain at the bottom of the AC layer was used as a predictor of fatigue cracking, and the vertical compressive strain at the top of the subgrade was used as a predictor of rutting based on asphalt institute (AI) distress model.

Pavement on service performance have been expressed in terms of structural condition of pavement distresses, pavement condition index, which is often a composite measure involving both the functional and structural condition, and pavement serviceability index, which includes user's evaluation of the condition of the pavement. This research is concern on structural condition of pavement to study only on fatigue crack causes due to radial strain at the bottom of asphalt layer and rutting deformation causes due to vertical strain on top of subgrade layer of pavement distress.

CHAPTER TWO
LITRATURE REVIEW

2.1 Introduction

Since the 1950s, as the techniques for analyzing pavement response to loading began to be available, there have been many attempts to develop rational design procedures, now commonly referred to as mechanistic-empirical (M-E) procedures, to define/describe the development of specific distresses in pavements. Also, the proposed revision of the *AASHTO Guide for Design of Pavements,* to be completed by the year 2002, will be based on M-E procedures. The M-E procedures typically involve the following steps:

1. Establishment of a hypothesis for the mechanism involved in the development of the specific distress. For example, the development of fatigue cracking in AC pavements is considered by many to be due to the repeated application of bottom tensile strain in the AC layer. This is the most critical step, as all the subsequent steps depend on the correctness of the hypothesis. The hypothesis determines the type of analysis needed to compute the critical response(s), as well as the material and traffic characterizations needed for the analysis.
2. Comprehensive material characterization, incorporating: changes in material properties as a function of the state of stress (stress dependency), environmental conditions (temperature and moisture), aging, and continual deterioration under traffic loading.
3. For each set of conditions, determination of critical responses (stresses, strains, deformations) within the pavement layers when subjected to traffic and environmental loadings.
4. Estimation of damage due to each set of conditions of traffic and environmental loading. This is typically done using distress prediction models or transfer functions that relate a critical structural response to specific distress damage. A different model is used for each distress and pavement type.
5. Evaluation of the damage accumulation over a period of time. Miner's fatigue damage hypothesis is generally used to account for this cumulative damage. Based on predefined relationships between accumulated damage and distress development, the amount of distress that may develop at the end of the selected service life is estimated.

The selected pavement may then be redesigned, if the estimated amount of distress exceeds the acceptable level, or is significantly less than that level.

6. Selection of the pavement design that results in acceptable levels of distresses at the end of the target service/design life.

Similar steps are followed to evaluate the performance of existing pavements. If the previous traffic loading, material properties, and environmental conditions are known (or can be estimated), the six steps may be followed to estimate accumulated distress-specific damages in the pavement and predict future pavement performance. Although these six steps may seem simplistic, the actual process is very complex, because of the many still-indefinable factors associated with pavement design and construction, traffic loading, and environmental conditions.

Over the years, the maximum allowable gross vehicle weights and axle loads were raise. This enhances allowable gross vehicle weight is led to more than proportional raise in the deterioration of pavement environment (Luskin and Walton 2001). The mechanistic – empirical design method mixed the elements of mechanistic modeling and performance models in calculating the required pavement life for a set of design conditions. A performance model, which is a set of laboratory and finite element based models, used to forecast the performance of pavement in terms of physical distresses such as rutting and fatigue during the design life. Effective properties of pavement materials are a solution requirement for a good design, maintenance and rehabilitation works. The proposed AASHTO guide is mechanistic-empirical in nature and advocates the use of a number of mechanical properties such as the young's modules, poisons ratio and resilient modulus of soft clay subgrade bound materials, which contain fine grain local soils materials.

FHWA (April 1998) M-E distress modeling fundamentals approach involves the following elements:

1. A structural analysis model that can consider the geometry of the pavement (principally, the layered system), the loading condition (multiple wheel loads), and the stress dependency of paving materials. The model must also be capable of reliably determining the critical responses appropriate to the distress being considered. For AC pavements, both linear-elastic and viscoelastic structural analysis models are available. However, most of the M-E distress model work has been done using linear-elastic models.

2. A fairly reliable estimate of traffic loading. Advanced M-E procedures consider the axle loading spectra, while other models are based on the use of equivalent loading (e.g., equivalent single axle load (ESAL)), in which case all loadings are transformed into a single load type using load equivalency concepts. However, the use of such equivalent traffic loading limits the usefulness of many of these models in developing rational design procedures.
3. A fairly reliable estimate of seasonal climatic conditions, to account for changes in material properties and, in the case of concrete pavements, also to account for the effect of internal-concrete temperature differentials on curling stresses.
4. Comprehensive material characterization. The AC material properties need to be characterized in terms of temperature effects and in terms of aging. The granular material properties need to be characterized in terms of stress dependency and in terms of seasonal variation as a result of seasonal moisture and temperature variations within these materials. For example, the spring-thaw characterization for fine-grained materials is very important. For PCC materials, seasonal effects are not considered.
5. Availability of "calibrated" mechanistic distress models, or transfer functions that incorporate mechanistic responses. The general approach has been to develop "absolute" models based on laboratory testing and laboratory failure criteria and then to extrapolate those laboratory models to field conditions, using a shift factor to account for different levels of distress development and other unaccounted for factors. For example, for AC fatigue cracking, a model was developed on the basis of laboratory testing and the first crack-initiation as the failure criterion. This model was then expanded to account for different levels of fatigue cracking, as observed at the pavement surface. For example, the Asphalt Institute version of the model uses 20 percent fatigue cracking.
6. Acceptance of Miner's fatigue damage hypothesis. Miner's hypothesis suggests a method for combining various levels of damage done by a combination of traffic and environmental loadings. Miner's hypothesis states that the structural fatigue and rutting damage are cumulative, and that a structure's fatigue and rutting life, defined by the allowable number of load applications prior to failure, is finite.

Our capability for realistically modeling pavement behavior has seen much progress in the last few decades. However, the capability to consider realistically the material

characterization (e.g., E or M_r for the pavement layers remains less than desired, because of a lack of knowledge of realistically accounting for seasonality effects, spatial variability, and deterioration effects due to traffic loading and environment.

2.2 Evaluation of In Situ Pavement Layers with the Dynamic Cone Penetrometer (DCP)

The dynamic cone penetrometer (DCP) is rapidly becoming the primary tool for assessing the in situ strength of unbound pavement layers. The U.S. Army Corps of Engineers (USACE) has adopted the DCP for use in the evaluation of existing unbound pavements and shallow foundations. This paper describes the USACE's recommended procedures for using the DCP to evaluate in situ pavement materials. Regression models have presented to describe the relationship between the penetration rate or DCP index and the California Bearing Ratio (CBR), as well as a method for converting DCP results into bearing capacity values. Analysis techniques for interpreting DCP results have presented, and limitations of the device are noted. The results of the analyses show that the correlations provide a simple means of obtaining estimates of key material properties. The relationships between penetration rate and CBR appear to be valid with some scatter associated with inherent variability of natural materials. The techniques and relationships described in this paper provide a relatively reliable means of estimating in situ material properties with the DCP (USACE, 2007).

The Dynamic Cone Penetration test (DCP) was first developed by Scala in South Africa as an in-situ pavement evaluation technique for evaluating pavement layer strength (Scala, 1956). Dynamic Cone Penetrometer (DCP) has been used to measure the in-situ shear resistance of soil because a soil's shearing resistance is its ability to withstand load. But a newer form of the Dynamic Cone Penetrometer was designed by Dr. D. J. van Vuuren with a 30° cone in 1969. Afterwards, the Transvaal Roads Department in South Africa started using DCP to investigate road pavement in 1973 (Kleyn, 1975) with a 30° cone tip. Afterwards the results ,which were obtained using 30° and 60° cone tip were reported by Kleyn. Kleyn found that when a DCP measurement is plotted against a CBR obtained from the lab experiments on a log-log graph, the relationship between these two parameters are linear. Despite giving much effort to find out a way to use the DCP curves as an indicator of pavement condition, Kleyn

was unable to find any pattern that would give any indication about the pavement condition. Then in 1982, the final conclusion about the Dynamic cone Penetrometer was drawn by Kleyn after comparing sound pavement sections with failed pavement sections where he found a minimum strength or suitability for the base course. It has been extensively used in South Africa, United Kingdom, Australia, New Zealand and several States in the U.S.A. such as California, Florida, Illinois, Minnesota, Kansas, Mississippi and Texas for the characterization of the pavement layers and subgrades. The U.S. Corps of Engineers has also used DCP as an in-situ testing tool. The Dynamic Cone Penetrometer has been proven as an effective tool in measuring the strength parameter of the pavement layers and subgrade conditions.

Figure 2. 1 DCP test equipment

California Bearing Ratio (CBR) values for a soil were used as an indicator of shear strength for the pavement applications in military. CBR is measured with a standardized penetration shear test and usually performed on laboratory compacted test specimens during the design phase of the pavement. In these situations to determine the CBR value, destructive test pits were usually dug to determine pavement layer thicknesses and characterization of subgrade materials. This test was time consuming and impractical during the construction of the pavement.

The Dynamic Cone Penetration (DCP) is a simple field test method, consumes less time in practical applications, require less maintenance and a continuous profile of the pavement layers can be achieved with higher accuracy. Manually driving mechanism is avoided in the operation of DCP. The greatest advantage of DCP over other in-situ pavement testing devices is that it can locate the zone of weakness within the pavement easily.

2.2.1 Principle

The Dynamic Cone Penetrometer Test is performed by dropping a hammer of a specific weight from a certain height, which constitutes features both of SPT and CPT. The DCP test is standardized by ASTM D 6951-03. The penetration depth per blow up to a depth needed is measured thus resembling this to SPT procedures which measures blow count using the soil sampler. A 60° cone is used to create a cavity during the DCP test instead of using the split spoon soil sampler, this operation makes it similar to CPT as well. The principles on which the DCP operates on seem to reduce many of the deficiencies that occurred during manually getting into the soil.

The Dynamic Cone Penetrometer can provide continuous measurements of the pavement layers and the underlying subgrade without digging the existing pavement which is encounters during CBR test. It constitutes an upper fixed travel shaft which is 22.6 inch (575 mm) long with a 17.6 lbs (8 kg) falling weight which exerts an energy of about 78.5 N and a lower shaft of 39.4 inch (1000 mm) which contains an anvil and a replaceable cone with an apex angle of 60° and 0.8 inch (20 mm) diameter. The anvil stops the hammer from falling further than the standard falling height which ensures a constant driving force of the cone into the ground. An additional rod which is attached to the lower shaft is used as scale to measure the penetration per blow. The shaft has a smaller diameter than the cone (16 mm) to reduce the skin friction during the penetration of the cone into the soil. A schematic of the DCP is given below in Figure 2.2.

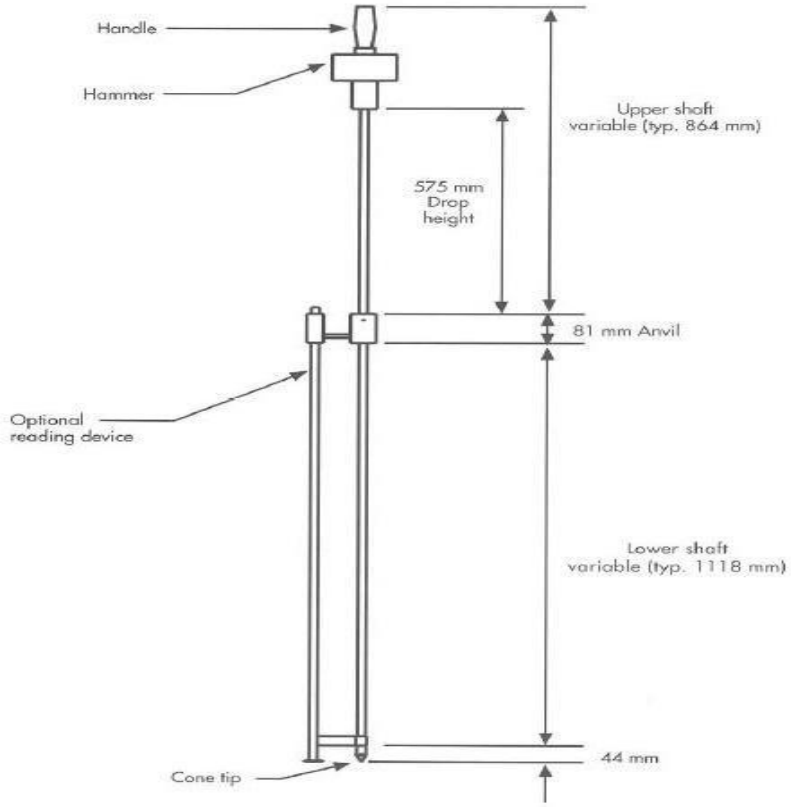

Figure 2. 2 Dynamic Cone Penetrometer Schematic (Source: MnDOT DCP Design)

Few configuration options are available for the DCP in the market for the use which include changing the mass of the falling weight, type of tip and recording method. The standard hammer mass is 17.6 lbs (8 kg) but 10.1 lbs (4.6 kg) mass is also available for a weaker soil. The smaller mass weight can be used on soils with a CBR value up to 80. The bigger between these two is usually used for the pavement application. The pavement layers are compacted and requires more energy from the falling weight for the proper penetration to occur. The tip which is attached to the lower portion of the DCP can be replaceable point or disposable cones. The replaceable point remains for a certain period of time until it becomes worn out or damaged beyond a certain limit and then it is replaced with a newer one. On the contrary, the disposable cone remains in the soil after every test. The main reason behind using disposable cones with the DCP is that it helps to remove the DCP shaft from the soil after the penetration process is performed.

Performing DCP test requires two persons where one person let the weight fall freely from a specified height and the other person records the measurement. The lower shaft can

move independently with the scale attached to it for the measurement to be recorded. The scale stays on the ground surface so that the penetration of the shaft can be measured with respect to the ground surface. The cone tip is being placed on the surface being tested at first and afterwards, the test is performed by letting the fall freely. The cone must have to penetrate a minimum of 25 mm between recorded measurements. Data which are taken at less than 25 mm penetration increments sometimes results in inaccurate strength determinations hence, to be avoided. The number of hammer blows between measurements should be between 1, 2, 3, 5, 10, 20 depending on the cone penetration rate. The initial reading recorded before any hammer blow is counted as initial penetration corresponding to blow 0. The falling of the mass is repeated until the desired depth is reached and the penetration depth for each blow is measured for each hammer drop. The penetration procedure performed with the DCP is shown in Figure 2.3 (Salgado and Yoon, 2003).

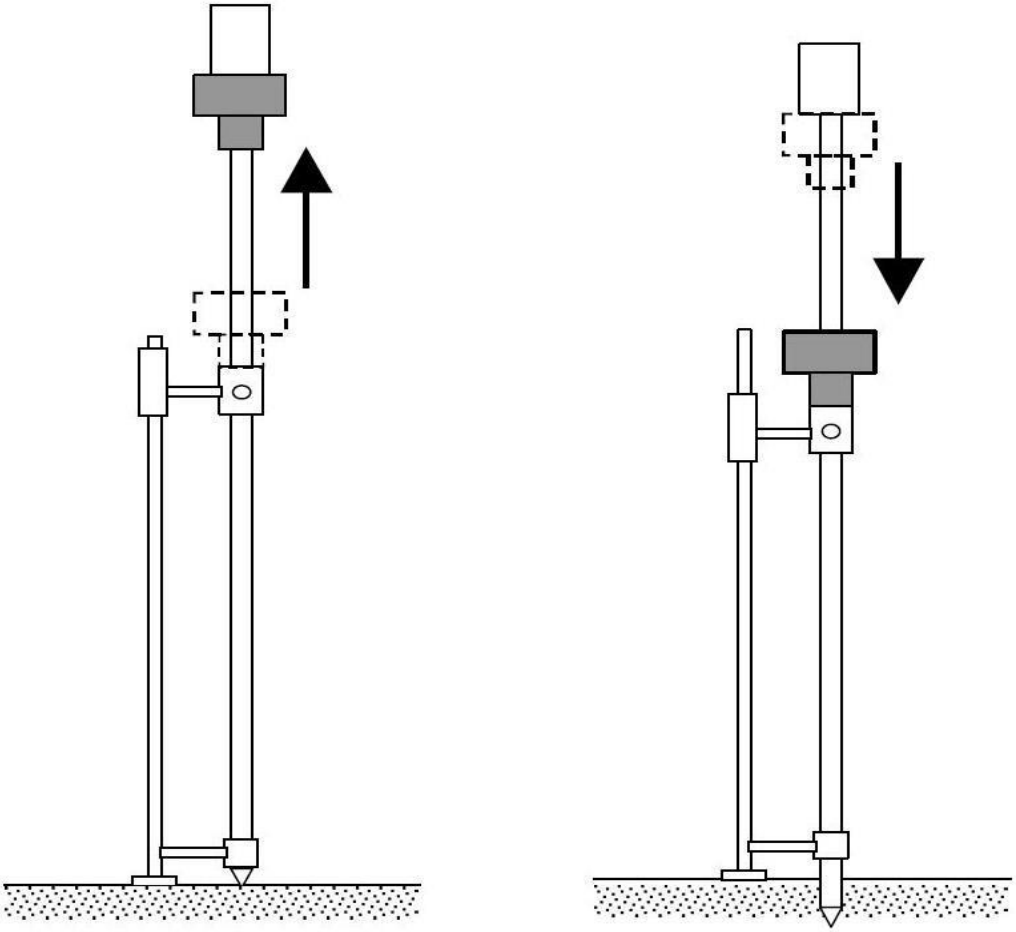

Figure 2. 3 The Dynamic Cone Penetration (DCP) Test Procedure (Salgado and Yoon, 2003)

While determining the layer thickness, the slope of the curve between number of blows and depth of penetration (mm/blow) is denoted as the DCP Penetration Index (DCPI). It can be calculated as (Embacher, 2005):

$$DCPI = {(i+1) - P(i)}\Big/{(i+1) - B(i)} \quad \text{.....Equation(2.1)}$$

Where, DCPI = Dynamic Cone Penetration Index (mm/blow)

P = Penetration at i^{th} or $(i+1)^{th}$ hammer drops(mm)

B = blow count for i^{th} or $(i+1)^{th}$ hammer drops

A typical plot of DCP test results is presented below in Figure 2.4. The slope of this graph at any point represents the value of Dynamic Cone Penetration Index (DCPI) in mm/blow which indicates the amount of resistance the material is exerting towards the cone. The lower DCPI values indicates a stiffer soil and vice versa.

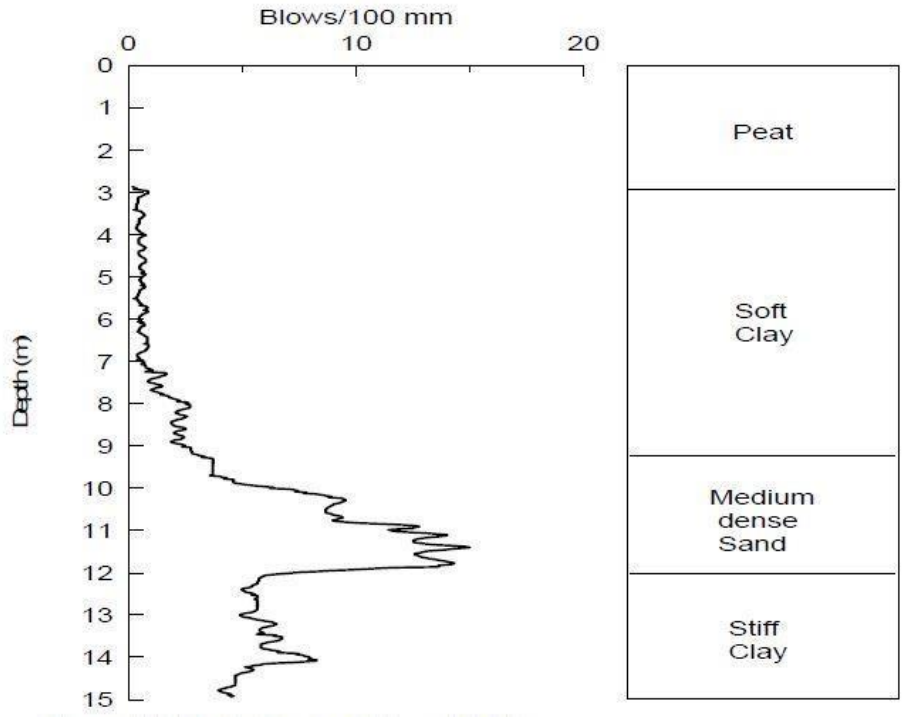

Figure 2. 4 DCPI Profile of a Flexible Pavement (Gudishala, 2004)

A standard procedure should be followed while analyzing the data recorded from DCP measurement for a representative value of penetration per blow. For a specific location, a representative DCPI value for a certain amount of depth being considered can be obtained

using any of the two methods mentioned below. The Wisconsin DOT identified DCP and rolling wheel deflectometer as an effective tool in identifying weak areas of in-situ subgrade for construction acceptance (Corvetti & Schabelski, 2001).

2.2.2 Existing correlations between DCP and California bearing ratio (CBR)

Penetration rates of the cone of Dynamic Cone Penetrometer into the base, sub-base and subgrade soil can be converted into CBR. Assessing the structural properties of a pavement layers often requires the DCP values to be converted into CBR. Different correlations were suggested between the DCPI (mm/blow) and CBR values. Based on the previously performed researches, it has been observed that the relationship between DCPI and CBR values are often one of the following forms presented below:

Log-Log Equation:

Log (CBR) = a + b (Log DCPI) …….……..…..Equation(2.2)

Where, CBR = California Bearing Ratio

DCPI = Dynamic Cone Penetration Index a = constant ranging from 1.55 to 3.93

b = constant ranging from -0.55 to -1.65

Inverse Equation:

CBR = D (DCPI) E + F ……..……..Equation(2.3)

Where, D, E, F = Regression Constants

U.S. Army Corps of Engineers developed a relation between DCPI and CBR based on a wide range of granular and cohesive materials which was adapted by many researchers

Log CBR = 2.465 – 1.12 (Log DCPI)……..Equation(2.4)

Or

$$CBR = {}^{292}/_{DCPI * 1.12}$$

This correlation can be presented by the chart presented below:

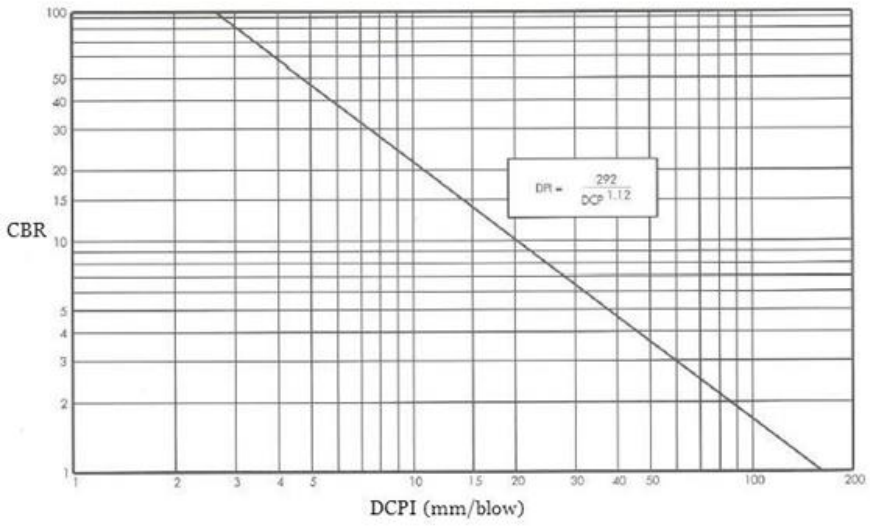

Figure 2. 5 Correlation chart between CBR vs DCPI

Based on the field CBR and the average of three measurements taken with the DCP within an area with a radius of less than 1 ft (0.3 m), the North Carolina Department of Transportation (NCDOT) (Wu, 1987) suggested the following relationship:

Log (CBR) 2.64 – 1.08 (Log DCPI)…….....Equation(2.5)

$$CBR = {}^{415}/_{PR} * 1.08 \qquad R^2 = 0.79$$

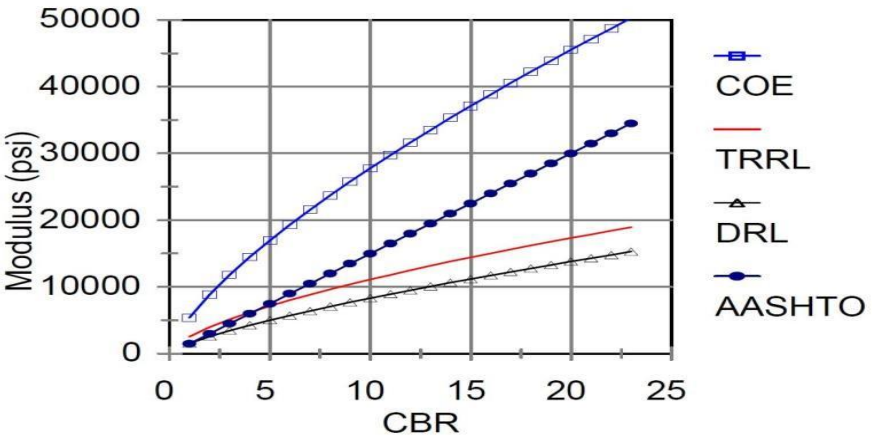

Figure 2. 6 Comparison of Different CBR-Moduli Relationships (Wu and Sargand, 2007)

The study conducted by U.S. Army Corps of Engineers was based on the CBR values obtained from the lab experiments and the CBR values obtained by NCDOT were from field. It has been observed that the CBR values obtained from field is twice than the values obtained from lab experiments. The results of these two experiments were in good agreements, Webster et al. (1994) refined this equation and suggested correlations

Suitable for different soil types.

For high plasticity clay soil (CH)

$$CBR = {}^{1}/_{(0.002871 * DCPI)} \cdots\cdots\cdots\cdots\cdots\cdots\cdots\cdots\cdots\cdots\cdots\cdots\cdots\cdots\cdots\text{Equation(2.6)}$$

For low plasticity clay soil (CL)

$$CBR = {}^{1}/_{(0.017019 * DCPI)^2} \cdots\cdots\cdots\cdots\cdots\cdots\cdots\cdots\cdots\cdots\cdots\cdots\cdots\cdots\cdots\text{Equation(2.7)}$$

After performing DCP tests on 2000 sample of pavement materials in standard molds, Kleyn recommended the following equation. He found out that the measurements taken from the DCP varied in a way as the CBR varies with the moisture content. According to him, DCP-CBR relationship was independent of moisture content.

Log CBR = 2.62 – 1.27 (log DCPI)…… …….....Equation(2.8)

Smith and Pratt suggested the following correlation based on a field study:

Log CBR = 2.56 – 1.15 (log DCPI)…….. Equation(2.9)

Observing the small difference between the two relationships above, Livneh et al. (1994) proposed the following equation as the best correlation:

Log CBR = 2.46 – 1.12 Log (DCPI)……... Equation(2.10)

Using a wide range of undisturbed and compacted fine-grained soil samples with or without saturation, Livneh and Ishia developed a correlation between DCPI and the in-situ CBR. Compacted granular soils were tested in flexible molds with variable controlled lateral pressures. The following relationship was developed by them:

Log CBR = 2.2 – 0.71 $(\text{Log DCPI})^{1.5}$…….Equation(2.11)

2.2.3 Existing correlation between DCP and elastic moduli

Structural analysis of Pavement requires moduli values and it can be derived based on the relation between moduli values and CBR. The following equation has been proposed by Huekelom and Klomp and adopted by the 1993 AASHTO Guide for Design of Pavement

Structures to calculate subgrade resilient modulus (M_R) which was derived for the fine-grained soils with a soaked CBR or 10 or less. The resilient moduli value calculated on which the correlation was developed was 750 to 3000 times higher than the CBR values.

$$M_R = 1500\ CBR\ (M_R \text{ in psi}) \text{ …… ……..Equation(2.12)}$$

Or,

$$M_R = 10.34\ CBR\ (M_R \text{ in MPa})$$

According to Chen et al., the CBR value should be computed using the equation adopted by U.S. Army Corps of Engineers and the following equation should be used to predict the resilient moduli value from the measurements taken with DCP tests. Powell et al., of the Transport and Research Laboratory (TRRL) in the United Kingdom suggested the relationship between subgrade resilient modulus and CBR which is presented below:

$$M_R = 2550\ CBR^{0.64}\ (MR \text{ in psi}) \text{ ……Equation(2.13)}$$

Or,

$$MR = 17.58\ CBR^{0.64}\ (MR \text{ in MPa})$$

The most effective properties of pavement materials are a base for solution requirement of good design. To be efficient and useful for pavement design, material characterization s should be depends on materials properties that correctly capture the material response to external stimulus of traffic load. The proposed AASHTO guide is mechanistic-empirical in nature and advocates the use of a number of mechanical properties such as the young's modulus, poisons ratio and resilient modulus of bound materials, which contain fine grain materials and local soils (Zaghloul, 1993).

D.M. Wood, (April 2004) assess the possibilities for performing real physical experiments on homogeneous soil samples (even ignoring for the moment the actual particulate nature of the soil) are limited by the ingenuity of the designers of soil testing devices; the possibilities for performing and deconstructing numerical experiments on assemblies of soil particles are much greater. Any general element of soil in a geotechnical system will experience changes in all of the six components of stress to which it subjected. Any constitutive model that is use in numerical analysis will be expect to make reasonable predictions of the soil behavior under such general stress changes. The reliability of the

constitutive model can be best to checked by pitting it against carefully conducted laboratory experiments, which expose uniform soil samples to similarly general stress or strain changes.

2.3. Mechanistic model

How pavements respond to applied loads and the environment determines how it will behave structurally. The stresses and resultant pavement response are the combined results of load, moisture conditions, and material layer characteristics. Therefore, the development of models to predict pavement behavior requires mechanistic relationships that relate loads to structural response, and empirical relationships that relate structural response to pavement damage (AI, 1982).

The mechanistic method of flexible pavement design is an emerging technology for design, which contains a number of distress models: mainly fatigue cracking and rutting. But, structural analysis of pavement systems started early century from the classical solutions of Boussinesq (1885) and Burmister (1943). But the design of pavement structure is not totally mechanistic, as dependence on observed performance is necessary because theory alone has not proved sufficient to realistic pavement design (Huang, 2004).

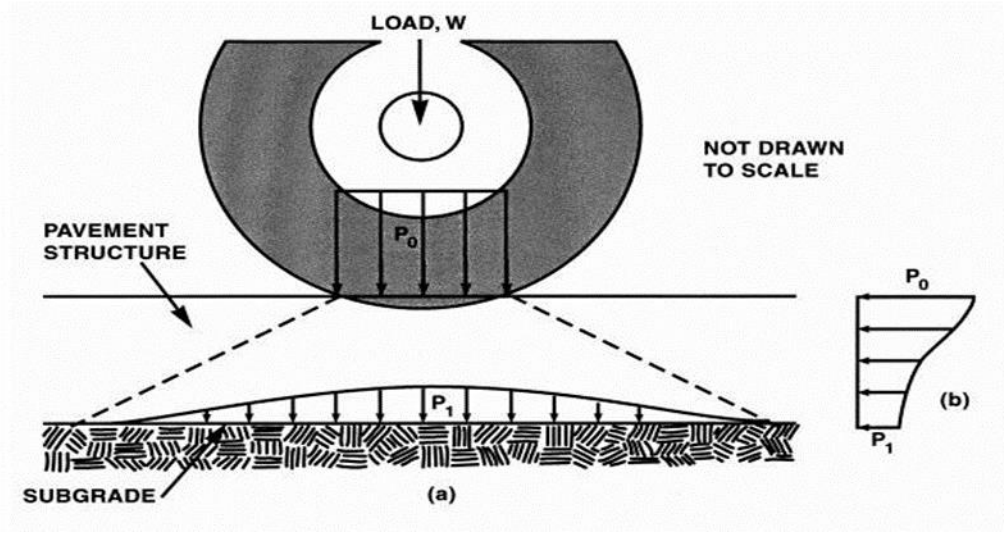

Figure 2. 7 Spread of wheel-load though pavement structure (ERA, 2002).

These critical strains are the mechanical responses of a material to loads. They can be related to the rate at which pavements deteriorate, and then calibrated against the performance of in-service or test pavements (Huang, 2004; Wardle et al, 2003). The critical tensile strain at the bottom of the asphalt layer (ε_t) is related to fatigue cracking. Fatigue cracking is

interconnected cracks in the AC layer caused by repeated load repetitions. The critical compressive strain at the top of the subgrade (ε_V) is related to rutting, which is permanent deformation in the material layers caused by repeated loads. Rutting is manifested in the pavement surface.

Wang (2001) investigated the response of flexible pavement structures with various materials, model dimensions and different loadings using three-dimensional finite element analysis. He developed an effective meshing tool for three-dimensional model incorporating multiple layers, interlayer debonding and slip, and various loadings. The effect of base material nonlinearity was studied with the stress-dependent K-θ model and the effect of spatially varying tire/pavement contact pressures on pavement surface. He concluded that spatially varying tire/pavement pressures affected the response of flexible pavement significantly.

2.3.1 Resilient Modulus

The elastic or resilient modulus is the measure of the stiffness of a material under repeated applied loads. The resilient modulus is the stress generated by an impulse load, similar to those experienced from a wheel load, divided by the recoverable strain after a loading cycle (Huang, 2004). The resilient modulus is used in structural response models to predict the pavement response to load. Poisson's ratio, which is lateral strain divided by axial strain, is also used with the resilient modulus in structural models.

The general form of the elastic or resilient modulus is shown in Equation 2.14 (after Newcomb and Birgisson, 1999).

$$E = Mr = \sigma/\varepsilon r \quad \ldots\ldots\ldots\ldots\ldots\ldots\ldots\ldots\ldots\ldots\ldots\ldots\ldots\ldots\ldots\ldots\text{Equation(2.14)}$$

Where:

$E=M_r$=elastic or resilient modulus

σ = applied stress

ε_R = recoverable strain

Figure 2.8 shows the resilient modulus as determined from a simplified load and unload stress-

strain diagram.

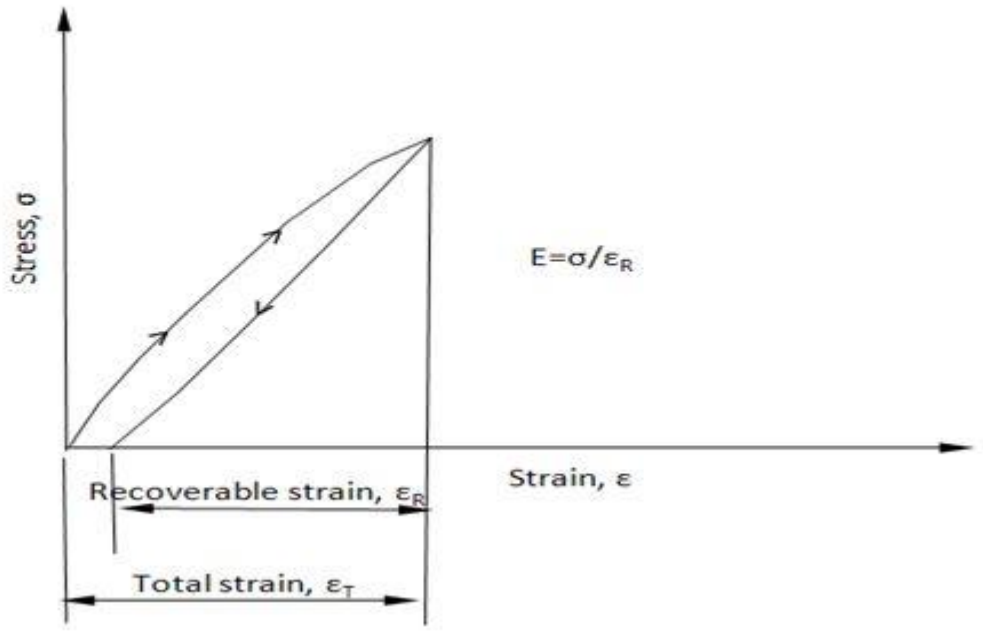

Figure 2.8: Resilient Modulus from Simplified Stress-Strain Diagram

Within the linear range of the stress-strain behavior of a material, strain is proportional to stress; this allows the prediction of the behavior of the material. This property is important when characterizing the ability of a material to return to its original shape and size immediately after deformation. The stress-strain diagram for soils and granular materials is often determined from the repeated load triaxial test. The stress-strain test for asphalt materials can be determined from the indirect tensile Protocol P07 Test Method for Determining Resilient Modulus for Asphalt Materials (FHWA, 2010). The uniaxial/triaxial tests from the simple performance test for Super pave mix design (NCHRP 9-29, 2002) may also be used to determine the resilient characteristics of asphalt concrete materials.

The resilient modulus of unbound granular aggregate and sub-grade soil materials can be non-linear and stress dependent. Brown (1997) demonstrated the non-linear elastic behavior of granular base and soils both from direct in-situ measurements of stress and strain, using field instrumentation, and through back-calculation of surface deflection bowls measured with the

falling weight deflectometer (FWD). Back-calculation is an iterative process that assigns layer modulus (stiffness) that theoretically matches computed deflections to measured deflections.

In resilient modulus tests of unbounded material, both resilient and permanent deformations occur during the initial stage of load application as indicated in Figure 2.9. However as the number of load repetitions increase, the amount of permanent deformation in each load application decreases. Finally permanent deformation does not increase significantly with each load application.

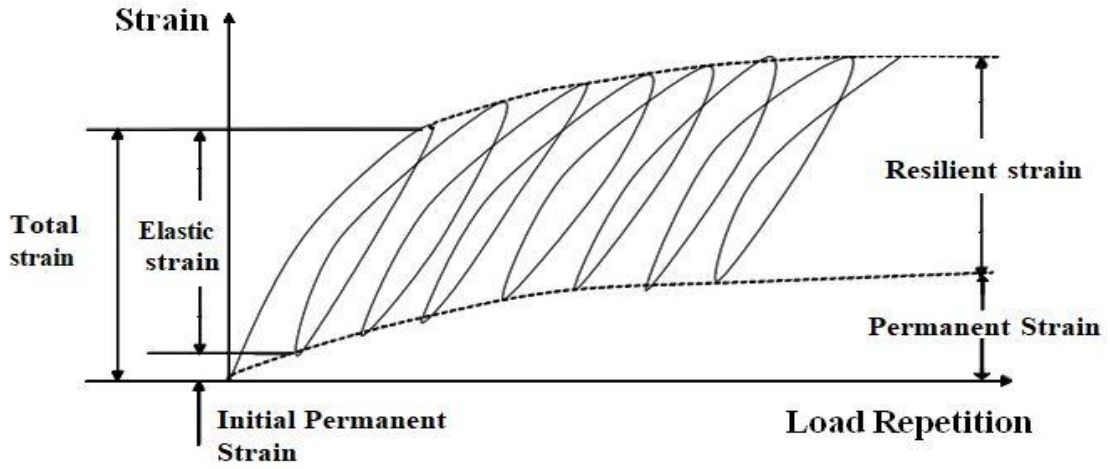

Figure 2.9 Deformation Response of a Pavement under cyclic Loading (Huang, 1993)

ERA (2013) design manual characterized resilient modulus of unbound granular base, sub-base and sub-grade soil through correlation with CBR value rather than direct measurement by falling weight deflectometer (FWD). DCP correlation with resilient modulus are described on ERA manual for determination of pavement unbounded layers thickness and strength property (resilient modulus). In this study we use resilient modulus obtained from correlation with CBR based on ERA standard manual and U.S army corps standard.

Ovik et al (2000) characterized the seasonal trends in pavement layer moduli using data from

the Minnesota Road Research Project (MnROAD) and long term pavement performance (LTPP) sites in the US. The relationships between climate factors, subsurface environmental conditions, and pavement material mechanical properties were investigated. Ovik et al related changes in layer temperature and moisture in the base and subgrade to layer modulus at the sites over five seasonal phases; frozen, spring thaw, spring recovery, summer, fall, and using the Minnesota mechanistic-empirical pavement design procedure.

Ovik et al found that pavement layer stiffness was highly responsive to changes in the average daily temperature and moisture content. The resilient modulus of a granular material typically increased with increasing density and confining pressure, and decreasing moisture content. The modulus of fine-grained soils typically decreased with increasing deviator stress, but was dependent on the soil type, moisture content and density.

2.3.2 Hierarchal Approach

The MEPDG uses various models to estimate pavement performances from material properties that are measured or predicted. Depending on the available information and the desired reliability, different levels of analysis are available in the MEPDG's hierarchal approach. The MEPDG hierarchal levels are based on design and analysis options and classified into three levels. The levels are based on accuracy, reliability, state-of-knowledge, and available data. Level 3 is the lowest level of the hierarchy. Level 3 uses predicted material properties and have the lowest degree of reliability. Level 1 is on top of the hierarchy and uses lab or field directly measured values for material properties resulting in the highest extent of reliability in the design and analysis of a pavement (Daniel and Chehab 2007). The MEPDG also uses a hierarchal approach to characterize materials. The resilient modulus at optimum moisture content is a desired property found by the MEPDG. The MEPDG hierarchy consists of three levels with different inputs based on the data available to the user. The overall objective of the three levels is to calculate or estimate the resilient modulus depending on what data has been collected.

A Level 1 input requires the use of lab or field direct testing of the resilient modulus as an input. If no resilient modulus lab or field test data are available, the MEPDG will calculate the

resilient modulus using other properties in a Level 2 approach. These properties generally are the California Bearing Ratio (CBR) and/or the Dynamic Cone Penetrometer indexes obtained through standard AASHTO or NCHRP testing methods. Finally, the Level 3 analysis will estimate the resilient modulus at optimum water content based on the material classification (Hill, Yohannes and Khazanovich, 2007). The three levels in the hierarchal approach are expounded on in the following list:

i. **Level 1** input requires the highest quality of data. The data are collected from direct testing of the actual material (e.g., nonlinear resilient modulus for unbound materials). This level represents the greatest knowledge of the input parameters for the specific job. In particular, the input data are site-specific truck volumes for individual truck types and the axle load spectra is project site specific. The desired material data for Level 1 designs are the resilient modulus values of base, sub base, subgrade, and bedrock, which are determined from direct testing. The recommended test to obtain the resilient modulus is through the repeated triaxial or cyclic triaxial test. The standard testing procedure can be followed by using the NCHRP 1-28 A method or the AASHTO T307 method (Rabab'ah and Liang, 2007).

ii. **Level 2** Inputs are obtained through empirical correlations with other parameters (e.g., resilient modulus estimated from CBR values). These correlations may be between the resilient modulus and physical properties of the material, such as dry unit weight, Atterberg limits, and specific gravity or between resilient modulus and strength properties such as the CBR, DCP, or unconfined compressive strength. Also the input data may be come from regional data, such as measured regional values that encompass the project but are not site specific. For traffic data, estimated classified truck volumes are used. Level 2 input supplies an intermediate level of accuracy that is closest to the typical procedures used with AASHTO guide. All of the traffic data, physical and strength properties material can be obtained by following standard NCHRP or AASHTO procedures(Rabab'ah and Liang, 2007).

iii. **Level 3** Inputs are selected from a database of national or regional default values according to the material type or highway class (e.g., soil classification to determine the range of resilient modulus, highway class to determine vehicle class distribution). These data are based on global or agency-wide default values, such as

the median value from a group of similar projects. Design is typically used for lower volume roads because it uses the lowest level of data accuracy. In this level, the resilient modulus for the optimum moisture content of the material is estimated based on the classification of the material. The ICM then adjusts the resilient modulus for the seasonal effects of the climate(Rabab'ah and Liang, 2007).

According to the NCHRP 1-37A report, level 1 is recommended for heavily trafficked highways where premature failure is economically undesirable. Level 2 can be used for intermediate projects, while level 3 is recommended for minor projects, usually low traffic roads. In addition, level 3 may be appropriate for pavement management programs widely implemented in highway state agencies.

MEPDG recommended to use the best available data regardless of the overall input level. That is, it is possible for Level 1 inputs to be classified truck volumes, Level 2 data to be axle configuration, and Level 3 inputs to be axle load. This is solely based on the quality of each individual piece of data and where it fits best in the hierarchal scheme (Swan, et al. 2007).

Level 2 and 3 was used throughout this study because of at present there are limitation of resource for level 1 input data to be used on a consistent basis and ERA standard uses CBR value for pavement design.

2.3.3 Finite element model

Finite element method is one of mechanistic pavement structural analysis and design method. Generally finite element solution technique is used to conducted through three basic stages of the analysis; those are Idealization of the system being investigated, formulation and solution of equations governing the phenomenon being investigated and evaluation of the structural response required for undertaking the design process (Anand B.Tapase and M.S. Ranadive, 2016). Pavement analysis has been transitioning from empirical methods to numerical approaches (Kim, 2007). Usually soils idealize as being linear elastic and isotropic materials only by using Hooke’s law to estimate the elastic strains associated with applied stresses within a soil mass (Helwany. s, 2007). Actually soils are neither linear elastic nor isotropic by its nature.

The FEM analysis discretizes the pavement and subgrade into a number of elements with the

load at each node of the element. The finite element extends horizontally and vertically from the influence of the load and assumes boundary conditions in the area of interest. The assumed boundary conditions and element geometry (size and shape) of the FEM can have a major influence on the overall performance of the model.

As per development of computer technology many finite element package soft wares are developed. Chen et al. (1995) have made a comprehensive study of various finite element pavement analysis program and showed that the results from ABAQUS were comparable to those from other programs. Al-Khateeb, et. al., (2011) developed two-dimensional finite element program using (ABAQUS) software for pavement structure to investigate the static repeated load effect on rutting of flexible pavement. They demonstrated that the rut depth increases with increasing temperature and tire pressure and decreasing subgrade strength. Abed, A. and Alazzawi, A. (2012) also Stated that the stress in leveling layer decrease by about (14%) and (27%) in the base layer and rut depth is increased by (12%) and (28%) in that layers respectively using ANSYS finite element program. Local models for rutting are applying to estimate parameters for related to pavement structure and environmental conditions.

ABAQUS analysis modules starts with a batch program, with the objective of assembling an input file which describes a problem so that ABAQUS can provide an analysis (Liang, 2000). ABAQUS input file contains Model data defines a FEM in terms of geometry, element properties, material definitions and any data that specifies the model itself (Liang, 2000; Britto, 2010; ABAQUS, 2013). Also contain history data which is define what happens to the model and the sequence of loading for which the model's response is sought, including the procedure type, control parameters for time integration or non-linear solution procedures, loading and output request (Liang, 2000; Britto, 2010; ABAQUS, 2013). Data can be defined by the user with relevant option blocks provided in the modules (ABAQUS, 2013).

Kim (2010) illustrated the significance of axisymmetric model in order to reduces computational effort from 3-D pavement structures to 2-D cases by assuming constant material properties in all horizontal planes within cylindrical coordinate systems. As such, it has been widely used in pavement modeling despite its limitation in terms of loading configuration it uses only circular single-tire loading.

Cho et al. (1996) investigated three different FE models, axisymmetric, 2-D plane strain and 3-D, to determine an appropriate model in terms of traffic loading effects on pavement responses. From linear elastic analysis, they found that axisymmetric and 3- D models yielded comparable results from typical layered elastic analyses, while the 2-D plane strain model overestimated responses.

Kim et al. (2005) investigated the effects of super-single (wide-base) tire loadings on pavements using 2-D plane strain and 3-D static or dynamic analyses. They examined the responses of pavement structure under two different sub-grade materials such as sand and clay. It was found that distresses from 2-D analysis were higher than those from 3-D analyses, and that the permanent strain induced by super-single tires was about four times greater than that of conventional tires.

Kim (2010) compare computational accuracy of axisymmetric, 2-D plane strain and 3-D finite element analysis. The result of comparison indicated that, axisymmetric analysis was limited to account for realistic tire-axle configurations, but it could be provided considerable savings in computational efforts. Furthermore, with the proper application of superposition, axisymmetric simulation results are quite equivalent to 3-D simulations. The 2-D plane strain modeling was very computationally efficient, but it generally produces overestimated responses that need calibrations for better accuracy. The 3-D simulation was the most accurate and versatile in applying any complex loading-axle-tire configurations, whereas it it was computationally intensive. Therefore, due to considering modeling efficiency and accuracy together, the axisymmetric modeling approach incorporated with the infinite elements and the superposition principle seems to perform best for pavement response analysis.

The advantage of the FEM is improved structural response predictions and representation of field conditions. The disadvantage is greater computational effort and more detailed material parameters and field condition inputs into the model.

2.3.4 Layer elastic model

The layered elastic approach works with simple closed-form mathematical models that assume that each pavement layer is homogenous, isotropic, and linear elastic. That is the layer materials are the same in all directions and will rebound to their original form once the

load is removed. The layers are assumed to extend infinitely in the horizontal direction (a limitation since fatigue failure frequently starts or is more predominant in the wheel path near the edge), the subgrade extends infinitely in the downward direction, and the materials are not stressed beyond their elastic range. The surface load is represented by a uniformly distributed stress, superimposed for multiple loads over a circular contact area (Huang, 2004).

The NCHRP 1-37A procedure utilizes three models to predict pavement structural responses (stresses, strains, and displacements). Multi-Layer Elastic Theory (MLET) and the Finite Element Model (FEM) are used to compute responses due to traffic loading and the Enhanced Integrated Climate Model (EICM) is used to predict temperature and moisture histories throughout the pavement structure. When non-linear behavior of unbound materials is desired–i.e., for level 1 inputs the FEM is chosen; otherwise the load-related analysis is done with MLET.

In the NCHRP 1-37A procedure, the MLET is implemented in a modified version of the JULEA algorithm (NCHRP, 2004). Using the principle of superposition, single wheels can be combined spatially into multi-wheel axles to simulate different axle configurations.

The small set of input parameters required by MLET facilitates its implementation and use. The only inputs required are the layer thicknesses, the elastic properties (Young's modulus of elasticity and Poisson's ratio) for each layer, the tire pressure, and the tire contact area. The main disadvantage of MLET is its inability to consider nonlinearities often exhibited by pavement materials.

LEDFAA, (Federal Aviation Administration, 1993) was developed by the Federal Aviation Administration (FAA). This was a computer program for performing thickness design of airport pavements. It implemented an advanced design procedure based on elastic layered theory. At the same time, elastic layered design better predicted the wheel load interactions for the aircraft because the landing gear configurations and layered pavement structures could be modeled directly using the elastic layered design procedure. WES Modulus procedure (Barker and Gonzales, 1991) included with sub-layering performed automatically calculated the modulus value of aggregate layers. The modulus values of the sub-layers decreased with increasing depth of a sub-layer within the aggregate layer and were also dependent on the

modulus of the subgrade/sub base layer below the aggregate layer. Sometimes, unusually high moduli were predicted on the top of base layer due to doubling of the modulus in the sub-layers from subgrade to the top of the base layer (Tutumluer and Thompson,1997).

MLET requires the layer thickness and modulus to adequately characterize the pavement structure and its response to loading. The advantage of the layered elastic system is the short computation time due to the simplified assumptions. The disadvantage is the reduced accuracy depending on the assumptions of the structural response predictions when compared to actual field conditions.

2.4. Causes and empirical Prediction of pavement damage

Yoder and Witczak (1975) define two types of pavement distress, or failure. The first is a structural failure, in which a collapse of the entire structure or a breakdown of one or more of the pavement components renders the pavement incapable of sustaining the loads imposed on its surface. The second type of failure is a functional failure; it occurs when the pavement, due to its roughness, is unable to carry out its intended function without causing discomfort to drivers or passengers or imposing high stresses on vehicles. The cause of these failure conditions may be due to inadequate maintenance, excessive loads, climatic and environmental conditions, poor drainage leading to poor subgrade conditions, and disintegration of the component materials. Excessive loads, excessive repetition of loads and high tire pressures can cause either structural or functional failures. In this research we concerned on structural failure related with fatigue and rutting failure.

Yoder and Witczak describe the possibility of Pavement failures that may occur due to the intrusion of subgrade soils into the granular base, which results in inadequate drainage and reduced stability. Distress may also occur due to excessive loads that cause a shear failure in the subgrade, base course, or the surface. Other causes of failures are surface fatigue and excessive settlement, especially differential of the subgrade. Volume change of subgrade soils due to wetting and drying, freezing and thawing, or improper drainage may also cause pavement distress. Inadequate drainage of water from the base and subgrade is a major cause of pavement problems (Cedergren, 1987). If the subgrade is saturated, excess pore pressures will develop under traffic loads, resulting in subsequent softening of the subgrade. Under dynamic loading, fines can be literally pumped up into the sub-base and/or base.

Improper construction practices may also cause pavement distress. Wetting of the subgrade during construction may permit water accumulation and subsequent softening of the subgrade in the rutted areas after construction was completed. Use of dirty aggregates or contamination of the base aggregates during construction may produce inadequate drainage, instability, and frost susceptibility. Reduction in design thickness during construction due to insufficient subgrade preparation may result in undulating subgrade surfaces, failure to place proper layer thicknesses, and unanticipated loss of base materials due to subgrade intrusion. Yoder and Witczak (1975) state that a major cause of pavement deterioration is inadequate observation and field control by qualified engineers and technicians during construction.

Performance prediction incorporated into the 2002 mechanistic – empirical design guide, developed in USA under the National Cooperative Highway Research Program (NCHRP) 1-37A, are typical examples. The pavement performance measures considered in the guide include permanent deformation (rutting), fatigue cracking (bottom-up), thermal cracking and smoothness. Pavement response was calculated by using either the elastic multilayer theory or the finite element method.

The strains that formed due to cracking and rutting have been considered more critical for the structural design of flexible pavements. The first strain is the horizontal tensile strain (εt) at lower of the asphaltic layer, which led to fatigue cracking, and the second strain is normal compressive strain (εc) at the upper of subgrade layer, which led to the permanent deformation or rutting (Asphalt Institute , 1981). These models could be used to forecast the design life of new flexible pavement with assuming pavement pattern and if the reliability for a certain distress is less than the minimum level necessary, the assumed pavement pattern should be changed *(*Huang, *2004).*

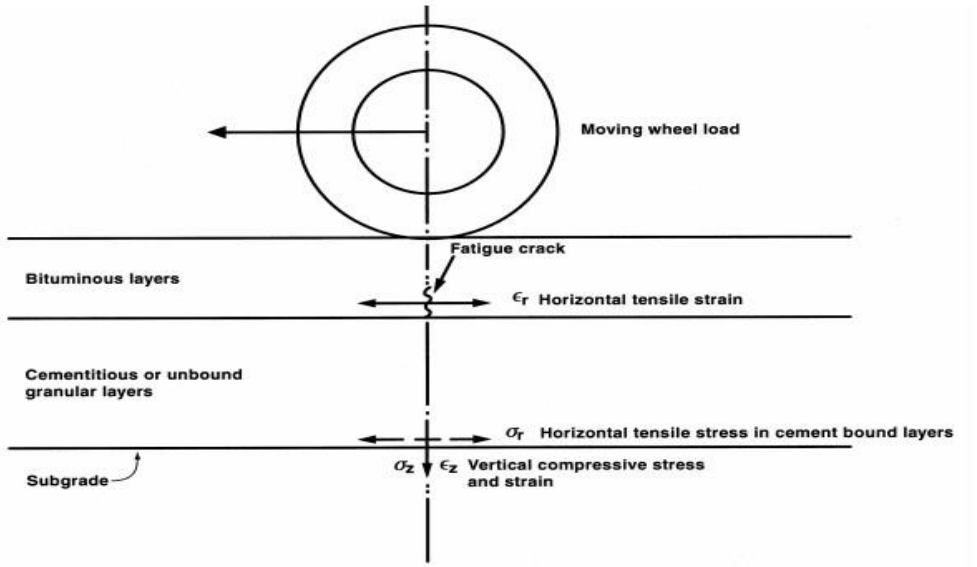

Figure 2. 10 Critical stress and strain in a flexible pavement (ERA, 2002)

2.4.1 Fatigue Cracking Models

Miner's cumulative damage theory has been widely used to forecast fatigue cracking (Miner, 1945). It is commonly approving that the allowable number of load repetitions is relating to the tensile strain at the bottom of the asphalt layer. The amount of damage is express as a damage ratio, which is the relation between predicted and allowable number of load repetitions. The damage occurs when the total of damage ratio reaches to one.

The main difference in the various design methods is the transfer formulas that transmit the HMA tensile strains to the allowable amount of load repetitions. The allowable amount of load repetitions (N_f) could be calculated by using Equation 2.14.

$$Nf = f_1 (\varepsilon_t)^{-f_2} (E)^{-f_3} \quad \text{.....Equation(2.15)}$$

where

ε_t is tensile strain at the bottom of HMA,

E is modulus of elasticity of HMA and

f_1, f_2 *and* f_3 are constants calculated by calibration.

Figure 2.11 illustrates the AI fatigue damage model. The graph (log-log scale) shows the horizontal tensile strains at the bottom of the AC layer versus the number of axle load repetitions to fatigue failure. Typical AC modulus of 500,000psi (3,500MPa) from AASHTO (1993) and a lower AC modulus of 200,000psi (1,350MPa) were used to show the

variation of AC modulus on the fatigue model.

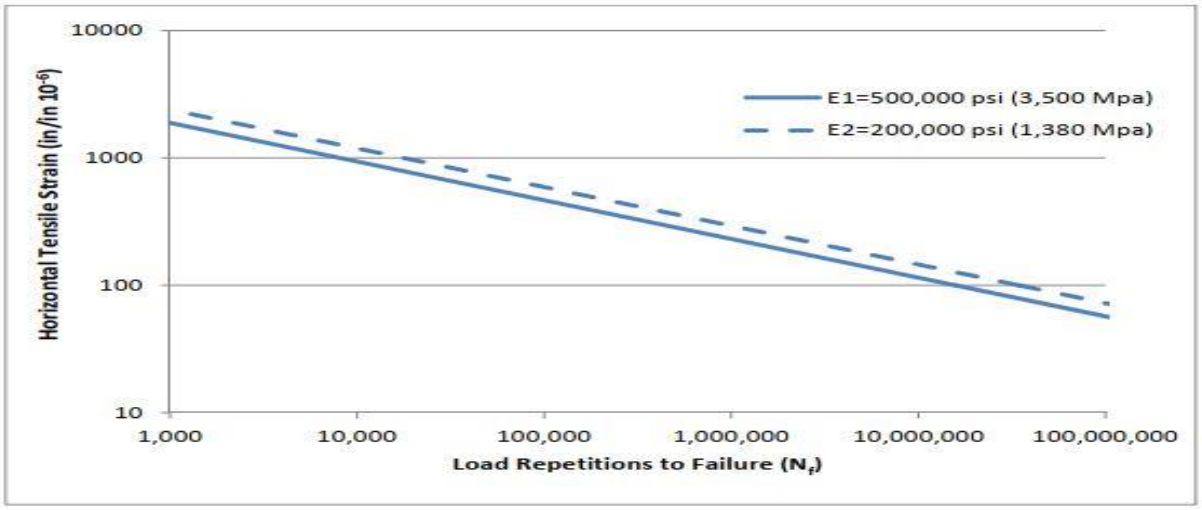

Figure 2.11: Illustration of AI Fatigue Damage Model

The AI fatigue model in Figure 2.9 shows that as horizontal tensile strains increase at the bottom of the AC layer, the number of load repetitions required to cause fatigue failure decreases. For the same horizontal strain, the number of repetitions to fatigue failure decreases with increase in the AC modulus.

Monismith et al (1969) has shown that for extremely low strains, the slope of the repetitions to failure line flattens out, resulting in near infinite loads to failure. Monismith et al(year) suggested that the relationship between strain at the bottom of the AC layer and repetitions to fatigue failure seems to undergo a significant slope change lower than approximately 70 micro strains. Below this strain level, the asphalt layer can undergo infinite repetitions without fatigue failure.

Carpenter et al (2003) also hypothesized that at low strains around 70 micro strains, asphalt mixtures have infinite fatigue. Carpenter et al suggested that a continuous physical-chemical healing reaction in the AC is occurring at low strain levels. Since research into the fatigue of asphalt mixtures has been limited to strain levels well above the hypothesized value of 70 micro strains, work is currently underway by the National Cooperative Highway Research Program, NCHRP 9-38, to identify the endurance limit of AC mixtures in flexible pavements (NCHRP, 2010).

2.4.2 Rutting

Asphalt institute (A1, 1982) develop two approaches for mechanistic modeling of rutting. The first approach, typically referred to as the sub grade strain model approach, assumes that most of the rutting is due to permanent deformation within the subgrade layer, and that the deformation within the AC and base/sub base layers is negligible, as the quality of these layers is controlled through mix design and construction specifications. This model included not only asphalt institute but also included on: Shell, Minnesota, Belgian Road Research Center, Chevron, U.S. Army Corps of Engineers, and U.K. Transport & Road Research Laboratory. The second approach considers permanent deformation within each layer of the pavement. Although several techniques have been proposed for the second approach, it has not been widely used because of the difficulty in obtaining elastoplastic or visco-plastic characterizations for the various paving materials.

Rutting models are used to estimate the normal compressive strain on the top of the subgrade and are extensively used. The allowable amount of load repetitions (Nd) is related to the normal compressive strain (ε_c) on top of the subgrade by Equation 2.15:

$N_d = f_4 \ (\varepsilon_c)^{-f_5}$……..Equation(2.16)

where

f_4 *and* f_5 are calibrated values using forecast performance and field inspection.

Figure 2.12 illustrates the AI rutting damage model. The graph (log-log scale) shows the vertical compressive strains at the top of the subgrade versus the number of axle load repetitions to rutting failure.

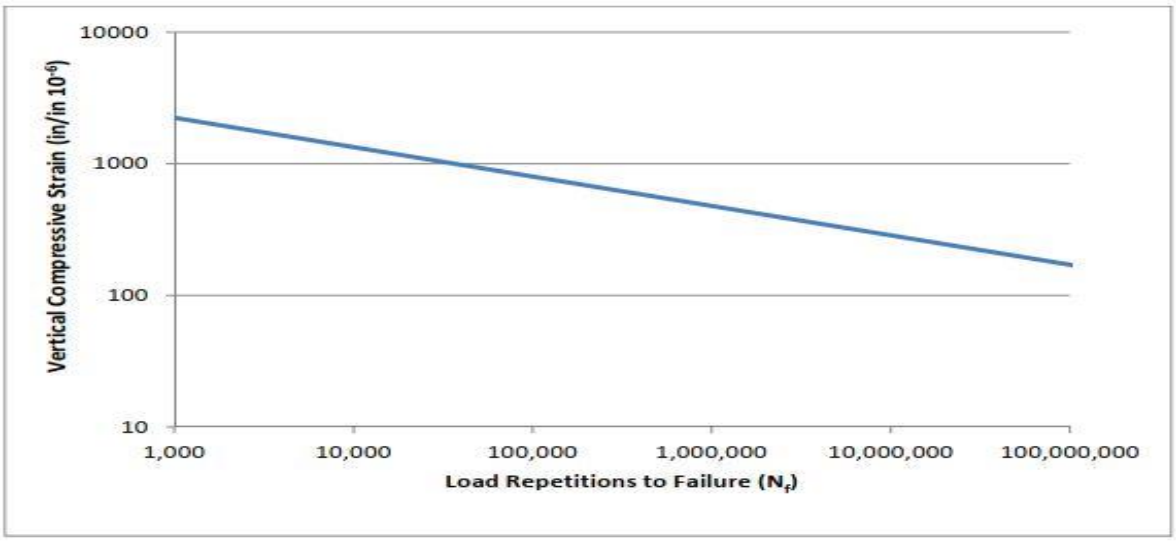

Figure 2.12: Illustration of AI Rutting Damage Model

The AI rutting model in Figure 2.10 shows that as the compressive strains at the top of the subgrade increases, the numbers of load repetitions required to cause failure decreases. Because subgrade moduli are relatively low compare to base or AC modulus, the AI rutting model is not sensitive to modulus.

The permanent deformations of structural layers and subgrade in low volume roads and heavily loaded fields have a significant influence on a pavements deterioration and service life. Rutting is defined as "permanent deformation in the wheel path" by Mamlouk (2006) or "depressions of the wheel paths as a result of traffic load" by Doré and Zubeck (2009). Pavement rutting is not desirable. It can become a safety hazard as lateral manoeuvrability of vehicles is often reduced, the risk of skidding on ponding water and ice increases, fuel consumption of pavement users increases, and the structural capacity of the pavement structure decreases as water concentrates on the surface and soaks into the pavement structure. Furthermore, the asphalt layers crack can when unbound layers rut underneath them, and the rutting is seldom uniform, causing unevenness of the pavement surface (Doré & Zubeck, 2009; Dawson & Kolisoja, 2004).

In the subgrade strain technique, it is assume that if the subgrade compressive strain is restricted, logical surface rut depths will not be exceeded. Unless standard depth and materials are used for design, the assessment of surface rutting that based on the subgrade

strain does not appear to be logical (Gedafa, *2006)*.

Different institutions have provided different distress models. The coefficients for rutting and cracking used by some of the institutions are given in Table 2.1.

Table 2. 1 Coefficient in rutting and cracking distress models

S.No	**Distress models**	f_1	f_2	f_3	f_4	f_5	**Sources**
1	AI Model	0.0796	3.291	0.854	$1.365*10^{-9}$	4.477	AI (1981)
2	Shell Model	0.0685	5.671	2.363	$1.05*10^{-7}$	4.0	Shell (1978)
3	Belgian RRC	$4.92*10^{-14}$	4.76	0	$3.05*10^{-9}$	4.35	Verstraeten et al. (1984)
4	Indian Model	$2.2*10^{-4}$	3.89	0.854	.4166E-05	4.534	IRC-37:2001 (2001)

CHAPTER THREE

MATERIALS AND METHOD

The research study area covers asphalt concrete road from Jimma to Bonga for evaluation of in situ pavement layers thickness and structural strength. In order to investigate pavement layer thickness and structural strength of pavement, dynamic cone penetration test (DCP) and mechanistic analysis are utilized. AI (Asphalt institute) method was used to determine pavement future structural performance under certain traffic load.

3.1. Study area

Jimma to Bonga concrete asphalt road branch is found in south western Ethiopia at 7°39’ 52’’ altitude and 36°50’10’’ longitude. It is first branch of Jimma–Mizan pavement road segment cover around 107 Km long.

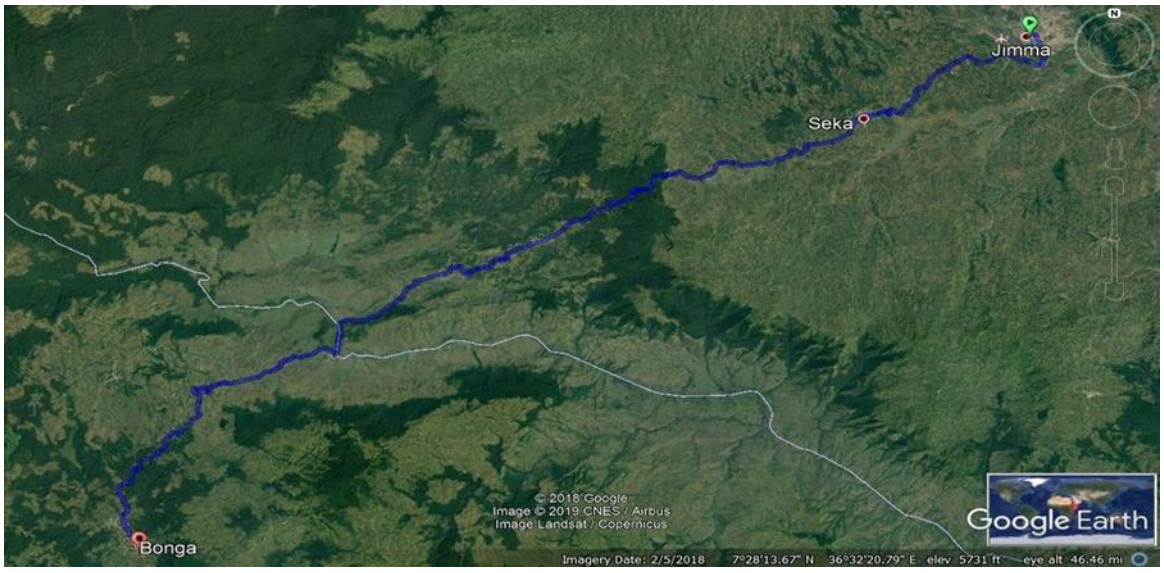

Figure3.1 Jimma –Bonga road alignment (Google map, 2012)

3.2. Climate condition of the area

Rainfall in the Project area is generally high with an average of 1600 mm, rising to 1784 mm at Bonga. There is considerable variation in annual rainfall figures, see Table below, and this variation is reflected in land use and agricultural production along the route.

Table 3. 1 Rainfall figures along the route

Village/town	Mean average annual rainfall (mm)
Jima	1,496
Gojeb	1,523
Bonga	1,784

Source: Omo-Gibe River Basin Development Master Plan, 1995; Draft EIA Report 2001

Approximately 60 to 65 per cent of annual rainfall falls during the wet season, between June and September. November to January are the driest months with average rainfall less than 100 mm. Mean annual temperatures range between 15 and 20^{o} C and are influenced by rainfall figures, with minimum temperatures being experienced in July and August (Draft EIA Report, 2001).

3.3. Geology of the Area

The geology of the area has characterized by the presence of Mesozoic rocks and the dominant group of soil is clayey red soils whose characteristics clay mineral is kaolinite. This clay mineral is derived from the weathering of the primary minerals found in Igneous rocks of the area. Such types of soil are found in high rainfall area. The soils are described as predominantly Dystric nitosols, brown to dark reddish brown clay (ERA report, 2008).

3.4. Construction History of Pavement

Jimma-Bonga flexible pavement road construct by dividing into three sections shown in the following table. Based on construction history in situ evaluation of pavement are carried out with DCP for all sections in order to determine pavement property and thickness properly along road cross section excluding asphalt layer because asphalt layer removed or cored during DCP test carried out.

Table3. 2 Jimma-Bonga flexible pavement road sections

Road Section No.	Length(km)
Section One	0.00-50.00km
Section Two	50.00-60.00km
	83.00-107.00km
Section Three	60.00-83.00km

From (ERA report, 2008) document

3.5. Sampling Procedures

The definition of targeting parameters has been in line with the objectives of performance perdition of flexible pavement along Jimma-Bonga asphalt concrete road . A sampling frame would be from the In situ DCP test result. DCP portable device which follows the procedures of ASTM D 6951in situ samples from each of three sections road segment,(specify the sections) were collected from September 27-29 (2019) at adjacent sides of the road from defect side of the road section. Figure 3.3 shows that sample collection and some of defect of road section.

Figure 3. 2 in situ Sample Collection procedures

3.6. Sampling Technique

The purposive collection technique was used by selecting particular section and parameters to have certain characteristics as applied in this research program. Inspected samples were selected based on US army corps standard manual of flexible pavement. It was forwarded to be normally targets at particular pavement layers structural property and mechanistic response.

3.7. Data processing and analysis

data from site investigation and laboratory testing, had arranged properly, the data analysis were conducted using (PCASE) software package, Microsoft excel and other tools. Then all the factors affecting flexible pavement road, are interpreted according to their magnitude of their effect on the road pavement. The results from the study, were analyzed and interpreted according to the standard specifications of AASHTO, ERA and AI. the findings of the results expressed using charts, graphs, figures and tabular formats by using excel and other pavement software.

3.8. Strength (CBR) and thickness of Pavement layers

DCP results from three selected sections is express in terms of correlation between penetration indexes to CBR value. The relationship was develop for the DCP penetration rate in mm per blow using the USACE standard DCP with the 17.6-lb hammer based upon numerous field tests including side-by-side in situ CBR and DCP measurements using equation (2.4).

Once the DCP test has been completed, the blows and corresponding penetration measurements can be used to compute the CBR using (PCASE) software package. By incorporating the number of blows and corresponding penetration.

Pavement layers thickness of the pavement is determined from significant different of material layers within a DCP profile plot. selected study sections of road layers has delineated by sudden increases or decreases in CBR strength with in CBR graph. For flexible pavement applications, a maximum of 4 individual material layers over the 39-in depth is identified from DCP test result. Webster et al.(1994) developed general guidance for determining layers as a function of changing CBR strengths. They recommend that a layer been delineated when there is a decrease, or an increase, in CBR strength in excess of 25 percent over a 4-in. interval. ERDC has developed a DCP analysis tool embedded in its Pavement Computer Aided Structural Analysis (PCASE) software package which is auto-layering with CBR

values of different pavement layers including Asphalt concrete layer thickness without considering CBR value of asphalt.

3.9. Elastic Modulus of Pavement layers

The flexible pavement road of Jimma – Bonga divide into three sections. Each of three section contains four layers component which are surface layer, base layers, sub-base layer and subgrade layer. It is difficult to get elastic modulus of each layers of flexible pavement directly. But. most of the time elastic modulus of pavement layers could be determine by California bearing ratio obtain from Dynamic cone penetration (DCP) test result. Direct comparative measurements between DCP penetration rate and dynamic modulus were not conducted. But, Powell et al provide a means of estimating dynamic modulus from the DCP-correlated CBR values of equation (2.13).

Hence: Elastic modulus of asphalt concrete is taken typical value from AASHTO and ERA standard manual. It is not conduct by dynamic cone penetration (DCP) test.

3.10. Poisons Ratio

For Poisson's ratio, the common practice is to use typical value based on the type of material from AASHTO and ERA standard specification value.

$$V = \frac{\Sigma D}{\Sigma L} \quad \text{Equation(3.1)}$$

Where

$$\Sigma D = \frac{\Delta D}{D} = is\ strain\ along\ diametrical\ (horizontal) axis.$$

$$\Sigma L = \frac{\Delta L}{L} = is\ strain\ along\ longitudinal\ (vertical) axis.$$

3.11. Assumptions of Mechanistic Pavement Response Analysis

Mechanistic pavement response analysis is performed based on multi-layer elastic theory which is developed by Burmister (1945) based on three dimensional continuum, elastic layered theory gives stress, strain and displacement in multilayer systems upon making the following basic assumptions such as:

1. All layers are weightless and infinite in horizontal directions.
2. All layers are homogeneous, isotropic and linearly elastic.
3. All layers have a finite thickness except the bottom layer, which is infinite.

4. Between any two layers, perfect bonding exists.
5. The upper layer subjected to a single uniformly distributed circular load.
6. At infinite depth, all stress and displacement are zero.

3.12. Traffic load

Load configuration has an effect on the stress distribution and deflection within a pavement. Many trucks have dual wheels which guarantee that the contact pressure is within the limits. In this study for simplification of the analysis, the dual wheels are converted into an equivalent 80 kN single axle load (ESAL). The contact area also is important to be determined so the axle load can be assumed to been uniformly distributed. In this study, only wheels on one side (the outer wheel path) need to been considered and each tire is assumed to have circular contact area. The tire spacing assumed with a typical distance between dual tires of 35 cm and tire radius of the contact area for commercial vehicles is 10.75 cm. Kim.M (2007) consider applied as a uniform pressure of 0.55-MPa over a circular area of 152.4-mm radius. The linear elastic solution then obtained using ABAQUS^{TM} finite element program. Since the load is analyzed using 80 kN single axle load (ESAL), then the tire pressure is calculated using Equation

$$P = \frac{F}{A} \quad \frac{F}{\pi r^2} \quad \frac{40kN}{2*\pi*0.1075^2} = 550.88 \text{ kN} \quad \ldots\ldots\ldots\ldots\ldots \text{Equation (3.2)}$$

Take 550 kN for mechanistic response analysis of pavement

The initial traffic loads used for the analysis in this study are based on the traffic data of ERA document N = 1.93 x 10^6 number of axle expected in design life of pavement.

3.13. Mechanistic Pavement response analysis

The MEPDG structural response model uses the multi-layer linear elastic program JULEA to calculate structural responses (stresses, strains, and deflections) based on axle loads, and material properties and environment conditions.(Schwartz and Carvalho, 2007). In addition, 2D ABAQUS is the most widely used to solve engineering problems based upon the finite element method applicable to linear solutions (Hibbit et al, 2005).

Pavement structural responses have to be relating to pavement failure through damage models. Damage models are mechanistic-empirical (M-E) equations that predict repetitions to pavement

failure based on critical structural responses to loads. The primary failure criteria considered in most mechanistic-empirical damage models are fatigue cracking and rutting

3.14. Performance Prediction of Flexible Pavement

The AI fatigue and rutting damage models were based on mechanistic-empirical and multi-layer theory in conjunction with empirical failure criteria. The AI damage models include equations to predict load repetitions to fatigue cracking and to rutting failures. The models were calibrated with data from the AASHO Road Test and a number of British test roads, and subsequently compared with the design procedures from the US. Army Corps of Engineers and several state agencies [Huang, 2004].

3.14.1. AI Fatigue Distress

The AI fatigue damage model is a global mechanistic-empirical equation between the critical tensile strain at the bottom of the asphalt layer (due to bending) and load repetitions to fatigue failure. The relationship is based on bottom-up fatigue cracking which initiates at the bottom of the AC layer due to repeated loads, and propagates to the surface. The AI fatigue failure criterion is fatigue cracking in the wheel path area, greater than 10% [AI, 1982].

The AI bottom-up fatigue cracking model is shown in Equation 3.2 [AI, 1982].

Fatigue Cracking:

$$N_f = 0.0769\ \varepsilon_t^{-3.291} E^{-0.854} \quad \text{…Equation (3.2)}$$

Where:

N_f = the predicted number of load repetitions to fatigue failure

ε_t = load-induced horizontal tensile strain at the bottom of asphalt layer

E_1 = stiffness or moduli of asphalt layer (psi), with typical asphalt properties for the AC layer of 10% asphalt by volume and 4% air voids

3.14.2. AI Rutting Distress

The AI rutting damage model is a global mechanistic-empirical equation between the vertical compressive stain at the top of the subgrade and load repetitions to rutting failure. The AI relationships develop based on permanent deformation of subgrade. By limiting the strains on the subgrade, the strains in other layers in the pavement structure will also be limited, and the

magnitude of permanent deformation on the pavement surface will be limited [Huang, 2004]. The failure criterion for rutting is rut depths greater than 12.5 mm (0.5 in) in the pavement surface [AI, 1982].

The AI rutting model is shown in Equation 3.3 [A1, 1982].

Rutting:

$$N_f = 1.36 \times 10^{-9} \ \varepsilon_v{}^{-4.477} \quad \text{..... Equation(3.3)}$$

Where:

N_f = the predicted number of load repetitions to rutting failure

ε_v = load-induced vertical compressive strain at top of subgrade

CHAPTR FOUR
RESULT AND DISCUSSION

4.1. Pavement evaluation Result

Material strength and thickness are important parameters for pavement performance evaluation with DCP. Strength parameters can be effectively estimating through the manipulation of the empirical relationships between DCP penetration indexes. The thickness and strength of Asphalt, Base, Sub-base and Sub-grade pavement layers for section one are shown in Figure 4.1 and Table 4.1. The result shows that, the thickness of asphalt (50mm), base course (200 mm), sub-base course (200 mm) and infinite depth of sub-grade soils

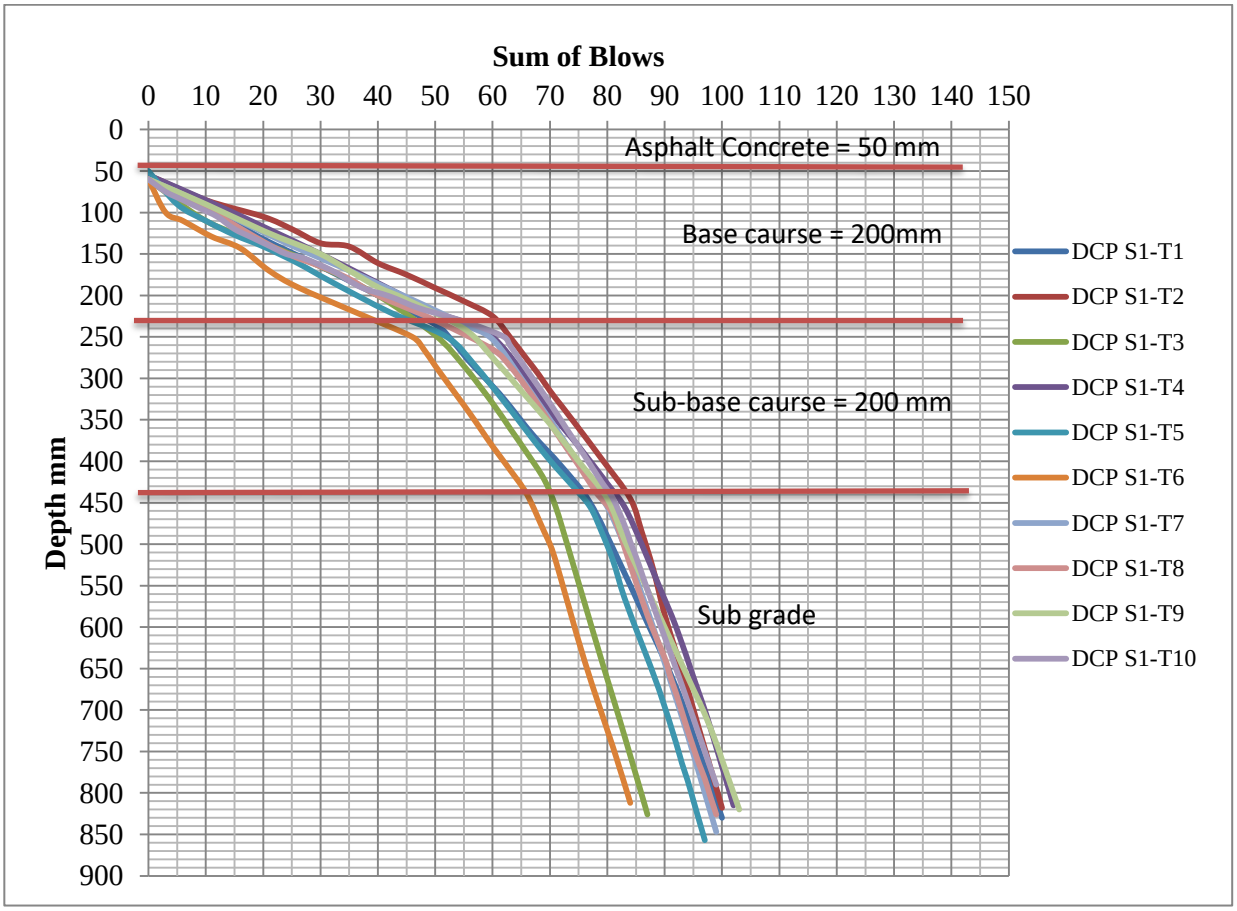

Figure 4. 1 Section one average thickness of Asphalt, Base, Sub-base and Sub-grade pavement layers

S_1-T_i (section one test number i^{th}(1-10))

Table 4.1 shows the pavement layers strength and thickness property as analyzed from **PCASE DCP**. Section one average thickness and CBR value shows that the thickness of asphalt layer

is 2.0 in (50 mm), base course layer average (CBR 71% and thickness 8.0 in or 200 mm), sub-base course average (CBR 25% and thickness 8.0 in 0r 200 mm) and sub-grade average CBR 10%.

Table 4. 1 Section one PCASE DCP analysis result

No. Test	Chainage (Km + m)		Asphalt	Base	Sub base	Sub grade
T1	01+050	Thickness(in)	2	8.14	8	
		CBR%		65.7	26.8	12.5
T2	03+200	Thickness(in)	2.17	7.83	8	
		CBR%		77.5	31.9	8.5
T3	12+500	Thickness(in)	2.01	8.14	8	
		CBR%		67.1	30.9	9
T4	17+800	Thickness(in)	2.17	7.83	8	
		CBR%		77	25.1	10.8
T5	29+100	Thickness(in)	1.97	8.03	8.05	
		CBR%		64.3	27.4	10.1
T6	31+000	Thickness(in)	2	8	8.03	
		CBR%		58.5	34.7	9.7
T7	35+700	Thickness(in)	2.14	8	8	
		CBR%		80.6	36.3	9.3
T8	42+050	Thickness(in)	2	7.85	7.92	
		CBR%		73.5	35.6	10.2
T9	43+300	Thickness(in)	2	8.14	7.93	
		CBR%		71.7	25.1	12.9
T10	47+000	Thickness(in)	2	8	8	
		CBR%		74.6	31.4	10.6

Similarly, thickness and strength of Asphalt, Base, Sub-base and Sub-grade pavement layers for section two are indicates in Figure 4.2 and Table 4.2. The result shows that, the thickness of asphalt (50mm), base course (200 mm), sub-base course (175 mm) and infinite depth of sub-grade soils.

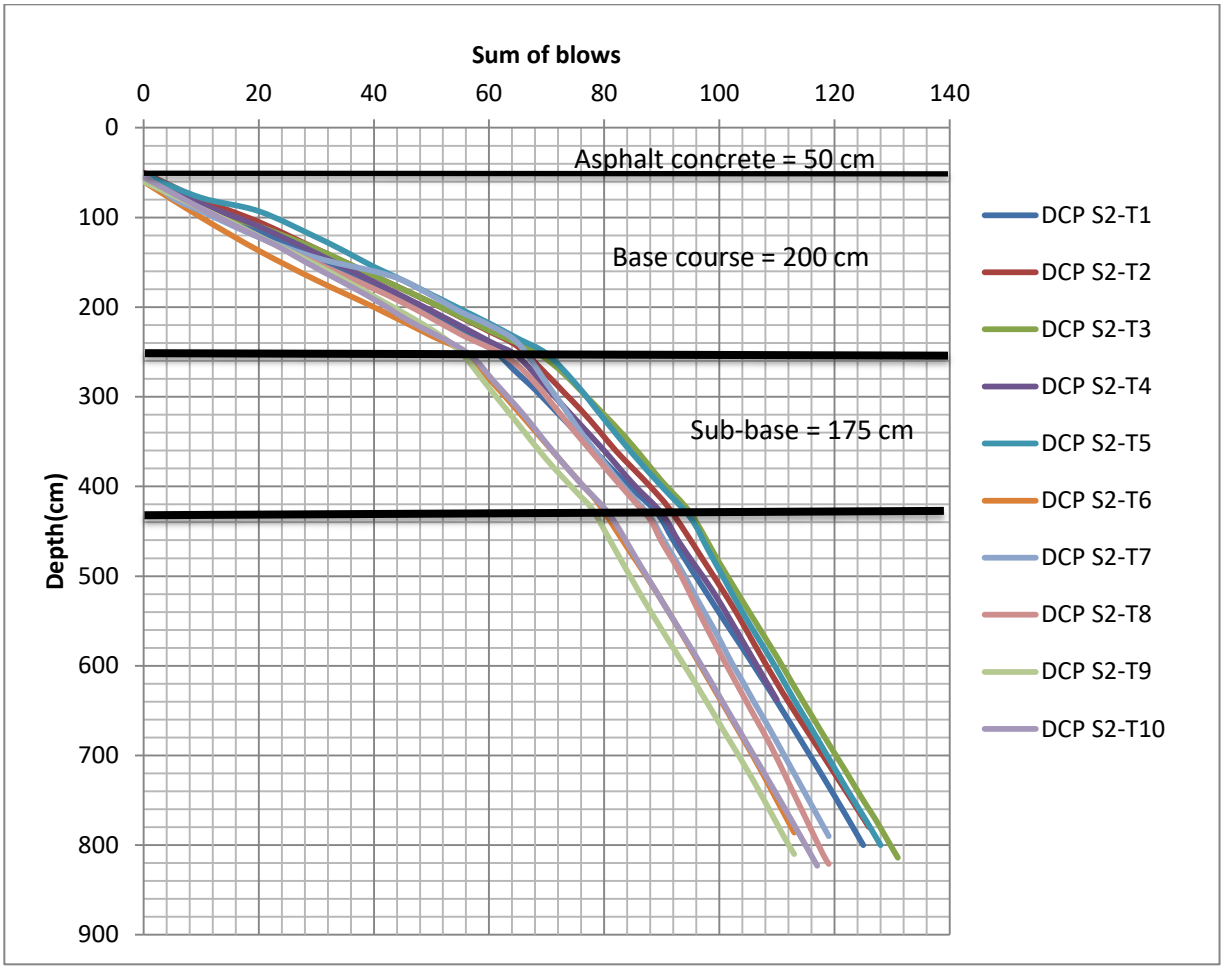

Figure 4. 2 Section two average thickness of Asphalt, Base, Sub-base and Sub-grade pavement layers

S_2-T_i (section two test number i^{th}(1-10))

Table 4.2 shows the pavement layers strength and thickness property as analyzed from **PCASE DCP**. Section one average thickness and CBR value shows that the thickness of asphalt layer is 2.0 in (50 mm), base course layer average (CBR 79% and thickness 8.0 in or 200 mm), sub-base course average (CBR 32% and thickness 8.0 in 0r 175 mm) and sub-grade average CBR 20%.

Table4. 2 Section two PCASE DCP analysis result

No. Test	Chainage (Km + m)		Asphalt	Base	Sub-base	Sub grade
T1	50+080	Thickness(in)	2.17	7.83	7	
		CBR%		78.9	36.2	21.4

T2	51+350	Thickness(in)	2	8.03	7	
		CBR%		82.9	33.1	21.6
T3	54+400	Thickness(in)	2	8.14	7	
		CBR%		85.1	32.4	20.6
T4	55+100	Thickness(in)	2.17	7.83	6.83	
		CBR%		82.5	33.1	21.9
T5	59+040	Thickness(in)	2.05	7.95	7.5	
		CBR%		83.6	36.6	19.8
T6	85+100	Thickness(in)	1.97	7.64	6.5	
		CBR%		72.6	32.2	20.4
T7	88+050	Thickness(in)	2	7.85	7.21	
		CBR%		78.8	35.2	19.5
T8	93+010	Thickness(in)	2	8.26	7.1	
		CBR%		79	30.1	17.4
T9	98+200	Thickness(in)	2	7.64	7	
		CBR%		72	29.6	20
T10	105+300	Thickness(in)	2	7.83	7	
		CBR%		71.5	31.5	20.2

Finally, evaluation of Section three pavement layers thickness and strength of Asphalt, Base, Sub-base and Sub-grade pavement layers for section two are indicates in Figure 4.3 and Table 4.3. The result shows that, the thickness of asphalt (50mm), base course (200 mm), sub-base course (275 mm) and infinite depth of sub-grade soils.

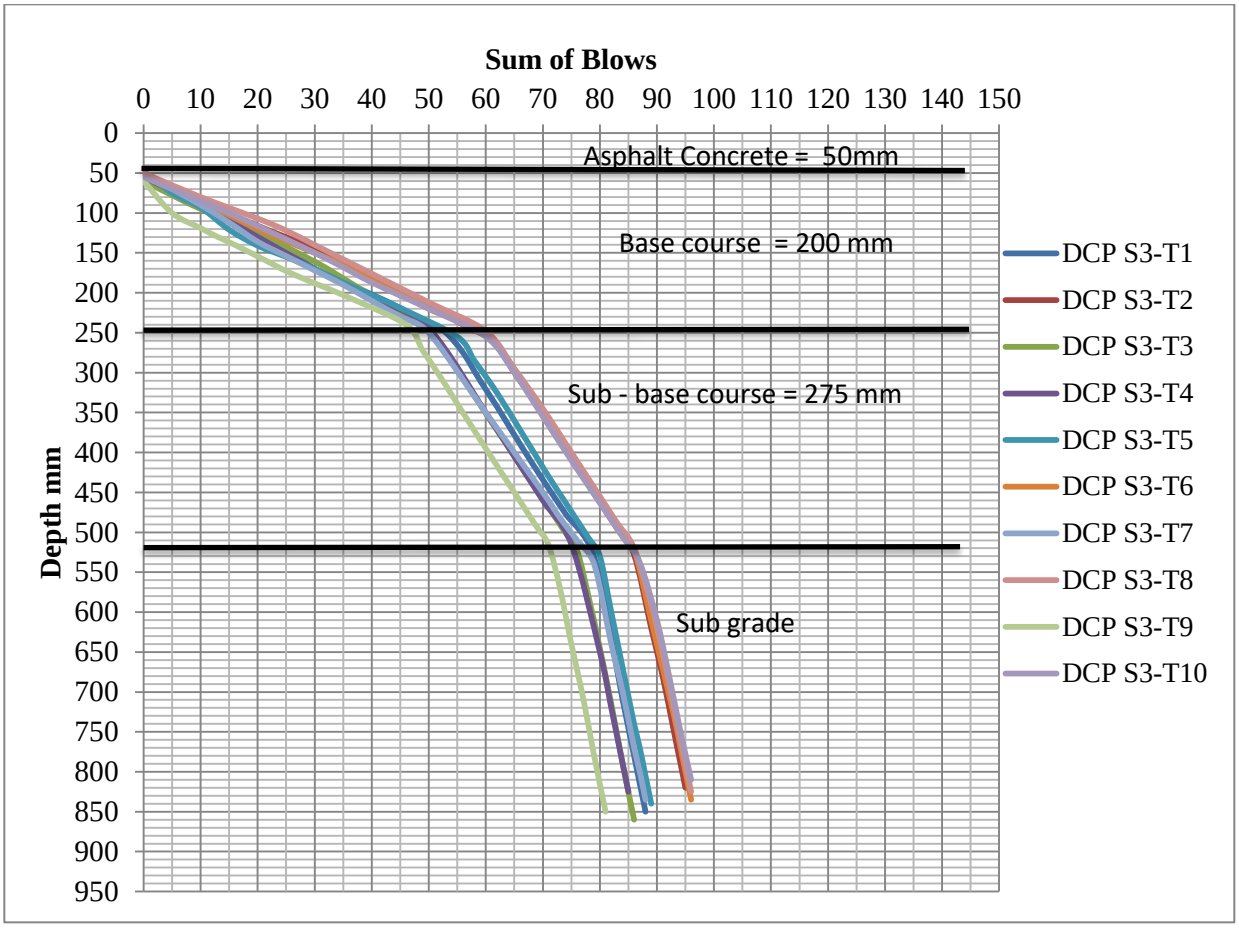

Figure 4. 3 Section three average thickness of Asphalt, Base, Sub-base and Sub-grade pavement layers

S_3-T_i mean section three test number i^{th}(1-10)

Table 4.3 shows the pavement layers strength and thickness property as analyzed from **PCASE DCP**. Section one average thickness and CBR value shows that the thickness of asphalt layer is 2.0 in (50 mm), base course layer average (CBR 70% and thickness 8.0 in or 200 mm), sub-base course average (CBR 20% and thickness 8.0 in 0r 275 mm) and sub-grade average CBR 5%.

Table4. 3 Section three PCASE DCP analysis result

No. Test	Chainage (Km + m)		Asphalt	Base	Sub-base	Sub grade
T1	60+750	Thickness(in)	2.17	8	11	
		CBR%		68.3	19.8	5.3
T2	61+000	Thickness(in)	1.97	8.01	11.1	

		CBR%		76.8	19.8	5.9
T3	63+500	Thickness(in)	2.21	8	11	
		CBR%		68.9	20.5	5.9
T4	67+500	Thickness(in)	2.17	8	10.85	
		CBR%		66.4	19.4	6.4
T5	69+050	Thickness(in)	1.89	8.11	11	
		CBR%		64	26.4	6.5
T6	70+000	Thickness(in)	1.97	8	11	
		CBR%		75.7	20.7	6.9
T7	73+080	Thickness(in)	1.97	8	11	
		CBR%		61.9	22.1	5.8
T8	78+100	Thickness(in)	1.97	8	11	
		CBR%		78.9	20	6
T9	80+250	Thickness(in)	2.13	8	11	
		CBR%		58.8	19.7	5.7
T10	82+030	Thickness(in)	2	8	11	
		CBR%		76.7	18.9	6.2

Pavement structure was delineated by sudden increases or decreases of CBR value in pavement structure. PCASE's DCP analysis tool automatically divides pavement layers with a maximum of four layers based on CBR values. ERA (2013) flexible pavement design manual described dynamic cone penetration (DCP) data analysis graphically and resulted in terms of penetration index, CBR value and thickness property of pavement structure with delineated graph curve line of each pavement layers.

Table 4.4 shows average pavement evaluation result of section one, two and three of Jimma-Bonga road.

Table4. 4 Average CBR and thickness result of pavement sections.

Pavement layers	Section one		Section two		Section three	
	CBR (%)	Thickness (mm)	CBR (%)	Thickness (mm)	CBR (%)	Thickness (mm)
Asphalt concrete		50		50		50
Base course	71	200	79	200	70	200
Sub-base course	31	200	33	175	21	275

Sub-grade soil	10		20		6	

Pavement evaluation was summarized by determined the adequacy of pavement structure for on service traffic. Pavement structural evaluations with average DCP are consider traffic load and climate of study area. Table 4.5 shows climate Jimma area.

Table 4.5 Climate data of Jimma area

	Jan	Feb	Mar	Apr	May	Jun	Jul	Aug	Sep	Oct	Nov	Dec
Mean daily max (^{o}C)	28	29	28	27	26	24	24	25	27	27	28	28
Mean (^{O}C)	23	24	24	23	23	21	21	22	23	23	23	22
Mean daily min (^{O}C)	18	19	20	20	20	19	19	19	19	19	18	17

Source: From (https://www.weather-atlas.com/en/ethiopia/jimma-climate)

Figure 4.4 shows the season from January to December are normal season and February are hottest month. Design pavement temperature and design air temperature of Jimma to Bonga road are 91.9 ^{o}F and 79.5 ^{o}F respectively.

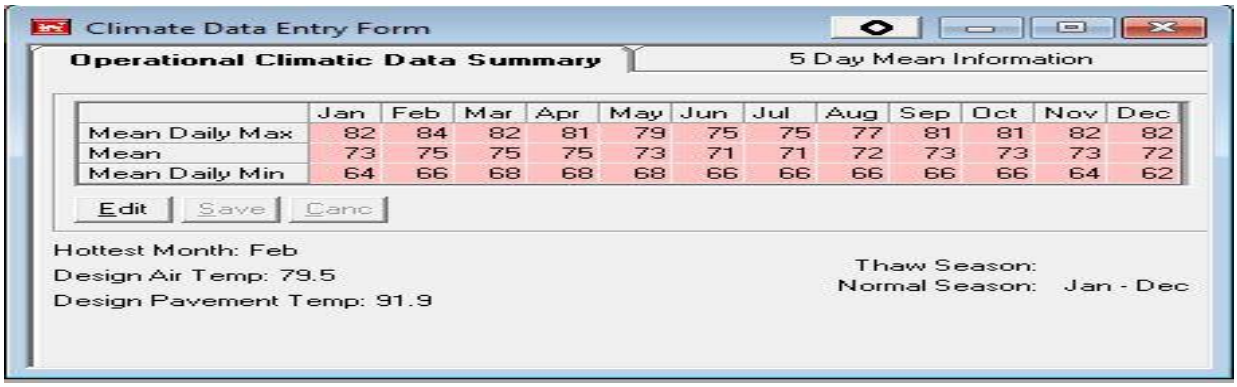

Figure 4.4: PCASE climate analysis result

JULEA multilayer elastic analyses consider design pavement temperature 91.9 ^{o}F for mechanistic pavement response analysis.

Pavement structural evaluation results are active as shown on figure (4.5- 4.7), which means our pavement structures are capable (adequate) to give traffic service.

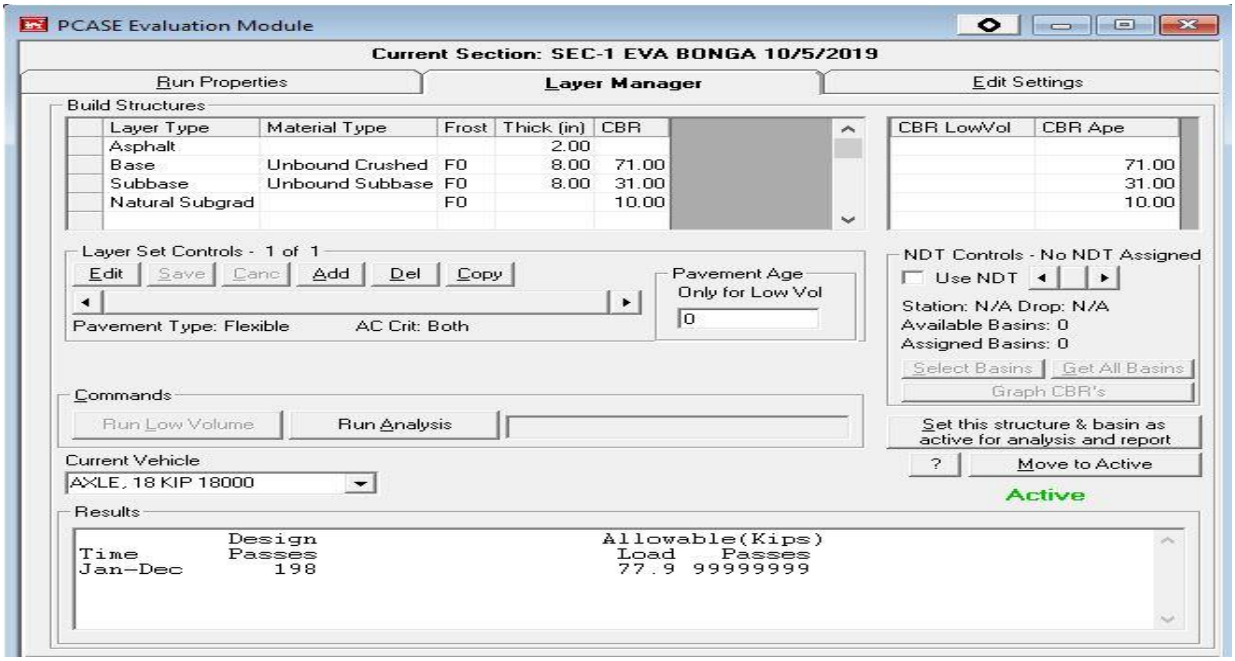

Figure 4.5: pavement evaluation result of section one

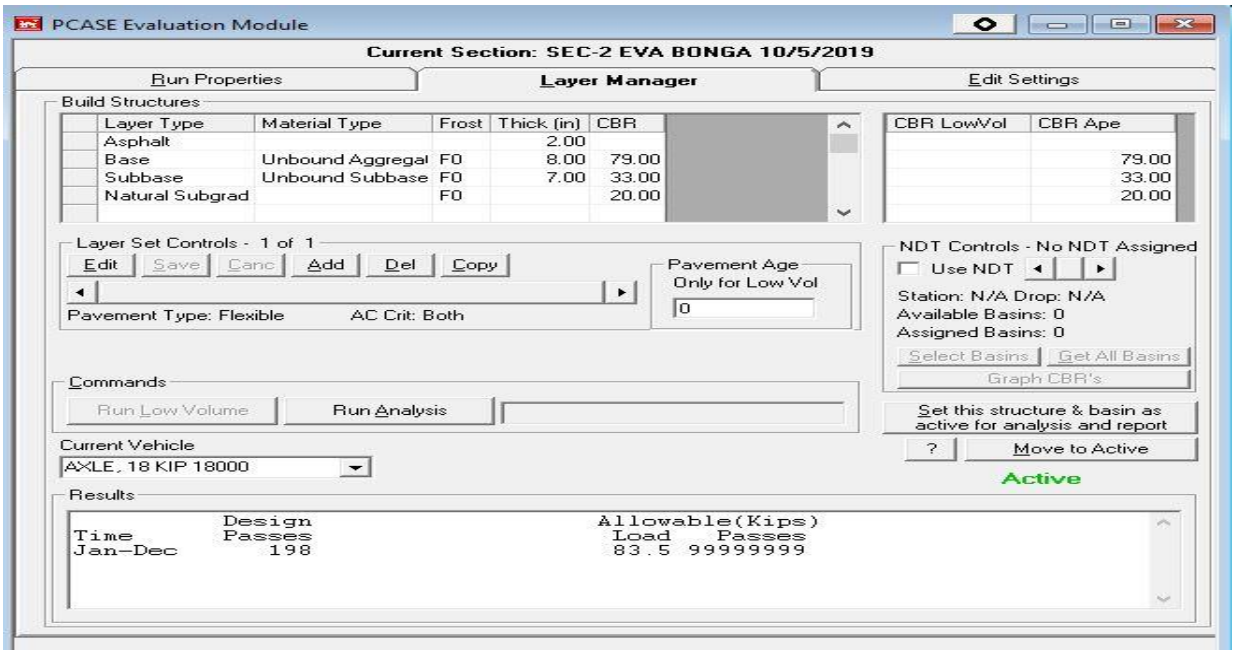

Figure 4.6: pavement evaluation result of section two

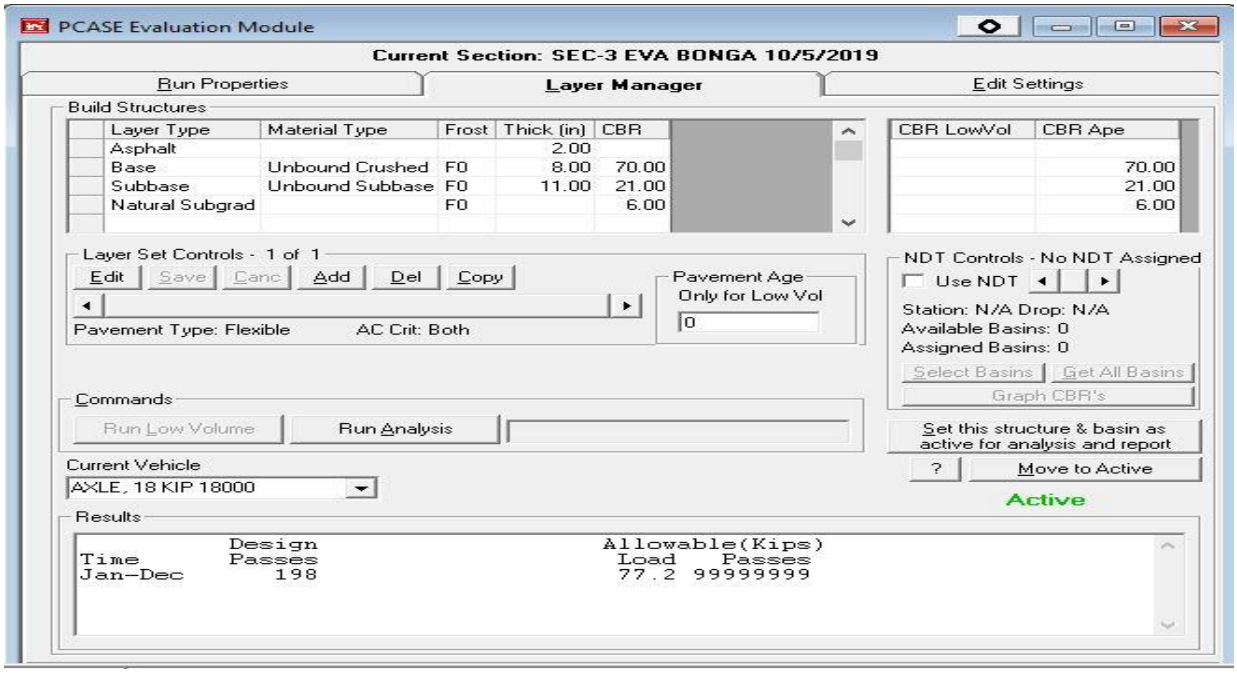

Figure 4.7: pavement evaluation result of section three

Therefore, as per evaluation the present (current) pavement structural condition of Jimma to Bonga road are capable to deliver traffic service.

4.2. Dynamic Modulus Result

A material in each layer of each section was defined by a modulus of elasticity (E) and a Poisson's ratio (υ). Poisson's ratio (υ) was considered as 0.35, 0.30, 0.30 and 0.45 for asphalt layer, base course, sub-base course and subgrade course, respectively from AASHTO and ERA standard specification. Traffic load considered in terms of repetitions of single axle load 80KN with dual tires radius 10.75 cm and 35 cm center-to-center spacing are apply on top of pavement surface. Over all pressure of tire apply on top of pavement surface is 550KPa.

Table 4. 6 AASHTO Typical moduli value for common pavement materials

Materials	General range (MPa)	Poison's ratio range	Typical value (MPa)	Poison's ratio
HMA	1500-4000	0.15-0.45	3000	0.35
PCC	20000-55000	0.10-0.20	30000	0.15
Asphalt-treated base	700-6000	0.15-0.45	1500	0.35
Lean concrete	7000-20000	0.15-0.30	10000	0.20
Cement treated base	3500-7000	0.15-0.30	5000	0.20
Granular base	100-350	0.30-0.40	200	0.35
Granular subgrade	50-150	0.30-0.40	100	0.35

Fine grained Subgrade soil	20-50	0.30-0.50	30	0.40

Source: AASHTO

Table 4.7 shows road component characteristics like elastic modulus, poison's ratio and their typical values, which are taken from ERA 2013.

Table4.7 ERA typical Pavement Material Properties

Material	Elastic modulus (MPa)	Poisson's ratio
Asphalt surface	3000	0.35
Base course layer	300	0.30
Sub-base layer	175	0.30
Subgrade layer		0.45

(source: ERA 2013)

Table 4.8 show Jimma-Bonga road pavement layers materials properties obtained from DCP test result. Elastic modulus was calculated by equation (2.13).

Table4. 8 Jimma-Bonga road pavement layers CBR value and elastic modulus

Pavement layers	Resilient (Elastic) modulus result					
	Section one		Section Two		Section Three	
	CBR %	E. MPa	CBR %	E. MPa	CBR %	E. MPa
Asphalt concrete	-	3000		3000		3000
Base course	71	269.0	79	288	70	267
Sub-base course	31	158	33	165	21	123
Subgrade course	10	77	20	120	6	55

AASHTO mechanistic empirical method NCHRP 1-37A, incorporates a hierarchical approach for specified all pavement mechanistic analysis inputs. Three levels are provided for the mechanistic analyses inputs in the NCHRP 1-37A procedure. In this thesis, we use level 2 and 3 of input value, because of Jimma to Bonga road design and constructed based on CBR value of material property and based on relative importance of Jimma-Bonga pavement road. Table 4.9

shows the input values for mechanistic response analysis of Jimma-Bonga road sections.

Table4. 9 Pavement layers input values for mechanistic response analysis.

No. of sections	Layers	Thickness (mm)	E (MPa)	ν	Material Properties		
Section one	AC	50	3000	0.35	Isotropic and Linear Elastic		
	Base	200	269	0.3	Nonlinear: Universal Model with octahedral shear stress, τ_{oct} (Witczak and Uzan, 1988))		
					K_1	K_2	K_3
					1,098	0.64	0.065
	Sub-base	200	158	0.3	Nonlinear: Universal Model with octahedral shear stress, τ_{oct} (Witczak and Uzan, 1988)		
					K_1	K_2	K_3
					1,098	0.64	0.065
	Sub-grade		77	0.45	Isotropic and Linear Elastic		
Section two	AC	50	3000	0.35	Isotropic and Linear Elastic		
	Base	200	288	0.3	Nonlinear: Universal Model with octahedral shear stress, τ_{oct} (Witczak and Uzan, 1988)		
					K_1	K_2	K_3
					1,098	0.64	0.065
	Sub-base	175	165	0.3	Nonlinear: Universal Model with octahedral shear stress, τ_{oct} (Witczak and Uzan, 1988)		
					K_1	K_2	K_3
					1,098	0.64	0.065
	Sub-grade		120	0.45	Isotropic and Linear Elastic		
Section three	AC	50	3000	0.35	Isotropic and Linear Elastic		
	Base	200	267	0.3	Nonlinear: Universal Model with octahedral shear stress, τ_{oct} (Witczak and Uzan, 1988)		
					K_1	K_2	K_3
					1,098	0.64	0.065

	Sub-base	275	123	0.3	Nonlinear: Universal Model with octahedral shear stress, τ_{oct} (Witczak and Uzan, 1988)		
					K_1 (kPa)	K_2	K_3
					1,098	0.64	0.065
	Sub-grade		55	0.45	Isotropic and Linear Elastic		

Base, sub-bas and subgrade layers thickness and resilient modulus estimated from correlations with measured CBR values is one of the most common level 2 input values. Poisons ratio, asphalt elastic modulus and nonlinear constant values are level 3 input values which are obtained from standard manuals and model.

4.3. Mechanistic Response Result

JULEA and ABAQUS 2D software package used for mechanistic pavement response analysis under uniform tire load 0.55Mpa over circular radius of 10.75 cm. According to Kim (2007) ABAQUS 2D defined geometrical domain of 140-times the radius of loading area in vertical direction and 20-times radius of loading area in the horizontal direction, but JULEA do not defined geometrical domain of pavement structure.

ABAQUS finite element analysis considered nonlinear material property of base course and sub-base course. However, JULEA was considered all pavement material as linear elastic element.

Kim (2010) compared the result of ABAQUS axisymmetric and plane strain model with 3D model. Axisymmetric model results are more similar with 3D model result and 2D plane strain model results are over estimated, when compared with 3D model result. So that, Kim conclude axisymmetric model are better in order to save computation time of 3D model and for accurate result of single axle loaded pavement analysis.

Figure 4.8 shows mechanistic response analysis results of vertical compressive stresses for section one, two and three respectively.

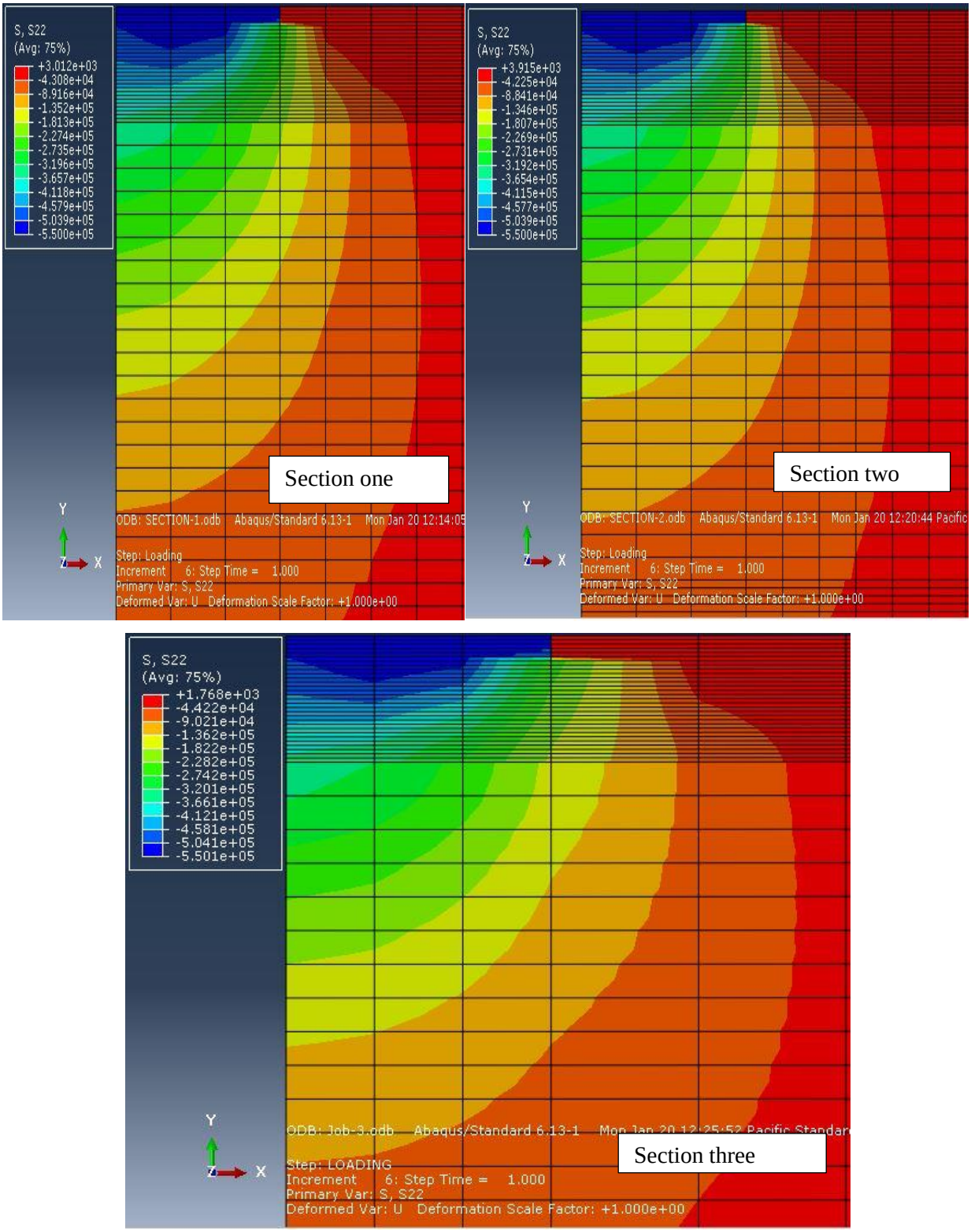

Figure 4. 8 ABAQUS 2D Vertical stress of section one, two and three results

Vertical stress is the main output of mechanistic response analysis critically shows the stress induced by traffic load passed over the pavement structure. According to (NCHRP, 2002)

resulted the contact pressure of the wheel on the road is equal to the tire pressure. The vertical stress on top of asphalt layer resulted 0.55 Mpa is equal with the wheel load of traffic is shown on the figure 4.8 by blue colure. Figure 4.9 shows vertical stress passed all over 5m depth of pavement structures by compared ABAQUS with JULEA.

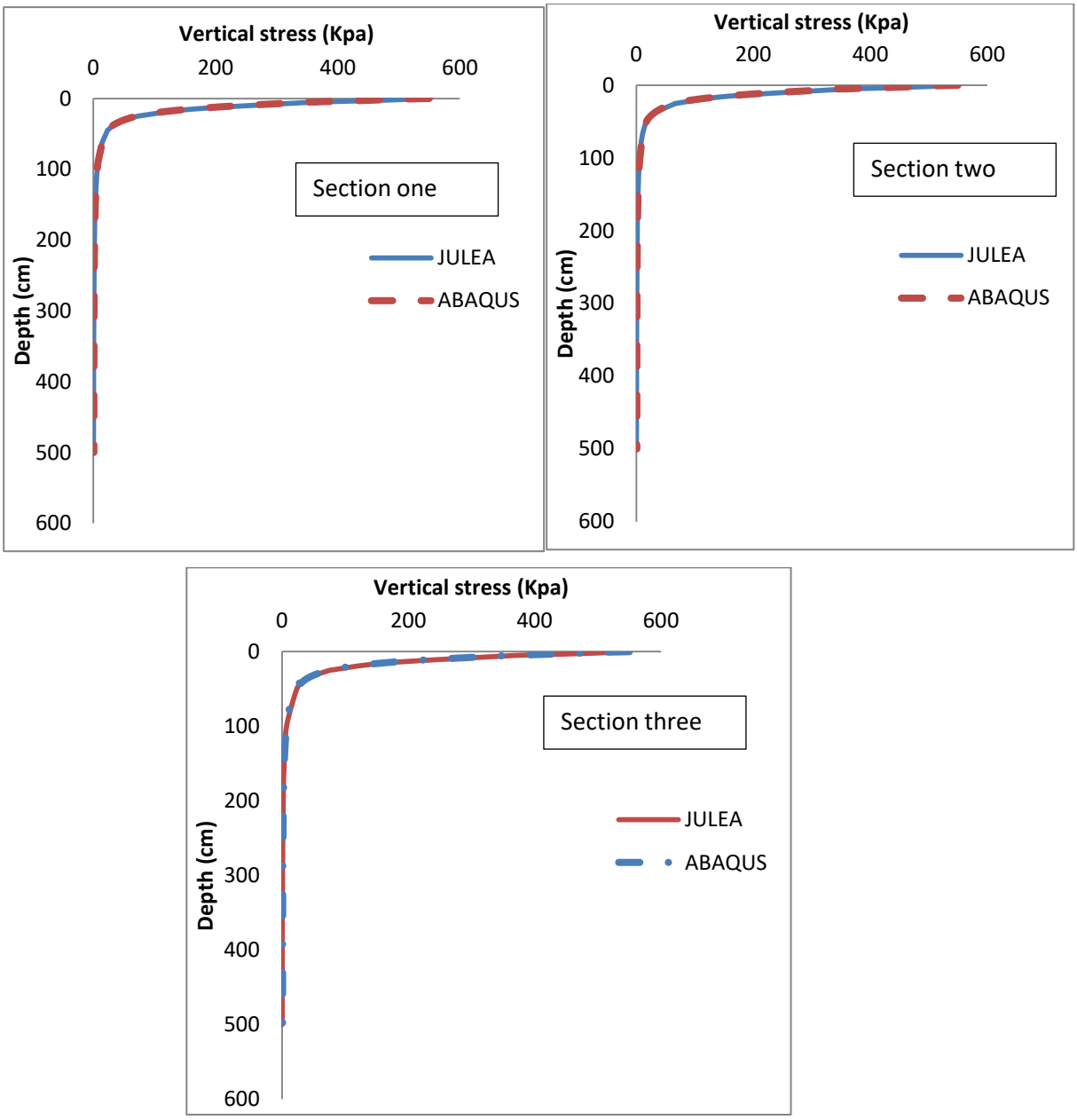

Figure4. 9 Vertical stress results of ABAQUS and JULEA

Kim (2007) obtained more accurate mechanistic response analysis result by comparing JULEA and ABAQUS in order to defined geometrical domain of pavement.

Critical strains are obtained from mechanistic pavement response analysis, which are horizontal

strain and vertical strain of pavement sections. Figure 4.10 shows ABAQUS horizontal strain results of section one, two and three respectively.

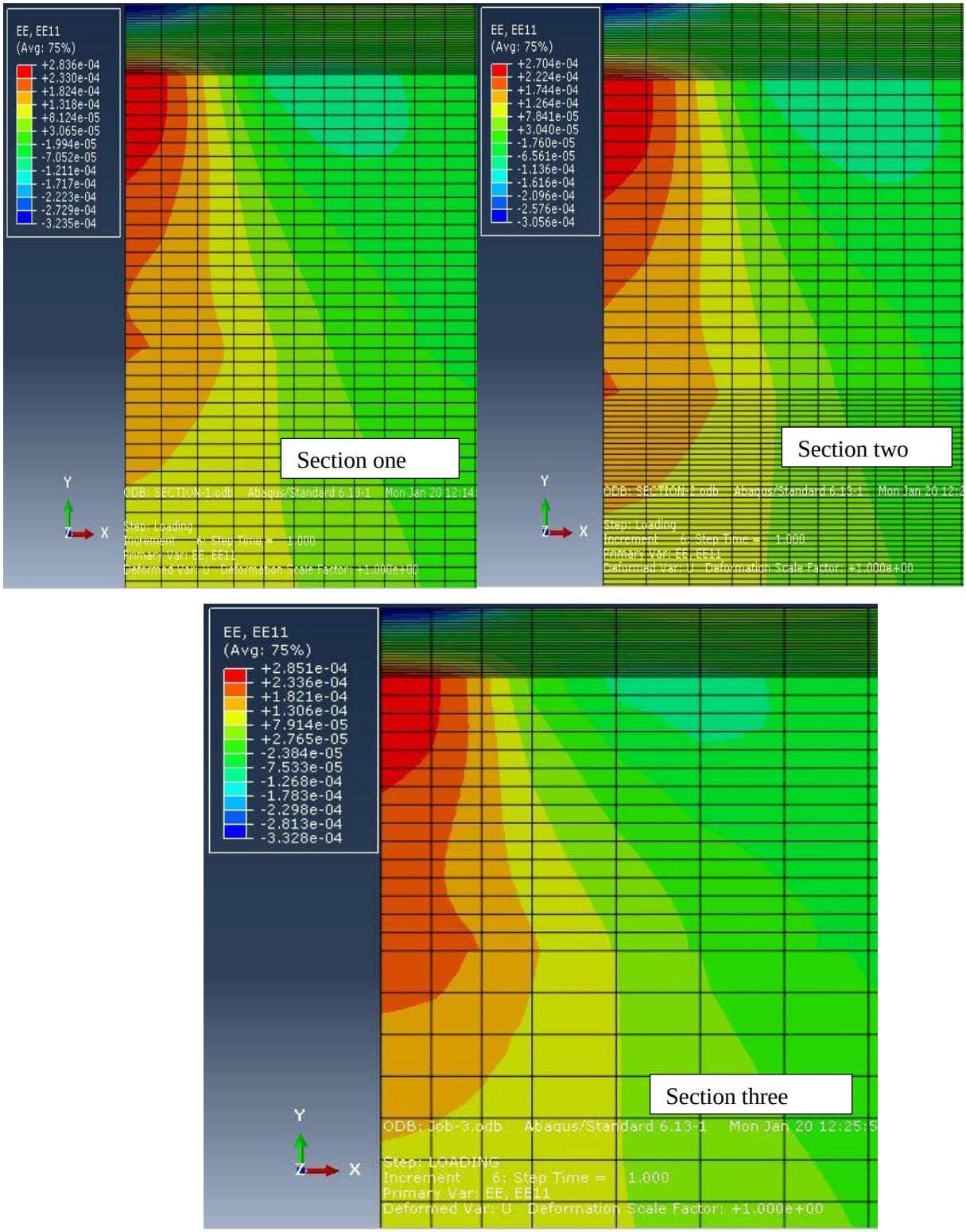

Figure4. 10 Horizontal strain results from ABAQUS for section one, two and three

Muniandy (2013) compared the analysis of KENPAVE and CHEV PC computer programs in order to differentiate the strain output results and determined the governed distress model. Figure 4.11 shows ABAQUS and JULEA horizontal strain results comparatively for section one, two and three.

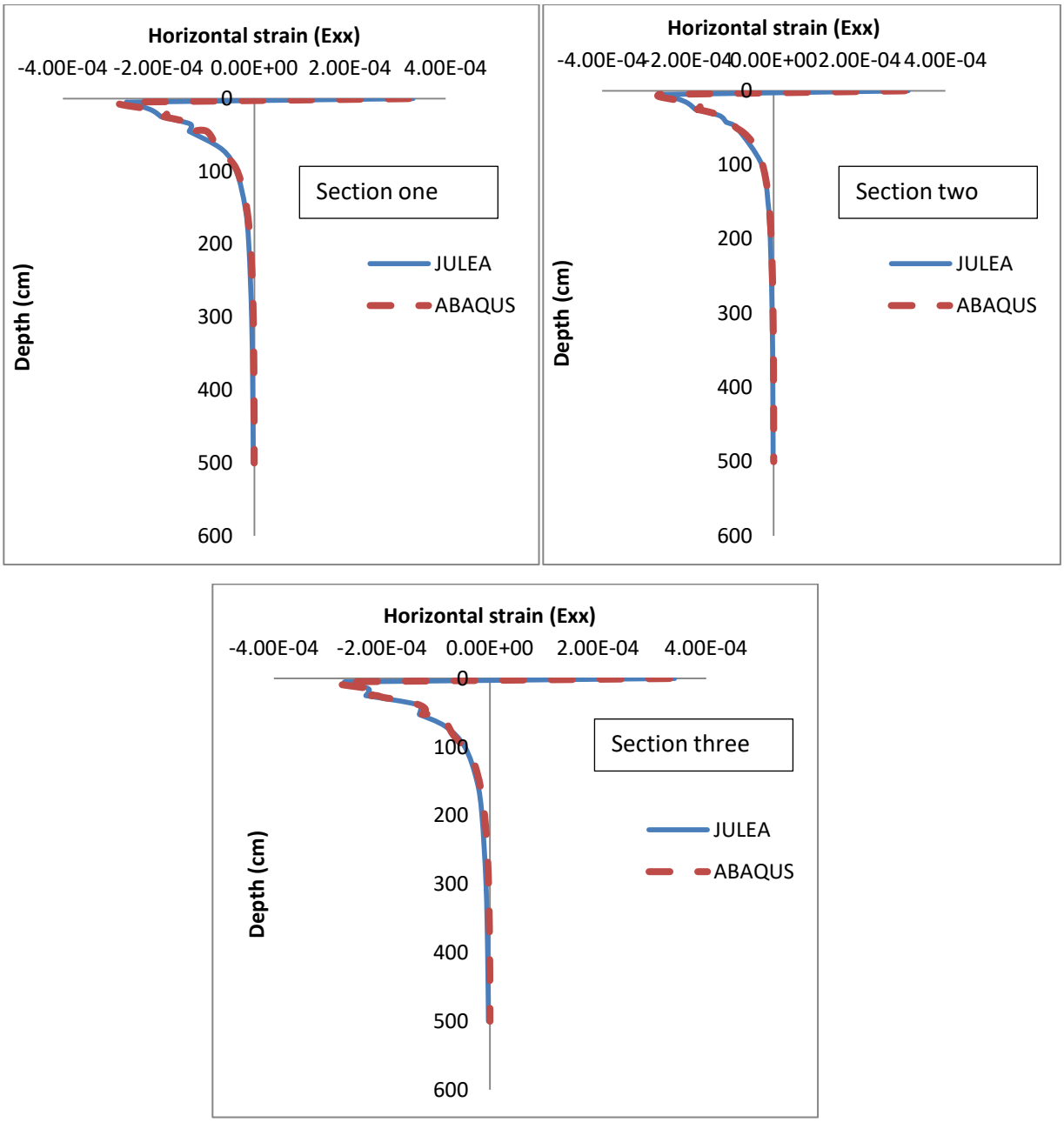

Figure4. 11 Horizontal strain results of ABAQUS and JULEA

Horizontal strain at the bottom of asphalt was critically resulted from mechanistic pavement response analysis. ABAQUS horizontal strain results at the bottom of asphalt of section one, two and three are 2.6705 x 10^{-4}, 2.5469 x 10^{4} and 2.6896 x 10^{-4} respectively. JULEA horizontal

strain results at the bottom of asphalt of section one, two and three are 2.6746 x 10^{-4}, 2.5474 x 10^{4} and 2.6967 x 10^{-4} respectively. The results of ABAQUS and JULEA are relatively similar. However, the small difference was occurred between ABAQUS and JULEA results because of JULEA considered pavement temperature for mechanistic response analysis.

Figure 4.12 shows ABAQUS mechanistic response analysis results of vertical strain output.

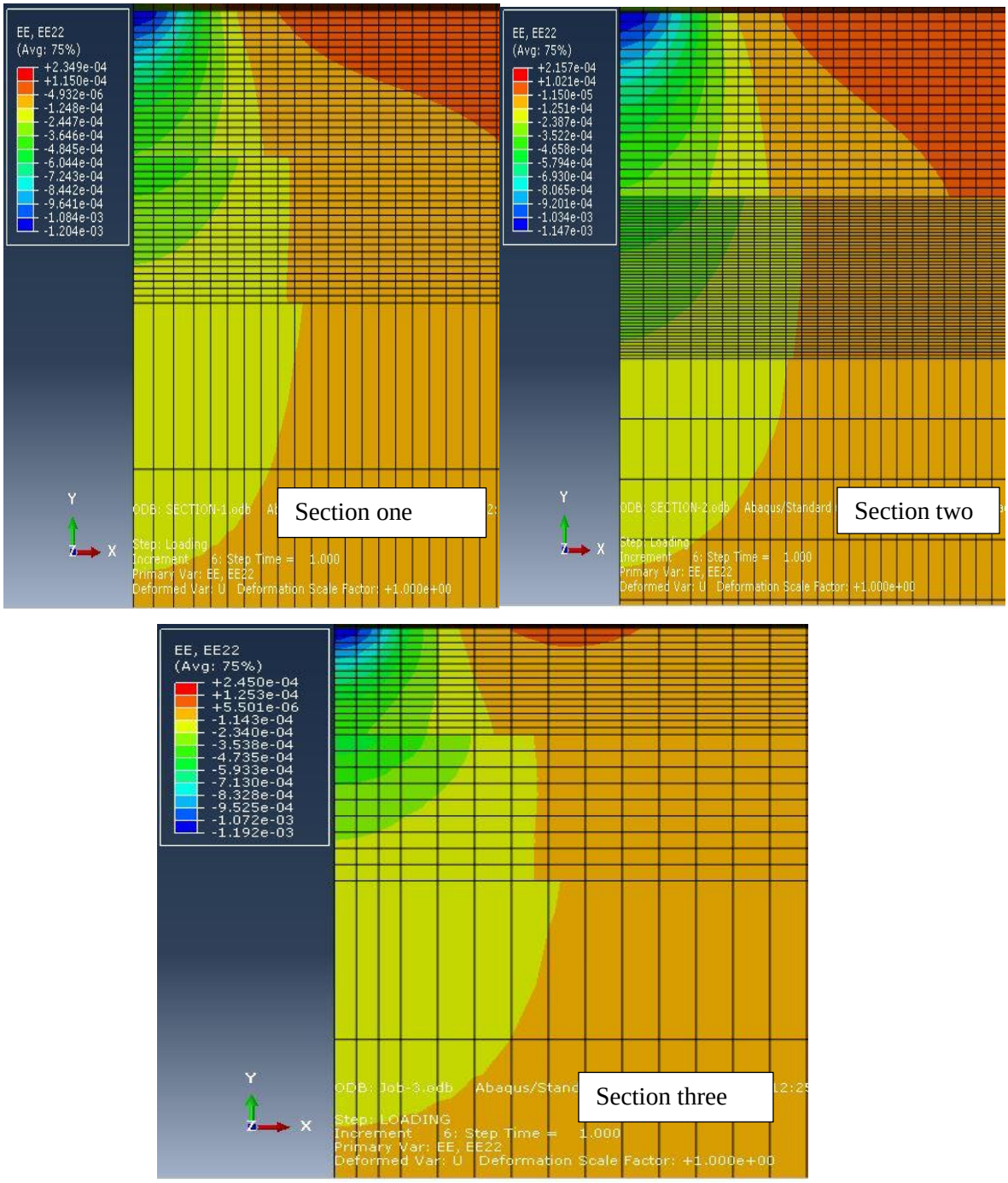

Figure 4. 12 Vertical strain result of ABAQUS for section one, two and three

Kim (2010) compared MEPDG and FEM for pavement failure by rutting deformation resulted to predict pavement life. The result shows MEPDG pavement failure predicted more realistic than FEM because of FEM analysis used viscoelastic energy dissipation to predict pavement life. However, MEPDG analysis used linear elastic method to predict pavement life.

Figure 4.13 shows vertical strain result of ABAQUS and JULEA comparatively.

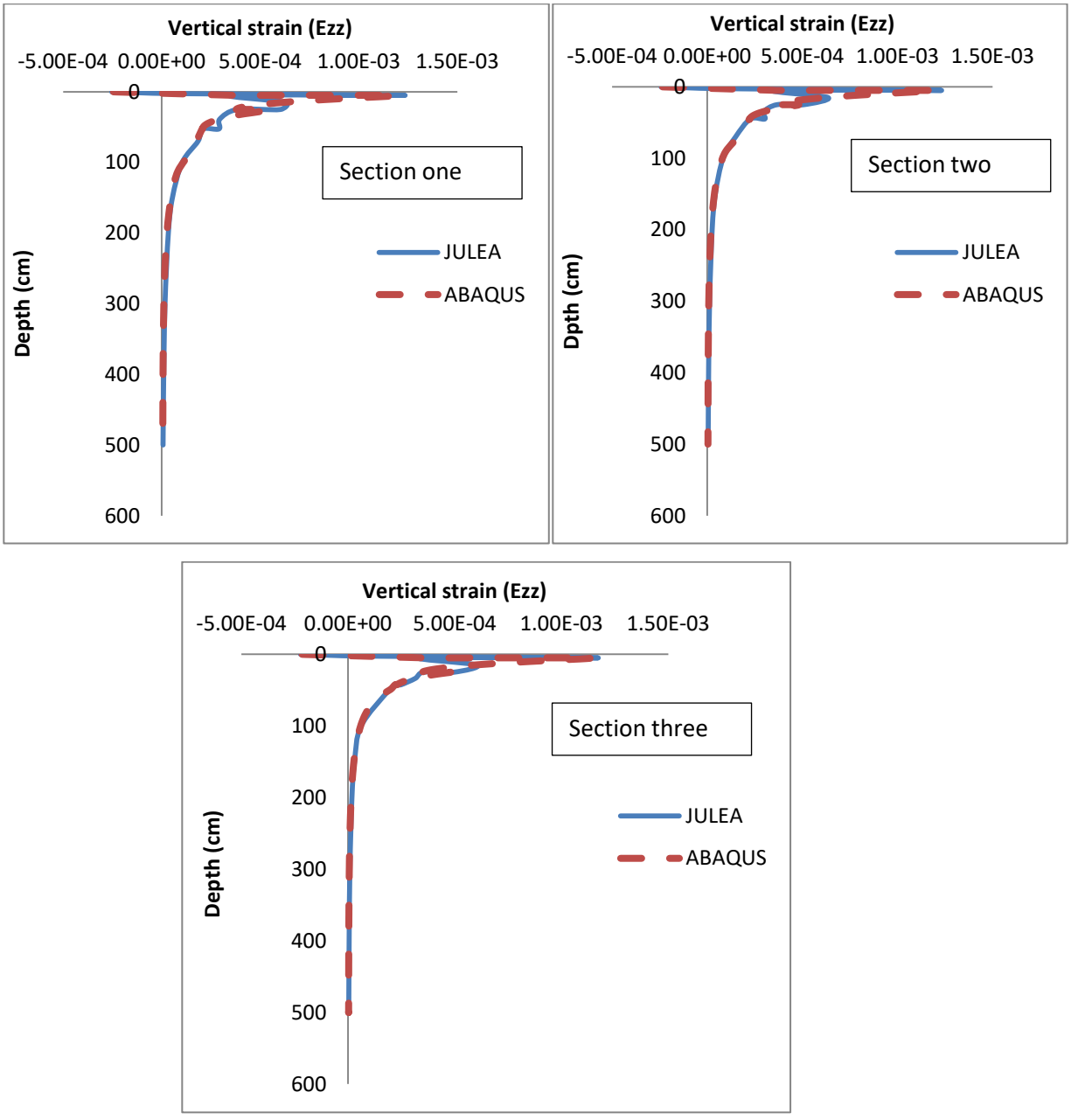

Figure 4. 13 Vertical strain results of ABAQUS and JULEA for section one, two and three

Vertical strain at the top of sub-grade soil was critically resulted from mechanistic pavement response analysis. ABAQUS vertical strain results at the top of sub-grade soil of section one,

two and three are 2.2143 x 10^{-4}, 2.2016 x 10^{4} and 2.0489 x 10^{-4} respectively. JULEA vertical strain results at the top of sub-grade soil of section one, two and three are 2.2636 x 10^{-4}, 2.3162 x 10^{4} and 2.083 x 10^{-4} respectively. The results of ABAQUS and JULEA are quite different because of ABAQUS analysis considered nonlinearity material property made a great difference.

Table 4.10 and table 4.11 shows critical strain results of JULEA and ABAQUS respectively.

:

Table 4. 10 JULEA linear analysis Critical strain at the bottom of asphalt and at top of subgrade soil results

Road section	Pavement layers	**Location of evaluation**	**Depth: Z Position (cm)**	**strain at the bottom of AC and top of subgrade**	
				Ɛxx	**Ɛyy**
Section one	Asphalt concrete	Bottom	5	-0.00026746	
	Sub-grade soil	Top	-45		0.00022636
Section Two	Asphalt concrete	Bottom	5	-0.00025474	
	Sub-grade soil	Top	-42.5		0.00023162
Section three	Asphalt concrete	Bottom	5	-0.00026967	
	Sub-grade soil	Top	-52.5		0.0002083

JULEA divide pavement intersection by minus sign for the top of next layer and positive for the bottom of first pavement layer in order to obtain accurate result of pavement interface.

Table 4. 11 ABAQUS nonlinear analysis critical strain result at the bottom of asphalt and top of sub-grade soil

Road section	Pavement layers	**Location of evaluation**	**Depth: Z Position (cm)**	**strain at the bottom of AC and top of subgrade**	
				Ɛxx	**Ɛyy**
Section one	Asphalt concrete	Bottom	5	0.000267054	
	Sub-grade soil	Top	45		-0.000221436
Section Two	Asphalt concrete	Bottom	5	0.000254697	

	Sub-grade soil	Top	42.5		-0.000220169
Section three	Asphalt concrete	Bottom	5	0.000268966	
	Sub-grade soil	Top	52.5		-0.000204895

4.4. Empirical performance Prediction Result

Table 4. 12 Pavement Performance prediction result base on JULEA linear analysis result

Road section	**Location**	**strain at the bottom of AC and top of subgrade**		**Number of axle repetition**		**Damage**	
		Ɛxx	**Ɛyy**	Fatigue distress (Nf)	Rutting distress(Nf)	**Ratio**	**Year**
Section one	AC Bottom	$-2.6746E^{-04}$		$48.9x10^6$		0.04	25
	SG Top		$2.2636E^{-04}$		$28.5x10^6$	0.068	15
Section Two	AC Bottom	$-2.5474E^{-04}$		$57.4x10^6$		0.034	30
	SG Top		$2.3162E^{-04}$		$25.71x10^6$	0.075	13
Section three	AC Bottom	$-2.6967E^{-04}$		$47.6x10^6$		0.041	25
	SG Top		$2.083E^{-04}$		$41.34x10^6$	0.047	21

Table 4.12 shows predicted Performance based on JULEA linear elastic analysis results. Based on the summation of damage ratio at the bottom of the asphalt concrete and on the top of the subgrade was compared and the smaller of the two was taken as the governed pavement life. Sum of damage ratio and governed performance life in years are 0.075 and 13 year respectively.

Gedafa (2007) obtained the Vertical compressive strain as governed performance at damage ratio of 0.0558, and design life in years is 18 based on AI model.

Table 4.13 shows Prediction based on ABAQUS analysis result.

Table 4. 13 Pavement performance prediction based on ABAQUS nonlinear analysis result

Road section	**Location**	**strain at the bottom of AC and top of subgrade**		**Number of axle repetition**		**Damage**	
		ε_{xx}	**ε_{yy}**	Fatigue distress (Nf)	Rutting distress(Nf)	**Ratio**	**Year**
Section one	AC Bottom	$2.67054E^{-04}$		$47.48x10^6$		0.041	25
	SG Top		$-2.21436E^{-04}$		$31.32x10^6$	0.062	16
Section Two	AC Bottom	$2.54697E^{-04}$		$55.49x10^6$		0.035	29
	SG Top		$-2.20169E^{-04}$		$32.14x10^6$	0.060	17
Section three	AC Bottom	$2.68966E^{-04}$		$46.34x10^6$		0.042	24
	SG Top		$-2.04895E^{-04}$		$44.34x10^6$	0.044	23

As the table 4.13 shows damage ratio and highest performance, life of pavement based on ABAQUS nonlinear analysis critical strain results are 0.062 and 16 year respectively.

Table 4.14 shows comparison of predicted performance and over all governed performance of Jimma to Bonga road.

Table 4. 5 Comparative pavement performance prediction based on JULEA and ABAQUS

Comparatively Predicted pavement performance in year				
	Distress	Section one	Section two	Section three
JULEA	Fatigue	25	30	25
	Rutting	15	13	21
ABAQUS	Fatigue	25	29	24
	Rutting	16	17	23

As illustrated on table 4.14 ABAQUS nonlinear model predicted results produces relatively longer life than the JULEA linear elastic approach prediction result. This is happened because of, JULEA accounts linear elastic material property for pavement damage due to truck loading by incorporated with pavement temperature. On the other hand, ABAQUS finite element

model consider nonlinear material property of base and sub-base layers to determine the pavement life by accounted only damage due to truck loading without incorporated with pavement temperature.

Over all governed performance life of pavement are 13 year, which are resulted from vertical compressive strain output of JULEA linear analysis. Rutting deformation are governed distress for performance life of the pavement. The result shows about 25.71 million of allowable equivalent standard axle loads are create large rutting distress throughout pavement section.

CHAPTER FIVE
CONCLUTION AND RECOMMENDATION

5.1. Conclusion

This thesis was focused on performance prediction of flexible pavement based on in situ evaluation of flexible pavement with DCP test taken as in put value for mechanistic response analysis of pavement structure in order to predicate pavement performance comparatively by using critical strain result of JULEA and ABAQUS based on asphalt institute (AI) prediction function. Jimma-Bonga flexible pavement road has three sections in 107 Km length of road alignment during construction.

In situ evaluation of pavement with DCP test carried out over three sections of road conducted strength (CBR %) and of pavement layers without asphalt concrete surface layer and thickness of pavement layers in each three sections of road alignment.

Elastic modulus of pavement layers has obtained from CBR and elastic modulus correlation formula of US army corps. Evaluation of Jimma-Bonga flexible pavement road resulted in terms of thickness and elastic modulus of each sections pavement structure. Asphalt, base course, sub-base course and sub-grade soil are structural component of Jimma-Bonga road sections. As per evaluation current pavement structural condition are capable to give traffic service.

Comparative prediction of pavement performance based on JULEA and 2D ABAQUS software critical strain resulted shows 13-years and 16-year respectively maximum performance of Jimma-Bonga road. Therefore, 13-year performance of pavement is governing predicted performance of Jimma-Bonga flexible pavement road.

5.2. Recommendation

Performance prediction of flexible pavement case study Jimma-Bonga road concerned on prediction of structural performance of future pavement life rather than riding quality or serviceability performance of the pavement surface. So that, other researcher and scholars may include serviceability performance prediction order to determine the riding quality and traffic efficiency of the road.

As flexible pavement performance prediction, there are several factors that affect pavement performance such as material property, traffic load, climate, environment, aging, construction, asphalt binding, sub-surface drainage, side drainage, ground water table and so on. In this research, we included only material property (strength/stiffness), climate factor (temperature) and traffic load. Other factors have their own effect on reducing pavement performance life, so researcher need to be including such factors for better accuracy of prediction.

This thesis only evaluates performance of pavement tested by DCP during September 2019. Therefore, other researcher and organization must assess that seasonally changed material property and traffic load effect on structural performance of Jimma-Bonga road in order to determine full of one-year pavement performance to predict more of accurate future pavement performance. Sensitivity analysis performed based on seasonal performance of pavement needed seasonal evaluation of in situ pavement structural and serviceability performance.

ERA standard specification does not have performance prediction function (model) at national level. In order to predict the performance of flexible pavement road in Ethiopia need prediction model at national level or local level respect to global prediction model like asphalt institute (AI). Accuracy of prediction more closes to reality if national prediction model are available in country because national level prediction model has formulated by considering Ethiopian different climate and environmental condition.

In this research included only fatigue crack at the bottom of asphalt and rutting deformation of subgrade soil for performance prediction. Other researcher will be looking through other distress such as: top down fatigue crack, rutting deformation of each layer, pothole, alligator crack and thermal crack.

REFERENCE

ABAQUS Inc. (2003), *Analysis of geotechnical problemswithABAQUS. 2003*. ABAQUS, Inc.

ABAQUS Theory Manual, Version, (2009), Hibbitt, Karlsson and Sorenson, Inc., INC.

Al-Khateeb, et.al. (2011), *Rutting Prediction of Flexible Pavements Using Finite Element Modeling*.Jordan Journal of Civil Engineering, Volume 5, No. 2.

Al-Azzawi,A. and Abed ,A. (2012), Evaluation of Rutting Depth in Flexible Pavements by using Finite Element Analysis and Local Empirical Model".

AMADEUS, (2000) Advanced Models for Analytical Design of European Pavement Structures, http://wwwext.lnec.pt/AMADEUS/

American Association of State Highway Officials (AASHTO). (1993). AASHTO Guide for Design of Pavement Structures., Washington.

Anand B.Tapase, M.S. Ranadive. (2016). Performance evaluation of flexible pavement using the finite element method, Forth Geo-China International conference, Material, design, construction, maintenance and testing of pavement, Shandong, China, GSP 266,pp.9-14.

ARA. (2004). *Guide for the Mechanistic Empirical Design of New and Rehabilitated pavement Structure*. (Report 1-37A), Washington, D. C: *Transportation Research Board of the National Academies*.

Asphalt Institute (AI). (1981). Thickness Design —Asphalt Pavement for Highways and Streets. Manual Series No. 1 (MS-1), Lexington.

Barker, W. R., and Gonzales, C. R. (1991) Pavement Design by Elastic Layer Theory, In Proceedings of Airfield Pavement Specialty Conference, Kansas City,MO

Bayomy F. and Abo-Hashema M. (2001), "WINFLEX 2000: mechanistic- empirical overlay design system for flexible pavements - program documentation and user guide," NIATT, University of Idaho, USA.

Boussinesq, J. (1885). Application des potentials a l'etude de l'equilibre et du Mouvement des Solids Elastiques, Gauthier-Villars, Paris,France.

Britto A. *Running ABAQUS 6.9* [Online].University of Cambridge.2010. Available at: http://www- h.eng.cam.ac.uk/help/programs/fe/abaqus/doc/aba69fdouble.pdf.[Accessed: 6 December 2014].

Brown, S., (1997), *"Achievements and Challenges in Asphalt Pavement Engineering"*, 8th International Conference on Asphalt Pavements, ISAP

Burmister, D.M. (1943).–TheTheory of Stresses and Displacements in Layered Systems and Applications to the Design of Airport Runways.‖ Highway Research Record 23, TRB, National Research Council, Washington, D.C., pp. 126-144.

Carpenter, S., Ghuzlan, K., and Shen, S, (2003), *"Fatigue Endurance Limit for Highway and Airport Pavements"*, Paper#03-3428, Transportation Research Board Annual Meeting

Cedergren, H.R. (1987). *Drainage of Highway and Airfield Pavements*, Robert E. Krieger Publishing Co. Inc., Malabar, FL

Chen, D.H.,Zaman,M., Laguros,J., and Soltani,A. (1995).–Assessment of Computer Programs for Analysis of Flexible Pavement Structures.‖ Transportation Research Record 1482, TRB, National Research Council, Washington, D.C., pp. 123-133.

Cho, Y. H., B. F. McCullough, and J. (1996). Weissmann. ―Considerations on Finite-Element Method Application in Pavement Structural Analysis.‖ Transportation Research Record. 1539: 96-101.

COST 333, (1999) "Development of New Bituminous Pavement Design Methods," Final Report on Action, European Commission, Brussels, ISBN 92-828- 6796-X.

Daniel, J.S. and G.R. Chehab (2007). "Use of RAP Mixtures in the Mechanistic Empirical Pavement Design Guide." Department of Civil Engineering, University of New Hampshire and Department of Civil and Environmental Engineering, The Pennsylvania State University, Durham, NH and University Park, PA: Transportation Research Board 87th Annual Meeting 2008 Washington DC.

Dawson, A. & Kolisoja, P. (2004). *Permanent Deformation*. Report on task 2.1, Roadex II, Northern Periphery, Lead Partner: The highland Council, Transport, Environmental & Community Service, Inverness, Scotland.

Doré, G. & Zubeck, H. K. (2009). *Cold Regions Pavement Engineering*. 1st ed. American Society of Civil Engineers, 1801 Alexander Bell Drive, Reston, USA.

ERDC Developed Software WinJULEA. (2003). Windows Layers Elastic Analysis, Engineering Research and Development Center, GSL-Airfields and Pavements Branch, Vicksburg, Mississippi.

Federal Aviation Administration (2004). Advisor Circular (AC) No:150/5320-6D, U.S.

Department of Transportation.

FHWA (Federal Highway Administration), (2010), *"LTPP Protocol P07 - Test Method for Determining the Creep Compliance, Resilient Modulus and Strength of Asphalt Materials using the Indirect Tensile Test Device*"

Gedafa Daba S., (2006)"Comparison Of Flexible Pavement Performance Using Kenlayer And Hdm-4",Midwest Transportation Consortium, Ames, Iowa.

Gudishala, R. (2004). Development of resilient modulus prediction models for base and subgrade pavement layers from in situ devices test results (Doctoral dissertation, Louisiana State University).

Helwany, s., *Applied Soil Mechanics: with ABAQUS Applications* 2007, New Jersey: JOHN WILEY & SONS, INC.

Hill, K., Y. Bereket, and L. Khazanovich (2007). "Toward A Unified Mechanistic Approach For Modeling Tests Of Unbound Materials." Department of Civil Engineering, University of Minnesota, Minneapolis, MN: Transportation Research Board 87th Annual Meeting 2008 Washington DC.

Huang, Y.H. (2004). Pavement Analysis and Design.2nd Edition, New Jersey, Prentice Hall.

Huekelom, W., and A.J.G. Klomp. (1962).Dynamic Testing as a Means of Controlling Pavements During and After Construction. Proceedings, *(1st) International Conference on the Structural Design of Asphalt Pavements*, pp. 667-685.

Kim, M. (2007).*Three-Dimensional Finite Element Analysis of Flexible Pavements Considering Nonlinear Pavement Foundation Behaviour*. Department of Civil Engineering, Graduate College of the University of Illinois at Urbana- Champaign.

Kim, Yong-Rak; Ban, Hokie; and Im, Soohyok. (2010). *Impact of Truck Loading on Design and Analysis of Asphaltic Pavement Structures*. *Final Reports & Technical Briefs from Mid-America Transportation Center*. 23.

Kleyn, E.G. (1975). *The Use of the Dynamic Cone Penetrometer*. Transvaal Roads Department, South Africa.

Liang, A. (2000). *Finite Element Analysis of Distortional bucking of Cold-formed Stainless Steel Columns*.Master's Thesis, University of Johannesburg.

Livneh, M. and Ishai, I. (1987). Pavement Material Evaluation by a Dynamic Cone Penetrometer. In *Proceedings of Sixth International Conference, Structural Design of Asphalt Pavements,* Vol. 1, pp. 665-676.

Luskin, D.M.and C.M.Walton, ―Effects of Truck Sizeand Weights on Highway Infrastructure and Operations. March2001. A Synthesis Report,‖ Research Report 2122- 1.

Maina, J., and Matsui, K., (2005). Elastic multilayered analysis using DEIntegration. *Publications of the Research institute for Mathematical Sciences, 41(5)*, pp. 853-867.

Mamlouk, M. S. (2006). Design of flexible pavements. In T.F. Fwa (ed.) *The Handbook of Highway Engineering*. Taylor & Francis Group, Boca Raton, Florida, USA.

Miner, M.A. (1945).CumulativeDamageinFatigue,‖TransactionsoftheASME,Vol.67, pp.A159-A164.

MIURA, T.S.N.a.N. (2001)., *Soft Clay Behaviour Analysis and Assessment* A.A.Balkema.

MnROAD (Minnesota Road Research), (2010), "*Low Volume Road Instrumentation"*, Minnesota Department of Transportation website, http://www.dot.state.mn.us/mnroad/instrumentation/pavementsensors.html

Monismith, C., Secor, K., and Blackmer, W., (1961), *"Asphalt Mixture Behavior in Repeated Flexure"*, Association of Asphalt Paving Technology, AAPT, Volume 30

Mousa. M.R., Abo-Hashema. M. A., Gadallah. A.A., and Mousa. R.M. (05 February 2016) Evaluation of pavement performance prediction models under difrente traffic and climet conditions. : <https://www.researchgate.net/publication/282348664

Muniandy, R., Aburkaba, E., Thamer, T. (2013). "Comparison of Flexible Pavement Performance Using Kenlayer and Chev PC Software Program" Australian Journal of Basic and Applied Sciences.

NCHRP (National Cooperative Highway Research Program), (2002) *"Simple Performance Test for Superpave Mix Design"*, NCHRP Report 465, Project 9-29, Transportation Research Board, Washington, DC

NCHRP. (2004). *Mechanistic-Empirical Design of New and Rehabilitated Pavement Structures*, National Cooperative Highway Research Program, NCHRP Project 1-37A, National Research Council, Washington, DC.

NCHRP 1-37A (2004): Mechanistic-Empirical Design of New & Rehabilitated Pavement Structures Guide. Available at: http://www.trb.org/mepdg/guide.htm [Accessed 16 February 2009]

NCHRP. (2007). Evaluation of Mechanistic-Empirical Design Procedure.National Cooperative Highway Research Program, NCHRP Project 1-37A. National Research Council,

Washington.

NCHRP (National Cooperative Highway Research Program), (2010), *"Validating the Fatigue Endurance Limit for Hot Mix Asphalt"*, NCHRP Project 9-38, Transportation Research Board

Newcomb, D., and Birgisson, B., (1999) *"Measuring In Situ Mechanical Properties of Pavement Subgrade Soils"*, NCHRP Synthesis 278, Transportation Research Board

Oscarsson, E. (2007): Prediction of Permanent Deformations in Asphalt Concrete using the Mechanistic-Empirical Pavement Design Guide. Licentiate Thesis. Lund University

Powell, W.D., J.F. Potter, H.C. Mayhew, and M.E. Nunn. (1984). *The Structural Design of Bituminous Roads*. TRRL Laboratory Report LR 1132. Transport and Road Research Laboratory, Crowthorne, United Kingdom.

Rabab'ah, S. and R.Y. Liang (2007). "Evaluation Of Mechanistic Empirical Design Approach Over Permeable Base Materials." Gannett Fleming, Inc., Audubon, PA: Transportation Research Board 87th Annual Meeting 2008 Washington DC.

Salgado, R., & Yoon, S. (2003). Dynamic cone penetration test (DCPT) for subgrade assessment. Joint Transportation Research Program, 73.

Schwartz, C., and Carvalho, R., (2007), "Implementation of the NCHRP 1-37A Design Guide, Final Report, Volume 2: Evaluation of Mechanistic-Empirical Design Procedure", Department of Civil and Environmental Engineering, University of Maryland.

Swan, D., R. Tardif, J.J. Hajek, and D.K. Hein (2007). "Development of Regional Traffic Data for the M- E Pavement Design Guide." Applied Research Associated, Inc., Toronto, ON: Transportation Research Board 87th Annual Meeting 2008 Washington DC.

Tutumluer, E.,and Thompson, M. R. (1997).‒Granular Base Moduli for Mechanistic Pavement Design.‖ In Proceedings of the ASCE Airfield Pavement Conference, ASCE, Seattle, Washington, pp. 33-47.

Tutumluer, E.,and Thompson, M. R. (1997).‒Anisotropic Modeling of Granular Bases in Flexible Pavements.‖ Transportation Research Record 1577, TRB, National Research Council, Washington D.C., pp. 18-26.

Van Vuuren, D.J. (1969). Rapid Determination of CBR with the Portable Dynamic Cone Penetrometer. In The Rhodesian Engineer, Vol. 7, No. 5, pp. 852-854.

Wang, J. (2001). Three-Dimensional Finite Element Analysis of Flexible Pavements. Master Thesis,

The University of Maine, ME.

Wayesss. S.G., Quezon. E.T., Kumela. T. (2017) Analysis of Stress- Strain and Deflection of Flexible Pavements Using Finite Element Method Case study on Bako-Nekemte Road. *Journal of Civil, Construction and Environmental Engineering*.

Webster, S.L., R.W. Brown and J.R. Porter. (1994). Force Projection Site Evaluation Using the Electronic Cone Penetrometer (ECP) and the Dynamic Cone Penetrometer (DCP). Technical Report GL-94-17, U.S. Army Engineer Waterways Experiment Station, Vicksburg, MS.

Witczak, M. W., and Uzan, J. (1988). The Universal Airport Pavement Design System: Granular Material Characterization, University of Maryland, Department of Civil Engineering, MD

Wu, S., & Sargand, S. M. (2007). Use of dynamic cone penetrometer in subgrade and base acceptance (No. FHWA/ODOT-2007/01). ORITE.

Wood, D.M., *Geotechnical modeling* ed. April 2004, Tehran: SOFTbank E-Book Center.

Yang H. Huang, 1993. *Pavement analysis and design,* Prentice Hall.

Yoder, E. J., and Witczak, M.W. (1975). *Principles of Pavement Design,* Wiley, New York.

APPENDIX

Appendix One

PCASE DCP analysis result figures and tables

Blows	Penn (mm)	Hamer type	corr	CBR	Depth (in)
0	60	1	1	0	2.4
10	110	1	1	48.1	4.3
10	137	1	1	96	5.4
10	165	1	1	92.2	6.5
10	200	1	1	71.8	7.9
10	248	1	1	50.4	9.8
5	285	1	1	31	11.2
5	330	1	1	24.9	13
3	360	1	1	22.2	14.2
3	390	1	1	22.2	15.4
3	422	1	1	20.6	16.6
2	455	1	1	12.6	17.9
2	500	1	1	8.9	19.7
3	570	1	1	8.6	22.4
3	640	1	1	8.6	25.2
3	708	1	1	8.9	27.9
2	755	1	1	8.5	29.7
2	802	1	1	8.5	31.6
1	826	1	1	8.3	32.5

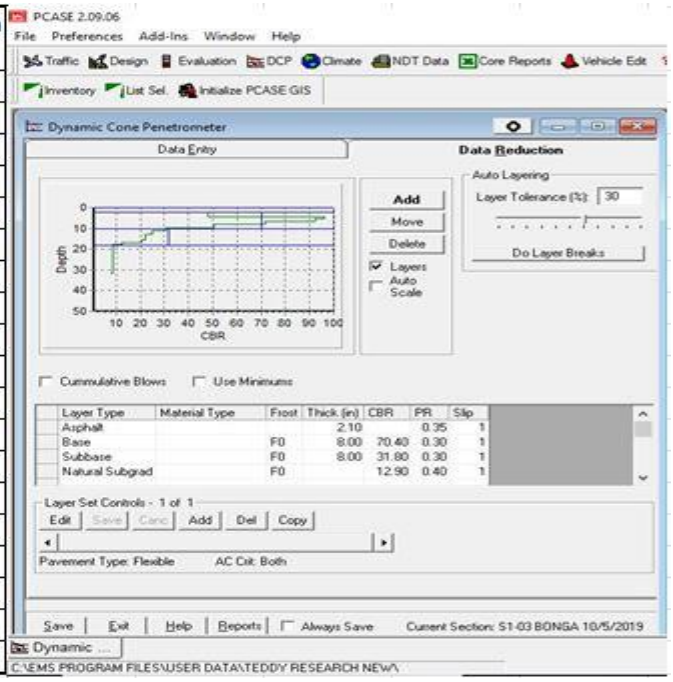

Blows	Penn(mm	Hamer type	corr	CBR	Depth(in)
0	52	1	1	0	2
10	78	1	1	100	3.1
10	93	1	1	100	3.7
10	122	1	1	88.6	4.8
5	138	1	1	79.4	5.4
5	155	1	1	74.2	6.1
5	170	1	1	85.3	6.7
5	186	1	1	79.4	7.3
5	202	1	1	79.4	8
5	218	1	1	79.4	8.6
5	235	1	1	74.2	9.3
5	252	1	1	74.2	9.9
5	285	1	1	35.3	11.2
5	325	1	1	28.4	12.8
5	364	1	1	29.3	14.3
5	400	1	1	32	15.7
5	435	1	1	33	17.1
3	470	1	1	18.6	18.5
3	505	1	1	18.6	19.9
3	540	1	1	18.6	21.3
3	572	1	1	20.6	22.5
3	604	1	1	20.6	23.8
3	638	1	1	19.3	25.1
3	670	1	1	20.6	26.4
2	692	1	1	19.9	27.2
2	714	1	1	19.9	28.1
2	736	1	1	19.9	29
2	757	1	1	21	29.8
2	778	1	1	21	30.6
2	800	1	1	19.9	31.5

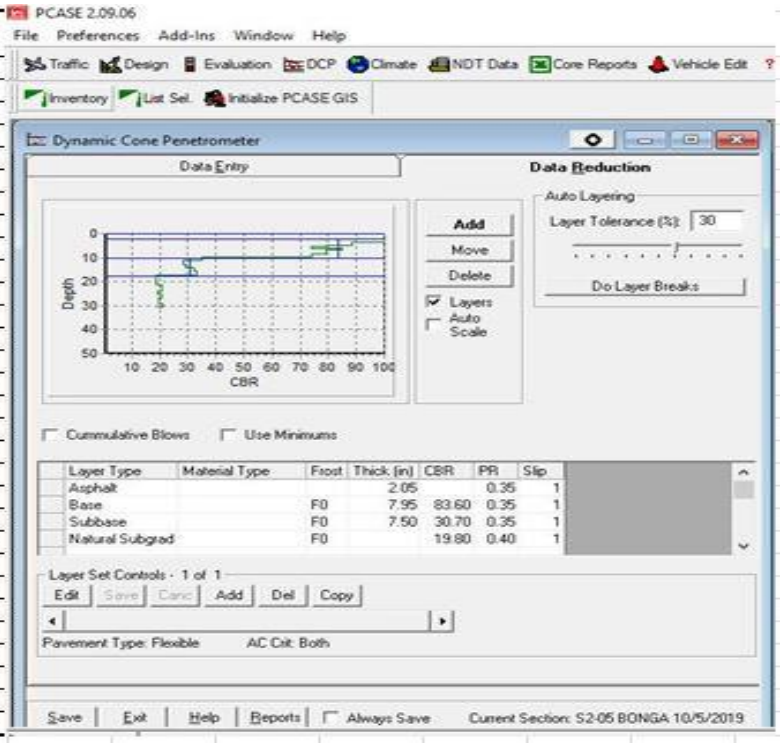

Blows	Penn (mm)	Hamer type	corr	CBR	Depth (in)
0	50	1	1	0	2
10	80	1	1	85.3	3.1
10	107	1	1	96	4.2
5	122	1	1	85.3	4.8
5	140	1	1	69.6	5.5
5	158	1	1	69.6	6.2
5	176	1	1	69.6	6.9
10	212	1	1	69.6	8.3
10	248	1	1	69.6	9.8
5	295	1	1	23.7	11.6
5	345	1	1	22.2	13.6
5	400	1	1	19.9	15.7
5	455	1	1	19.9	17.9
3	488	1	1	19.9	19.2
3	520	1	1	20.6	20.5
3	590	1	1	8.6	23.2
2	650	1	1	6.5	25.6
2	720	1	1	5.4	28.3
1	755	1	1	5.4	29.7
1	790	1	1	5.4	31.1
1	825	1	1	5.4	32.5

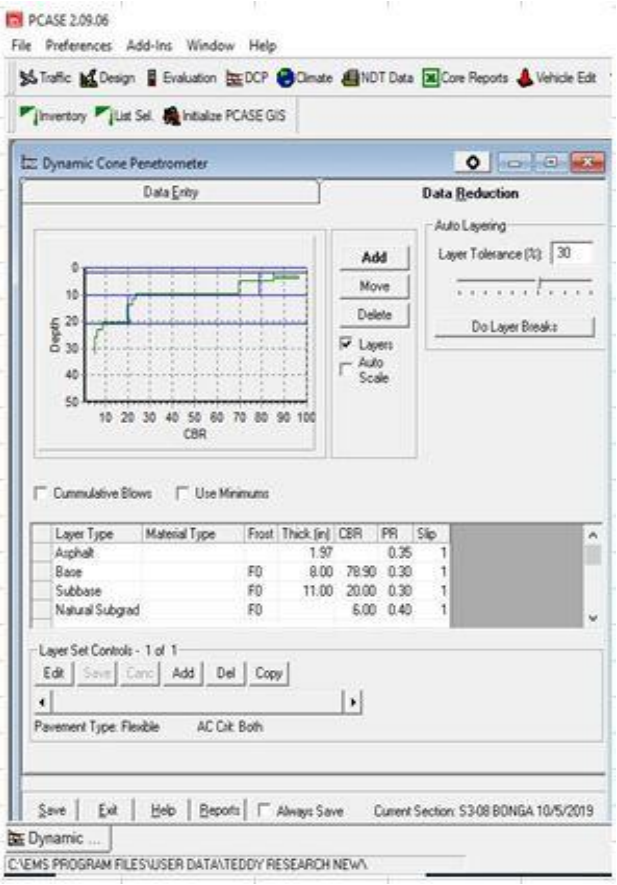

Appendix Three
Mechanistic response analysis result tables

SECTION ONE JULEA RESULT								
	Z-COORD	STRESS-X	STRESS-Y	STRESS-Z	STRAIN-X	STRAIN-Y	STRAIN-Z	DISPLT-Z
Point 1	0	1826.9	1826.9	550.09	3.32E-04	3.32E-04	-2.43E-04	3.97E-02
Point 2	2.5	372.2	372.2	472.05	2.56E-05	2.56E-05	7.05E-05	3.99E-02
Point 3	5	52.812	52.812	363.05	-2.67E-04	-2.67E-04	1.23E-03	3.93E-02
Point 4	-5	-1038.9	-1038.9	363.05	-2.67E-04	-2.67E-04	3.63E-04	3.93E-02
Point 5	15	-13.914	-13.914	162.48	-2.17E-04	-2.17E-04	6.35E-04	3.02E-02
Point 6	25	-12.926	-12.926	72.328	-1.95E-04	-1.95E-04	5.07E-04	2.54E-02
Point 7	-25	-43.785	-43.785	72.328	-1.95E-04	-1.95E-04	3.67E-04	2.54E-02
Point 8	35	-13.581	-13.581	38.638	-1.34E-04	-1.34E-04	2.96E-04	2.16E-02
Point 9	45	6.42E-02	6.42E-02	23.348	-1.36E-04	-1.36E-04	3.02E-04	1.91E-02
Point 10	-45	-20.692	-20.692	23.35	-1.36E-04	-1.36E-04	2.26E-04	1.91E-02
Point 11	70	0.11629	0.11629	11.578	-6.68E-05	-6.68E-05	1.49E-04	1.38E-02
Point 12	100	7.70E-02	7.70E-02	6.4783	-3.73E-05	-3.73E-05	8.32E-05	1.04E-02
Point 13	150	2.51E-02	2.51E-02	3.2818	-1.90E-05	-1.90E-05	4.23E-05	7.47E-03
Point 14	200	5.31E-03	5.31E-03	1.9861	-1.16E-05	-1.16E-05	2.57E-05	5.81E-03
Point 15	300	-3.26E-03	-3.26E-03	0.94702	-5.56E-06	-5.56E-06	1.23E-05	4.00E-03
Point 16	400	-5.87E-03	-5.87E-03	0.55602	-3.29E-06	-3.29E-06	7.29E-06	3.05E-03
Point 17	500	-5.18E-03	-5.18E-03	0.36369	-2.16E-06	-2.16E-06	4.78E-06	2.46E-03

SECTION TWO JULEA RESULT								
`	Z-COORD	STRESS-X	STRESS-Y	STRESS-Z	STRAIN-X	STRAIN-Y	STRAIN-Z	DISPLT-Z

Point 1	0	1741.7	1741.7	550.09	3.13E-04	3.13E-04	-2.23E-04	3.35E-02
Point 2	2.5	359.99	359.99	475.73	2.25E-05	2.25E-05	7.46E-05	3.37E-02
Point 3	5	53.733	53.733	369.92	-2.55E-04	-2.55E-04	1.17E-03	3.32E-02
Point 4	-5	-976.47	-976.47	369.92	-2.55E-04	-2.55E-04	3.51E-04	3.32E-02
Point 5	15	-13.431	-13.431	166.02	-2.06E-04	-2.06E-04	6.04E-04	2.44E-02
Point 6	25	-10.803	-10.803	75.343	-1.83E-04	-1.83E-04	4.96E-04	2.00E-02
Point 7	-25	-42.926	-42.926	75.343	-1.83E-04	-1.83E-04	3.51E-04	2.00E-02
Point 8	33.5	-10.06	-10.06	46.048	-1.26E-04	-1.26E-04	3.16E-04	1.66E-02
Point 9	42.5	0.66106	0.66106	30.353	-1.11E-04	-1.11E-04	2.48E-04	1.42E-02
Point 10	-42.5	-13.108	-13.108	30.353	-1.11E-04	-1.11E-04	2.32E-04	1.42E-02
Point 11	50	0.44341	0.44341	23.474	-8.60E-05	-8.60E-05	1.92E-04	1.26E-02
Point 12	100	7.38E-02	7.38E-02	7.3838	-2.74E-05	-2.74E-05	6.10E-05	7.16E-03
Point 13	150	1.12E-02	1.12E-02	3.6135	-1.35E-05	-1.35E-05	3.00E-05	5.02E-03
Point 14	200	-3.29E-03	-3.29E-03	2.1356	-8.02E-06	-8.02E-06	1.78E-05	3.85E-03
Point 15	300	-5.77E-03	-5.77E-03	0.99083	-3.74E-06	-3.74E-06	8.30E-06	2.62E-03
Point 16	400	-6.45E-03	-6.45E-03	0.57326	-2.18E-06	-2.18E-06	4.83E-06	1.99E-03
Point 17	500	-5.37E-03	-5.37E-03	0.37244	-1.42E-06	-1.42E-06	3.14E-06	1.60E-03

SECTION THREE JULEA RESULT								
	Z-COORD	STRESS-X	STRESS-Y	STRESS-Z	STRAIN-X	STRAIN-Y	STRAIN-Z	DISPLT-Z
Point 1	0	1873.1	1873.1	550.09	3.42E-04	3.42E-04	-2.54E-04	4.52E-02
Point 2	2.5	389.39	389.39	471.05	2.94E-05	2.94E-05	6.62E-05	4.54E-02
Point 3	5	51.701	51.701	360.64	-2.70E-04	-2.70E-04	1.23E-03	4.48E-02
Point 4	-5	-1050.4	-1050.4	360.64	-2.70E-04	-2.70E-04	3.65E-04	4.48E-02
Point 5	15	-18.461	-18.461	157.2	-2.25E-04	-2.25E-04	6.30E-04	3.57E-02
Point 6	25	-11.695	-11.695	67.021	-2.30E-04	-2.30E-04	6.02E-04	3.10E-02
Point 7	-25	-59.013	-59.013	67.021	-2.30E-04	-2.30E-04	3.84E-04	3.10E-02
Point 8	38.75	-10.324	-10.324	29.953	-1.32E-04	-1.32E-04	2.94E-04	2.52E-02
Point 9	52.5	-8.72E-02	-8.72E-02	15.897	-1.31E-04	-1.31E-04	2.90E-04	2.19E-02
Point 10	-52.5	-16.201	-16.201	15.901	-1.31E-04	-1.31E-04	2.08E-04	2.19E-02
Point 11	70	4.30E-02	4.30E-02	10.14	-8.25E-05	-8.25E-05	1.84E-04	1.79E-02
Point 12	100	6.68E-02	6.68E-02	5.7709	-4.65E-05	-4.65E-05	1.04E-04	1.37E-02
Point 13	150	3.35E-02	3.35E-02	2.9959	-2.42E-05	-2.42E-05	5.39E-05	9.99E-03

Point 14	200	1.30E-02	1.30E-02	1.8479	-1.50E-05	-1.50E-05	3.34E-05	7.86E-03
Point 15	300	-3.33E-04	-3.33E-04	0.90459	-7.40E-06	-7.40E-06	1.65E-05	5.49E-03
Point 16	400	-4.59E-03	-4.59E-03	0.53845	-4.45E-06	-4.45E-06	9.87E-06	4.21E-03
Point 17	500	-4.58E-03	-4.58E-03	0.35497	-2.95E-06	-2.95E-06	6.53E-06	3.40E-03

SECTION ONE ABAQUS RESULT				
Depth (m)	V. Stress (S22)	V. Strain (E22)	H. Strain (E11)	Displacement (m)
0	-550000	0.00023483	-0.00032342	-0.000539089
0.001667	-542278	0.00022346	-0.00031205	-0.000539092
0.003333	-532816	0.00020205	-0.00029036	-0.000539022
0.005	-522746	0.00018224	-0.00027002	-0.000539008
0.006667	-513696	0.00016264	-0.00025008	-0.000539042
0.008333	-505900	0.00014287	-0.00023021	-0.000539116
0.01	-499219	0.0001228	-0.00021029	-0.000539215
0.011666	-493394	0.00010246	-0.00019027	-0.000539327
0.013333	-488148	8.19E-05	-0.00017017	-0.00053944
0.015	-483236	6.12E-05	-0.00014999	-0.000539546
0.016666	-478452	4.04E-05	-0.00012977	-0.000539637
0.018333	-473636	1.96E-05	-0.00010952	-0.000539707
0.020001	-468673	-1.18E-06	-8.93E-05	-0.000539751
0.021667	-463488	-2.19E-05	-6.90E-05	-0.000539766
0.023334	-458038	-4.25E-05	-4.88E-05	-0.000539748
0.025	-452309	-6.31E-05	-2.86E-05	-0.000539695
0.026667	-446308	-8.36E-05	-8.42E-06	-0.000539607
0.028334	-440065	-0.00010402	1.17E-05	-0.000539481
0.03	-433622	-0.00012439	3.19E-05	-0.000539317
0.031667	-427031	-0.00014474	5.21E-05	-0.000539115
0.033334	-420352	-0.00016509	7.23E-05	-0.000538873
0.035	-413650	-0.00018546	9.25E-05	-0.000538592
0.036667	-406992	-0.00020589	0.00011272	-0.000538272
0.038333	-400441	-0.00022641	0.00013303	-0.000537913
0.04	-394060	-0.00024704	0.00015342	-0.000537514
0.041667	-387904	-0.00026781	0.00017389	-0.000537076
0.043333	-382025	-0.00028873	0.00019445	-0.0005366
0.045	-376459	-0.00030983	0.00021512	-0.000536085
0.046667	-371233	-0.0003311	0.00023588	-0.000535532
0.048333	-366356	-0.00035256	0.00025675	-0.000534942
0.05	-364005	-0.00036333	0.00026705	-0.000534316

0.05	-348728	-0.00120407	0.0002812	-0.000534316
0.06	-335847	-0.00117008	0.00028305	-0.000521744
0.07	-310502	-0.00110073	0.0002838	-0.000509824
0.08	-286208	-0.00103009	0.00027966	-0.000498589
0.09	-263308	-0.00096059	0.00027235	-0.000488087
0.1	-241971	-0.00089383	0.00026321	-0.000478308
0.11	-222237	-0.00083074	0.00025318	-0.00046923
0.12	-204066	-0.00077175	0.00024291	-0.00046081
0.13	-187377	-0.00071704	0.00023285	-0.000453008
0.14	-172072	-0.00066659	0.0002233	-0.000445772
0.15	-158045	-0.0006203	0.00021449	-0.000439061
0.16	-145195	-0.00057802	0.00020656	-0.000432824
0.17	-133427	-0.00053959	0.00019965	-0.000427023
0.18	-122658	-0.00050487	0.00019384	-0.000421612
0.19	-112815	-0.00047374	0.00018923	-0.000416556
0.2	-103840	-0.00044611	0.00018591	-0.00041181
0.21	-95687	-0.00042195	0.00018399	-0.000407344
0.22	-88324.3	-0.00040128	0.0001836	-0.000403111
0.23	-81734.5	-0.00038416	0.00018486	-0.000399084
0.24	-75912.1	-0.00037072	0.00018793	-0.000395213
0.25	-73192.8	-0.00036493	0.00018994	-0.000391471
0.25	-68425.1	-0.00048267	0.00018778	-0.000391471
0.26	-66270.1	-0.00046874	0.00018336	-0.000386526
0.27	-62123.2	-0.00044203	0.00017494	-0.000381881
0.28	-58286	-0.00041748	0.00016735	-0.000377491
0.29	-54728.9	-0.00039491	0.00016052	-0.000373359
0.3	-51427.5	-0.00037414	0.00015441	-0.000369435
0.31	-48360.4	-0.00035505	0.00014896	-0.000365735
0.32	-45509	-0.00033753	0.00014415	-0.000362206
0.33	-42856.8	-0.00032146	0.00013996	-0.000358869
0.34	-40389.6	-0.00030678	0.00013636	-0.000355671
0.35	-38095.3	-0.00029341	0.00013334	-0.000352639
0.36	-35963.8	-0.00028129	0.0001309	-0.000349716
0.37	-33986.3	-0.00027039	0.00012903	-0.000346935
0.38	-32155.9	-0.00026067	0.00012773	-0.000344237
0.39	-30467.5	-0.00025212	0.00012701	-0.000341655
0.4	-28917.5	-0.00024473	0.0001269	-0.000339134
0.41	-27503.5	-0.00023851	0.0001274	-0.000336704
0.42	-26225	-0.00023348	0.00012855	-0.000334312
0.43	-25082.7	-0.00022968	0.00013037	-0.000331983
0.44	-24077.9	-0.00022713	0.00013291	-0.000329672
0.45	-23610.4	-0.00022617	0.00013436	-0.000327395

0.45	-17371.5	-0.00022143	0.00010136	-0.000327395
0.6775	-13460.5	-0.00017512	7.87E-05	-0.000275604
0.905	-7996.66	-0.00010471	4.72E-05	-0.000247235
1.1325	-5581.76	-7.42E-05	3.36E-05	-0.000227842
1.36	-4194.32	-5.68E-05	2.59E-05	-0.000213424
1.5875	-3320.06	-4.58E-05	2.10E-05	-0.000201985
1.815	-2728.25	-3.83E-05	1.77E-05	-0.000192569
2.0425	-2308.53	-3.29E-05	1.52E-05	-0.000184556
2.27	-1999.83	-2.87E-05	1.34E-05	-0.000177611
2.4975	-1767.19	-2.55E-05	1.19E-05	-0.000171471
2.725	-1588.76	-2.30E-05	1.07E-05	-0.000165985
2.9525	-1450.71	-2.09E-05	9.75E-06	-0.000161011
3.18	-1343.41	-1.93E-05	8.95E-06	-0.000156463
3.4075	-1260.15	-1.79E-05	8.30E-06	-0.00015225
3.635	-1195.77	-1.68E-05	7.77E-06	-0.000148318
3.8625	-1146.39	-1.59E-05	7.34E-06	-0.000144602
4.09	-1108.86	-1.52E-05	7.00E-06	-0.000141066
4.3175	-1080.67	-1.47E-05	6.73E-06	-0.000137663
4.545	-1059.78	-1.43E-05	6.52E-06	-0.000134373
4.7725	-1044.55	-1.40E-05	6.35E-06	-0.00013116
5	-1032.13	-1.37E-05	6.21E-06	-0.000128014

SECTION TWO ABAQUS RESULT				
Depth (m)	V. Stress (S22)	V. Strain (E22)	H. Strain (E11)	Displacement (m)
0	-550000	0.000216726	-0.0003066	-0.000429753
0.001667	-542450	0.000205848	-0.0002957	-0.000429721
0.003334	-533101	0.000185459	-0.000275	-0.000429616
0.004999	-523136	0.000166691	-0.0002557	-0.000429573
0.006666	-514214	0.000148128	-0.0002367	-0.000429579
0.008333	-506571	0.000129365	-0.0002178	-0.000429628
0.01	-500075	0.000110292	-0.0001988	-0.000429704
0.011667	-494465	9.09E-05	-0.0001798	-0.000429794
0.013334	-489465	7.13E-05	-0.0001606	-0.000429888
0.014999	-484826	5.16E-05	-0.0001414	-0.000429976
0.016666	-480337	3.17E-05	-0.0001221	-0.00043005
0.018333	-475835	1.19E-05	-0.0001028	-0.000430106
0.020001	-471202	-7.99E-06	-8.34E-05	-0.000430137
0.021668	-466360	-2.78E-05	-6.41E-05	-0.00043014
0.023333	-461263	-4.75E-05	-4.48E-05	-0.000430112
0.025	-455889	-6.72E-05	-2.55E-05	-0.000430052
0.026667	-450243	-8.67E-05	-6.27E-06	-0.000429957

0.028334	-444350	-0.00010625	1.30E-05	-0.000429827
0.030001	-438250	-0.0001257	3.22E-05	-0.00042966
0.031666	-431991	-0.00014511	5.14E-05	-0.000429457
0.033333	-425625	-0.00016451	7.07E-05	-0.000429216
0.035	-419213	-0.00018393	9.00E-05	-0.000428938
0.036667	-412817	-0.0002034	0.00010928	-0.000428622
0.038334	-406499	-0.00022294	0.00012864	-0.000428269
0.040001	-400318	-0.00024256	0.00014805	-0.000427879
0.041666	-394327	-0.00026229	0.00016753	-0.000427452
0.043333	-388567	-0.00028216	0.00018709	-0.000426987
0.045	-383073	-0.00030219	0.00020675	-0.000426487
0.046667	-377874	-0.00032238	0.0002265	-0.000425951
0.048334	-372983	-0.00034272	0.00024633	-0.00042538
0.049999	-370616	-0.00035293	0.00025469	-0.000424776
0.049999	-355118	-0.0011535	0.00026963	-0.000424776
0.06	-342040	-0.00112105	0.00027139	-0.000412718
0.07	-316297	-0.00105475	0.00027206	-0.000401303
0.08	-291605	-0.00098709	0.00026795	-0.000390534
0.09	-268322	-0.00092044	0.00026075	-0.00038047
0.1	-246631	-0.00085638	0.00025173	-0.000371096
0.110001	-226580	-0.00079582	0.00024185	-0.000362396
0.120001	-208132	-0.00073923	0.00023173	-0.000354327
0.129999	-191206	-0.00068677	0.00022181	-0.000346852
0.139999	-175700	-0.00063842	0.0002124	-0.00033992
0.15	-161504	-0.00059409	0.0002037	-0.000333489
0.16	-148516	-0.00055363	0.00019586	-0.000327515
0.17	-136638	-0.0005169	0.00018899	-0.000321957
0.18	-125784	-0.00048374	0.0001832	-0.000316773
0.190001	-115880	-0.00045405	0.00017857	-0.000311925
0.200001	-106866	-0.00042775	0.0001752	-0.000307376
0.209999	-98695.6	-0.0004048	0.00017319	-0.000303091
0.219999	-91336.9	-0.00038522	0.00017264	-0.000299031
0.23	-84772	-0.00036908	0.00017371	-0.000295161
0.24	-78996.5	-0.00035651	0.00017654	-0.000291443
0.25	-76306.2	-0.00035113	0.00017842	-0.000287839
0.25	-73024.5	-0.0004823	0.00017912	-0.000287839
0.2535	-72245.8	-0.00047741	0.00017751	-0.00028611
0.257	-70710.8	-0.00046778	0.00017433	-0.000284417
0.2605	-69219.6	-0.00045844	0.00017127	-0.000282759
0.264	-67770.4	-0.00044937	0.0001683	-0.000281135
0.2675	-66361.4	-0.00044057	0.00016544	-0.000279543
0.271	-64991.1	-0.00043203	0.00016267	-0.000277983

0.2745	-63658.2	-0.00042373	0.00015999	-0.000276454
0.278	-62361.3	-0.00041568	0.0001574	-0.000274954
0.2815	-61099.3	-0.00040785	0.0001549	-0.000273483
0.285	-59871	-0.00040024	0.00015248	-0.00027204
0.2885	-58675.4	-0.00039286	0.00015014	-0.000270625
0.292	-57511.3	-0.00038568	0.00014788	-0.000269235
0.2955	-56377.9	-0.00037871	0.0001457	-0.000267872
0.299	-55274.2	-0.00037193	0.00014359	-0.000266533
0.3025	-54199.3	-0.00036535	0.00014156	-0.000265219
0.306	-53152.3	-0.00035896	0.0001396	-0.000263928
0.3095	-52132.5	-0.00035275	0.00013771	-0.00026266
0.313	-51139	-0.00034672	0.0001359	-0.000261415
0.3165	-50171.1	-0.00034086	0.00013415	-0.000260191
0.32	-49228.1	-0.00033518	0.00013247	-0.000258987
0.3235	-48309.3	-0.00032966	0.00013085	-0.000257804
0.327	-47414	-0.0003243	0.0001293	-0.000256641
0.3305	-46541.8	-0.0003191	0.00012782	-0.000255497
0.334	-45691.8	-0.00031406	0.0001264	-0.000254371
0.3375	-44863.7	-0.00030916	0.00012504	-0.000253263
0.341	-44056.8	-0.00030442	0.00012375	-0.000252173
0.3445	-43270.8	-0.00029983	0.00012252	-0.000251099
0.348	-42505	-0.00029537	0.00012134	-0.000250042
0.3515	-41759.1	-0.00029106	0.00012023	-0.000249001
0.355	-41032.6	-0.00028689	0.00011918	-0.000247975
0.3585	-40325.2	-0.00028286	0.00011819	-0.000246963
0.362	-39636.4	-0.00027896	0.00011726	-0.000245967
0.365499	-38966	-0.0002752	0.00011639	-0.000244983
0.368999	-38313.5	-0.00027156	0.00011558	-0.000244014
0.372499	-37678.8	-0.00026806	0.00011483	-0.000243056
0.375999	-37061.5	-0.00026469	0.00011414	-0.000242112
0.379499	-36461.4	-0.00026145	0.00011351	-0.000241179
0.382999	-35878.2	-0.00025833	0.00011293	-0.000240259
0.386499	-35311.7	-0.00025534	0.00011242	-0.000239347
0.389999	-34761.8	-0.00025248	0.00011197	-0.000238449
0.393499	-34228.2	-0.00024974	0.00011158	-0.000237558
0.396999	-33710.8	-0.00024713	0.00011125	-0.00023668
0.400499	-33209.4	-0.00024465	0.00011099	-0.000235807
0.403999	-32723.9	-0.00024229	0.00011078	-0.000234948
0.407499	-32254.2	-0.00024005	0.00011064	-0.000234091
0.410999	-31800.1	-0.00023794	0.00011057	-0.000233249
0.424999	-30331.7	-0.00023154	0.00011081	-0.000229936
0.424999	-27100.6	-0.00022017	9.94E-05	-0.000229936

0.490356	-24493.8	-0.00020173	9.01E-05	-0.000215204
0.686428	-14145	-0.00011766	5.28E-05	-0.000185131
0.751785	-12176.7	-0.00010166	4.57E-05	-0.000177992
1.07857	-6710.12	-5.73E-05	2.60E-05	-0.000153193
1.14393	-6091.55	-5.23E-05	2.38E-05	-0.000149618
1.66679	-3322.18	-2.98E-05	1.37E-05	-0.000129166
2.05893	-2407.46	-2.21E-05	1.03E-05	-0.000119135
2.64714	-1697.06	-1.58E-05	7.40E-06	-0.000108173
2.84321	-1552.45	-1.45E-05	6.75E-06	-0.000105207
3.03929	-1436.92	-1.33E-05	6.22E-06	-0.000102486
3.56214	-1229.6	-1.12E-05	5.18E-06	-9.61E-05
3.69286	-1194.54	-1.08E-05	4.99E-06	-9.47E-05
4.01964	-1127.5	-1.00E-05	4.61E-06	-9.13E-05
4.47714	-1069.71	-9.30E-06	4.25E-06	-8.69E-05
4.93464	-1038.66	-8.89E-06	4.04E-06	-8.27E-05
5	-1032.56	-8.80E-06	3.99E-06	-8.22E-05

SECTION THREE ABAQUS RESULT				
Depth (m)	V. Stress (S22)	V. Strain (E22)	H. Strain (E11)	Displacement (m)
0	-550000	0.000162515	-0.00034732	-0.00045183
0.001667	-541647	0.000153576	-0.00033562	-0.00045166
0.0033331	-532039	0.000136719	-0.00031318	-0.00045148
0.0050001	-522033	0.000121046	-0.00029201	-0.00045136
0.0066671	-513086	0.000105451	-0.00027123	-0.0004513
0.0083332	-505411	8.96E-05	-0.00025053	-0.00045128
0.0100002	-498857	7.35E-05	-0.00022979	-0.0004513
0.0116663	-493157	5.70E-05	-0.00020896	-0.00045133
0.0133333	-488030	4.04E-05	-0.00018804	-0.00045138
0.0150003	-483227	2.36E-05	-0.00016706	-0.00045142
0.0166664	-478540	6.69E-06	-0.00014603	-0.00045145
0.0183334	-473809	-1.02E-05	-0.00012498	-0.00045147
0.0200005	-468919	-2.70E-05	-0.00010393	-0.00045147
0.0216665	-463793	-4.38E-05	-8.29E-05	-0.00045144
0.0233335	-458391	-6.05E-05	-6.19E-05	-0.00045139
0.0249996	-452697	-7.71E-05	-4.09E-05	-0.00045131
0.0266666	-446722	-9.36E-05	-1.99E-05	-0.00045121
0.0283337	-440496	-0.00011	1.10E-06	-0.00045107
0.0299997	-434063	-0.00012638	2.21E-05	-0.0004509
0.0316668	-427476	-0.00014273	4.30E-05	-0.0004507
0.0333338	-420797	-0.00015907	6.40E-05	-0.00045046
0.0349998	-414096	-0.00017543	8.51E-05	-0.00045019

0.0366669	-407438	-0.00019184	0.000106129	-0.00044989
0.0383329	-400893	-0.00020833	0.000127258	-0.00044956
0.04	-394524	-0.00022493	0.000148462	-0.0004492
0.041667	-388392	-0.00024165	0.00016975	-0.0004488
0.0433331	-382548	-0.00025853	0.000191126	-0.00044837
0.0450001	-377027	-0.00027557	0.000212599	-0.00044791
0.0466671	-371849	-0.00029277	0.000234162	-0.00044741
0.0483332	-367005	-0.00031011	0.0002558	-0.00044688
0.0500002	-364662	-0.00031882	0.00026896	-0.00044633
0.0500002	-349152	-0.00121279	0.00028159	-0.00044633
0.0600004	-336012	-0.00117826	0.000283956	-0.00043372
0.0699997	-310128	-0.00110766	0.000285605	-0.00042169
0.0799999	-285290	-0.00103559	0.000282149	-0.00041038
0.0900002	-261877	-0.00096474	0.000275484	-0.00039982
0.1	-240056	-0.00089676	0.000267007	-0.00039
0.11	-219858	-0.00083257	0.000257675	-0.00038089
0.12	-201242	-0.00077262	0.000248162	-0.00037245
0.13	-184127	-0.00071709	0.000238939	-0.00036464
0.14	-168417	-0.00066601	0.00023034	-0.00035741
0.15	-154011	-0.0006193	0.000222607	-0.0003507
0.16	-140810	-0.00057685	0.000215927	-0.00034448
0.17	-128725	-0.00053853	0.000210452	-0.00033869
0.18	-117679	-0.00050426	0.000206318	-0.00033329
0.19	-107607	-0.00047396	0.000203661	-0.00032823
0.2	-98460.9	-0.00044762	0.000202626	-0.00032348
0.21	-90205.9	-0.0004253	0.000203376	-0.00031899
0.22	-82826.8	-0.0004071	0.000206101	-0.00031472
0.23	-76327.6	-0.00039324	0.000211028	-0.00031062
0.24	-70729.1	-0.00038399	0.0002184	-0.00030664
0.25	-68158.3	-0.00038054	0.000222726	-0.00030273
0.25	-63962	-0.00057674	0.000222186	-0.00030273
0.259167	-62169.8	-0.00056138	0.000216894	-0.00029732
0.268333	-58710.7	-0.00053179	0.000206742	-0.00029221
0.2775	-55490.6	-0.00050434	0.000197405	-0.00028736
0.286667	-52488.4	-0.00047884	0.000188805	-0.00028277
0.295834	-49685.5	-0.00045512	0.000180888	-0.00027841
0.305	-47064.7	-0.00043305	0.000173601	-0.00027426
0.314167	-44611	-0.00041249	0.000166902	-0.00027032
0.323334	-42310.9	-0.00039332	0.000160749	-0.00026657
0.3325	-40152.3	-0.00037545	0.000155111	-0.00026299
0.341666	-38124.5	-0.00035879	0.000149956	-0.00025958
0.350833	-36217.7	-0.00034325	0.00014526	-0.00025631

0.36	-34423.3	-0.00032875	0.000140998	-0.00025319
0.369166	-32733.6	-0.00031525	0.000137152	-0.0002502
0.378333	-31141.7	-0.00030269	0.000133705	-0.00024733
0.3875	-29641.6	-0.000291	0.000130645	-0.00024458
0.396667	-28227.7	-0.00028016	0.000127959	-0.00024193
0.405833	-26895.5	-0.00027013	0.00012564	-0.00023938
0.415	-25640.6	-0.00026087	0.000123682	-0.00023692
0.424167	-24459.5	-0.00025236	0.000122081	-0.00023455
0.433333	-23349.2	-0.00024459	0.000120837	-0.00023225
0.4425	-22307.2	-0.00023754	0.00011995	-0.00023002
0.451667	-21331.4	-0.00023119	0.000119424	-0.00022785
0.460834	-20420.2	-0.00022556	0.000119265	-0.00022574
0.47	-19572.7	-0.00022062	0.000119481	-0.00022368
0.479167	-18788.3	-0.0002164	0.000120085	-0.00022166
0.488334	-18066.9	-0.00021291	0.000121089	-0.00021968
0.4975	-17409	-0.00021015	0.000122511	-0.00021773
0.506667	-16815.7	-0.00020816	0.000124368	-0.0002158
0.515833	-16288.3	-0.00020696	0.000126681	-0.00021388
0.525	-16041.2	-0.00020655	0.000127952	-0.00021198
0.525	-11521.3	-0.00020489	9.23E-05	-0.00021198
0.823334	-8735.82	-0.00015384	6.84E-05	-0.00015009
1.12167	-4951.81	-8.27E-05	3.60E-05	-0.00011979
1.42	-3402.29	-5.33E-05	2.26E-05	-0.00010069
1.71833	-2530.81	-3.64E-05	1.48E-05	-8.79E-05
2.01667	-2007.41	-2.59E-05	9.98E-06	-7.90E-05
2.315	-1673.58	-1.91E-05	6.78E-06	-7.25E-05
2.61333	-1455.59	-1.46E-05	4.63E-06	-6.76E-05
2.91167	-1310.63	-1.15E-05	3.16E-06	-6.38E-05
3.21	-1213.66	-9.34E-06	2.15E-06	-6.07E-05
3.50833	-1148.46	-7.90E-06	1.46E-06	-5.82E-05
3.80667	-1104.67	-6.91E-06	9.89E-07	-5.60E-05
4.105	-1075.24	-6.24E-06	6.66E-07	-5.41E-05
4.40333	-1055.54	-5.79E-06	4.48E-07	-5.23E-05
4.70167	-1042.35	-5.49E-06	2.99E-07	-5.06E-05
5	-1032.87	-5.26E-06	1.92E-07	-4.90E-05